

Dissertation zur Erlangung des Doktorgrades  
der Fakultät für Chemie und Pharmazie der  
Ludwig-Maximilians-Universität München



**PLGA-based micro- and nanoparticle development for chemically  
modified messenger RNA delivery**

Maximilian Utzinger

aus Prien, am Chiemsee, Deutschland

2017

## Erklärung

Diese Dissertation wurde im Sinne von § 7 der Promotionsordnung vom 28. November 2011 von Herrn Prof. Dr. Gerhard Winter betreut und von der Fakultät für Chemie und Pharmazie vertreten.

## Eidesstattliche Versicherung

Diese Dissertation wurde eigenständig und ohne unerlaubte Hilfe erarbeitet.

München, 21.02.2017

Maximilian Utzinger

Dissertation eingereicht am 24.02.2017

1. Gutachter: Prof. Gerhard Winter

2. Gutachter: Prof. Christian Plank

Mündliche Prüfung am 11.05.2017

**„Bub, mach wenigstens einen Abschluss“**

**Für meine Mama**

“There we were, now here we are  
All this confusion, nothing's the same to me”

(Noel Gallagher)

## Table of Contents

1	Introduction .....	4
1.1	Transcript therapy .....	4
1.1.1	Chemically modified messenger RNA .....	5
1.2	cmRNA as a therapeutic tool .....	6
1.3	Challenges in nucleic acid delivery .....	7
1.4	Delivery systems for nucleic acids .....	7
1.4.1	Polyplexes in nucleic acid delivery .....	9
1.4.2	Lipoplexes in nucleic acid delivery .....	10
1.4.3	Scaffolds for nano-carrier systems .....	12
1.5	Poly (lactic-co-glycolic acid) (PLGA).....	13
1.6	Aim of the thesis .....	15
2	Materials and methods .....	18
2.1	Materials .....	18
2.1.1	Chemicals - microparticle project.....	18
2.1.2	Chemicals - nanoparticle project .....	19
2.2	Methods – general protocols .....	21
2.2.1	Measurement of nanoparticle size .....	21
2.2.2	Measurement of nanoparticle zeta potential.....	21
2.2.3	Cell culture .....	22
2.2.4	Scanning electron microscopy .....	22
2.3	Methods - microparticle project.....	23
2.3.1	Lipoplex formation .....	23
2.3.2	Fluorescence labelling for fluorescence microscopy .....	23
2.3.3	Microparticle formation .....	24
2.3.4	Measurement of microparticle size .....	25
2.3.5	cmRNA quantification protocol in microparticles .....	27
2.3.6	Surface topology investigation .....	27
2.3.7	<i>In vitro</i> transfection efficiency .....	29
2.3.8	Composite mixing with bone substitute materials .....	29
2.3.9	$\mu$ -CT analysis of composites.....	30
2.4	Methods – nanoparticle project.....	31
2.4.1	Preparation of chitosan and co-formulated PLGA/chitosan polyplexes.....	31

2.4.2	Fluorescence labelling for FRET analysis .....	32
2.4.3	cmRNA quantification in polyplexes .....	33
2.4.4	Agarose gel electrophoresis .....	33
2.4.5	Fluorescence resonance energy transfer (FRET) .....	34
2.4.6	<i>In vitro</i> transfection efficiency .....	34
2.4.7	<i>In vitro</i> cell viability assay (MTT).....	35
3	Results .....	36
3.1	Optimization of the microparticle formation process.....	36
3.1.1	Influence of the organic phase: PLGA (Resomer®) .....	38
3.1.2	Influence of the surfactant: poly (vinyl alcohol) (PVA) solutions.....	41
3.1.3	Influence of the energy input for phase interaction: sonication.....	43
3.1.4	Aqueous phase: cmRNA/lipid-complex .....	46
3.2	Visualization of release of lipoplexes <i>in vitro</i> .....	52
3.3	Development of a composite ceramic/polymer bone substitute .....	54
3.3.1	$\mu$ -CT analysis of composite specimens for porosity analysis .....	55
3.3.2	Transfection efficiency of composite and microparticle specimens .....	57
3.4	PLGA in nanoparticle carriers.....	58
3.4.1	Chitosan nanoparticle development and characterization .....	59
3.4.2	Screening of O/W emulsion mixing techniques .....	62
3.4.3	Screening of different PLGA polymers for the co-formulation .....	66
3.5	Investigation of co-formulation effects .....	68
3.5.1	Polyplex size and zeta potential comparison.....	68
3.5.2	Polyplex imaging <i>via</i> SEM .....	70
3.5.3	Influence on complexation and particle stability .....	71
3.5.4	Influence of co-polymerization on cytotoxicity .....	74
3.5.5	Influence on transfection efficiency.....	75
	Discussion .....	79
3.6	PLGA microparticles as a lipoplex distribution system .....	79
3.7	PLGA microparticles as composite in injectable calcium phosphate cements .....	82
3.8	The enhancement of chitosan/cmRNA complexes by co-formulation with PLGA ..	82
	Summary .....	86
4	References .....	88
5	Appendix .....	95
5.1	Abbreviations .....	95
5.2	Publications .....	97

5.3	Supplementary information.....	98
5.3.1	Supplementary Information to 2.3.9 $\mu$ -CT analysis of composites .....	104
6	Acknowledgements .....	105

# 1 Introduction

## 1.1 Transcript therapy

“Gene therapy uses the nucleic acids as medicine to cure genetic deficiencies and a large variety of acquired diseases”, according to Midoux *et al.* (2009, p.166) [1]. The related and more progressive approach of transcript therapy however does not cure diseases but treats the symptoms by adjusting and interfering with pathways in protein production. Transcript therapy is defined as the utilization of single-stranded ribonucleic acids as a therapeutic agent and contains many forms of ribonucleic acids like, small interfering RNA (siRNA) and messenger RNA (mRNA). These different forms of transcripts are all desired to be introduced into cells, without being metabolized and damaged before they arrive at the site of interest. Even though polycations were the first agents used for introducing nucleic acids into cells, the later developed recombinant viral vectors have been far more efficient in doing so. These vehicles have already proven their functionality to treat some diseases where classic “small molecule” medicine reached its limits, but the side-effects often outweigh their potential, like *i.e.* insertional mutagenesis or immunogenicity [2, 3]. Hence, the search for novel innovative carrier systems especially in transcript therapy is one of the imminent challenges, where basically parts of the main strategy of viruses is tried to be imitated. For successful applications where nucleic acids are the therapeutic agent, the protection of the cargo, trespassing the cell wall, the transfer into the cytosol and in the case of DNA into the nucleus, are necessary steps [1]. The mere fact that up to 2400 different therapeutic nucleic acid clinical trials were ongoing or approved worldwide until mid of 2016 is just an indicator how contemporary this field of research is at the moment and how important progress in the development of appropriate carrier systems for these therapeutic approaches are [4, 5].

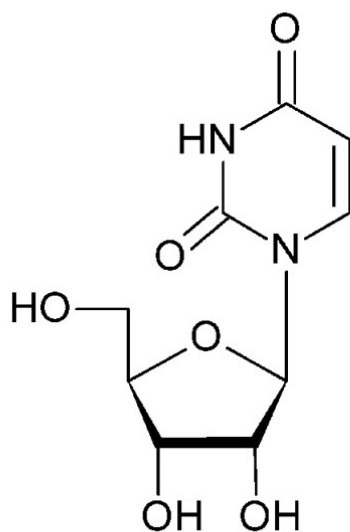
### 1.1.1 Chemically modified messenger RNA

As protein therapy comes with adverse effects like a lack of stability *in vivo*, and an often too complex chemical structure for synthetic development and carrier system development, the idea of letting the body produce its own therapeutic *via* transcript therapy emerged. Plasmid DNA transfection and the direct introduction into the genome comes with the danger of mutagenesis which makes it a risky alternative for protein therapy, as well. Also, as the transport into the nucleus only happens during cell division, plasmid DNA as a therapeutic tool only makes sense in dividing cells in general. Here, the introduction of transcript therapy and messenger RNA delivery in special, which is not being internalized into the genome and solely translated in the cytosol, could be one of the most promising candidates for treating patients with gene defects [6, 7].

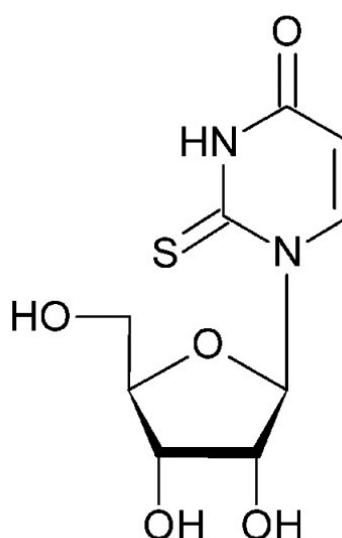
One of the most challenging obstacles for using mRNA as a therapeutic agent is the immune system. Immunogenicity and stability from the application to translation have so far been the major obstacles to be overcome in mRNA therapy research, especially for getting into clinical trials [8]. The innate immune system is trained by evolution to detect foreign nucleic acids and protect cells from those, to enter *via* pattern recognition of *i.e.* toll-like receptors (TLR). The activation of TLRs leads to production of mainly interferons and pro-inflammatory cytokines [9]. Furthermore, the existence of RNases in the blood stream and the cells hinder foreign mRNA from being translated, which is beneficial for health but a challenging task for therapeutic mRNA approaches [10]. Hence, the modification of single nucleosides was introduced which not only lowered the immune response but had the potential of increasing the translation potential. Chemical modifications like pseudouridine, 2-thiouridine (Scheme 1) or methyl-cytidine have proven to lower response by TLRs significantly [11].

By the incorporation of a certain ratio of chemical modifications to nucleosides without changing the protein encoding parts in mRNAs, the therapeutic window gets widened by lowering the immune system's ability to detect the product before it gets translated [6, 11, 12].

A



B



Scheme 1 - Exemplary modification scheme of A) uridine to B) 2-thio-uridine. By exchanging the oxygen with sulphur on position 2 of the phenyl group, the activation of the immune system is lowered [13].

## 1.2 cmRNA as a therapeutic tool

Chemically modified RNA has been of interest in clinical and non-clinical trials for the last years in several different research groups placed around the globe. Kormann *et al.* succeeded in the *in vivo* translation of erythropoietin (EPO) by cmRNA transfection and a subsequent substantial increase of hematocrit by a single intramuscular injection of EPO encoding cmRNA complexes in mice [6]. Another example would be the trials by Balmayor *et al.* where cmRNA encoding for bone morphogenic protein 2 (hBMP-2) was incorporated in scaffolds for bone defect filling. Here the authors could show that the internalization of cmRNA could even lead to faster bone growth [14]. Even in the delicate field of cardiology cmRNA technology was introduced as Abraham *et al.* showed that cmRNA containing stent coatings could potentially protect patients against angioplasty associated complications in atherosclerotic blood vessels [15]. These are just a few examples for fields in medicine where cmRNA could have a substantial impact in a near future. It also already hints at the potential of such nucleic acids to be used in a wide range of unrelated fields of applications.

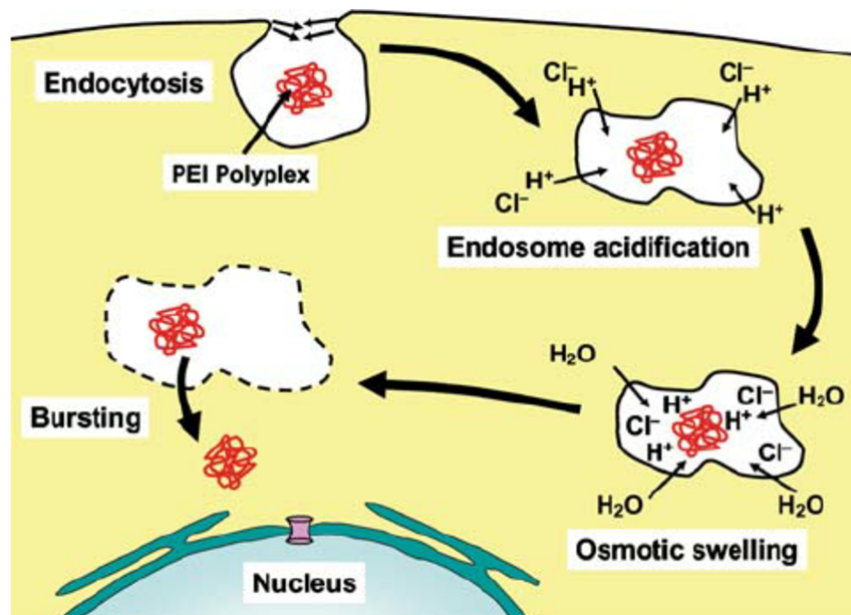
### 1.3 Challenges in nucleic acid delivery

As already mentioned nucleic acid delivery comes with certain challenges as the macromolecules need to be delivered to the interior of the target cell. In many cases, this task could not be overcome by non-viral vectors which led to employing viral vectors despite their enormous safety concerns [16, 17]. Furthermore, even though many different delivery agents have been developed over the last decades for an *in vitro* environment, an overwhelming majority of those agents lacked in efficiency in *in vivo* situations [18]. The most used carrier systems in nucleic acid delivery are cationic liposomes and polymers, as both families bind and complex nucleic acids *via* electrostatic interactions with negatively charged phosphodiester backbones [19].

### 1.4 Delivery systems for nucleic acids

Nucleic acids are considered robust macromolecules but the presence of nucleases *in vivo* and their poor cellular uptake imply the need for compacting agents which serve as a delivery mediator. Although there are some established physical delivery application routes like magnetofection [20] or the “gene gun” technology (gold particle bombardment) [21], chemical carrier systems like cationic lipids or polymers are often preferred. The requirements for an appropriate synthetic delivery system for nucleic acids in general are besides high functionality, the ability to compact the cargo, shield the negative charge and to transport the therapeutic agent to its target. Furthermore, as already mentioned, toxicity, immunogenicity and the potential to be repeatedly administered play major roles in the task to open the therapeutic window as wide as possible [22, 23]. Consequently, synthetic approaches which mimic viral features are desired in which functionality can be maintained while immune response and toxicity are reduced [4]. Understanding the pathway of nucleic acid delivery in general is crucial for the development of applicable delivery agents. The first hurdle is the plasma membrane, which is a barrier designed for lipophilic macromolecules, where the complex needs to bind to the cell surface before being internalized [24]. The pathway described mainly for polyplex- or lipoplex mediated cell uptake is endocytosis where extracellular macromolecules are internalized *via* vesicles which are basically pinched

off parts of the cell membrane (Scheme 2) [25]. The binding or docking to the cellular membrane can be achieved *via* unspecific charge interaction between carrier and extracellular matrix or ligand-receptor mediated binding. This pathway is common for mammalian cells and normally occurs for the internalization of essential nutrients, growth factors, antigens, and cholesterol-loaded lipoprotein for example. If a carrier successfully binds to receptors and the clathrin-coated vesicles (CCVs) are fused to endosomes, these have to be ruptured before being lysed or transported back to the cell membrane [26]. As the pH-level drops in endosomes, the carrier system's escape can be triggered by *i.e.* fusogenic lipids like DOPE which change their physiology pH-dependently and destabilize the endosomal membrane [27]. Furthermore, the so-called proton sponge effect was proposed especially for polymer-based carriers like polyethyleneimine (PEI) where the theory suggests that *i.e.* PEI gets protonated at lower pH levels, which triggers influx of ions like  $\text{Cl}^-$  in combination with water, which swells the endosome until it bursts. Once released from the endosome and detached from their complexing agent, nucleic acids can be translated in the cytosol or even transferred into the nucleus (DNA) [28].

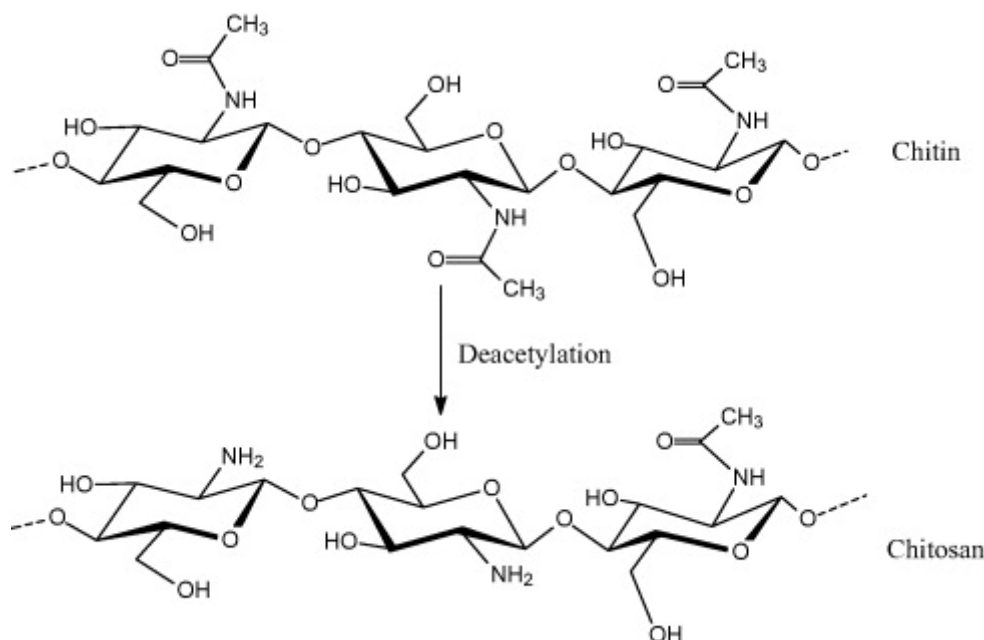


Scheme 2 – Transfection scheme for a PEI-nucleic acid complex. Cell uptake leads to encapsulation in the endosome which is followed by a pH-level drop. *Via* osmotic effects the endosome swells to a critical point where the endosome ruptures and releases the cargo [29].

### 1.4.1 Polyplexes in nucleic acid delivery

Polymer-based nucleic acid delivery has been investigated over the last 50 years. Cationic proteins which enhanced the infectivity of poliovirus RNA in the 1960s [30] or transfection complexes containing polyornithine and DNA which were first described in the 1970s [31] were the beginnings of exploiting the possibilities of cationic polymers. Over the years many different carrier systems based on this technology were introduced, including polymerosomes, polymer micelles, hydrogels and cationic polymers (polyplexes) [32]. All of these carrier systems form carrier families which have favorable application sites [33]. Pulmonary applications *i.e.* where surfactants play a major role extracellularly on the endothelial cells, provides an environment where liposome-mediated delivery is hindered [34]. Therefore, although lipoplex formulations tend to be more efficient *in vitro*, polymers as condensing agents are still relevant for several application routes *in vivo*. Furthermore, polymers used for nucleic acid transfection usually are able to condense their cargo more than lipid-based formulations which can lead to increased stability [24]. Generally, most of the polymers which have been successfully used in nucleic acid delivery bear free amines, which can be protonated in their structure. Prominent examples for polymer-based nucleic acid complexation agents are linear and branched PEI, polylysine, and biopolymers like chitosan or poly(lactic-co-glycolic acid) (PLGA) [33]. The transfection efficiency of polyplexes can be affected by the ratio of positive charges of the polymers, to negative charges of the nucleic acid's backbone (nitrogen (N)/phosphate (P) ratio) as positively charged complexes with free amines can interact with the anionic extracellular matrix. However, it was observed that an increasing amount of free cationic polymer leads to higher cytotoxicity which limits its applicability. These attributes lead to a specific therapeutic window which differs for each nucleic acid type and complexing polymer [35]. The endosomal escape or release of polymer-based transfection agents can additionally be enhanced by the addition of lysosomotropic agents like chloroquine, although in the case of PEI such agents are not needed as endosomal escape is triggered by the polymer itself. This may be due to their efficient endosomal escape *via* the controversially discussed proton-sponge effect [36]. Chitosan as a complexing agent for nucleic acid delivery has proven its validity in various cases especially where mucus barriers have to be crossed before cell uptake.

These application routes include nasal, intratracheal, pulmonary and even oral application for nucleic acid delivery. Its deacetylated backbone reveals primary amines in each monomer which is perfectly fitting to interact with the phosphate backbone of nucleic acids (chemical structures are shown in Scheme 3) [37-39].



**Scheme 3 - Deacetylation of chitin to chitosan leads to free primary amines which can be utilized for nucleic acid backbone binding [40].**

PLGA as a nanocarrier on its own for nucleic acids gathered some attention, as well, but low encapsulation and transfection efficiency made them unattractive for various applications [41]. However the combination of the chitosan's complexing capacity and biocompatibility paired with the colloidal stability contributed by PLGA made both polymers a highly promising choice for cmRNA complexation, as well [42].

### 1.4.2 Lipoplexes in nucleic acid delivery

Lipid mixes containing nucleic acids are commonly denominated as lipoplexes where cationic lipids serve as the complexing agent. These lipids usually have a polar head group and one or various hydrophilic alkyl moieties. This surfactant-like structure forms molecules to carrier-vesicles in which the hydrophilic cargo can be entrapped [24]. The use of cationic lipids in transcript therapy goes back to researchers like Felgner [43] or

Wu [44] in the mid-1980s and have been one of the most favorable delivery agents for nucleic acids ever since. Similar to polyplexes the cationic lipid binds to the negatively charged nucleic acid backbone but it hardly ever is formulated alone. Helper lipids like *i.e.* dioleoylphosphatidylethanolamine (DOPE) are needed to enhance endosomal escape. It could be shown that DOPE is able to fuse with other lipids when pH levels are dropping, just as it is happening in the endosome [27]. In this environment DOPE can adopt hexagonal structures that disturb the endosomal membrane which among other factors like the buffering capacity of the lipoplex, enhances the endosomal escape [45]. Also, the trans-bilayer flip-flop of negatively charged phospholipids can detach the nucleic acid from the cationic lipids and release the cargo into the cytosol [46]. Recent investigations about the mechanisms concerning the endosomal escape showed that buffering capacity of the cationic lipid in the pH level area of the endosome plays a major role in functionality of lipo- or polyplexes, as well [47].

Furthermore cholesterol is used to enhance lipoplex structure stability in physiological fluids [48] and to enhance binding to the extracellular matrix *via* scavenger receptors [49]. The particle's charge mainly determines the size as neutral particles tend to agglomerate due to hydrophobic interactions. On the contrary, highly negatively- or positively charged particles exhibit small mean hydrodynamic diameters. To enhance interaction with the extracellular matrix positively charged lipoplexes are needed but the necessary charge for cell attachment also increases unspecific binding and therefore limits the use in systemic administration [50]. Especially unspecific binding to negatively charged substances in the serum may lead to aggregation and subsequently clearance. A common strategy to overcome this is PEGylation. polyethylenglycol (PEG) bearing lipids can form a hydrophobic shielding layer on the surface of lipoplexes [51]. The composition of lipid mixes for nucleic acid delivery therefore requires fine-tuning for each and every application for each cargo [52].

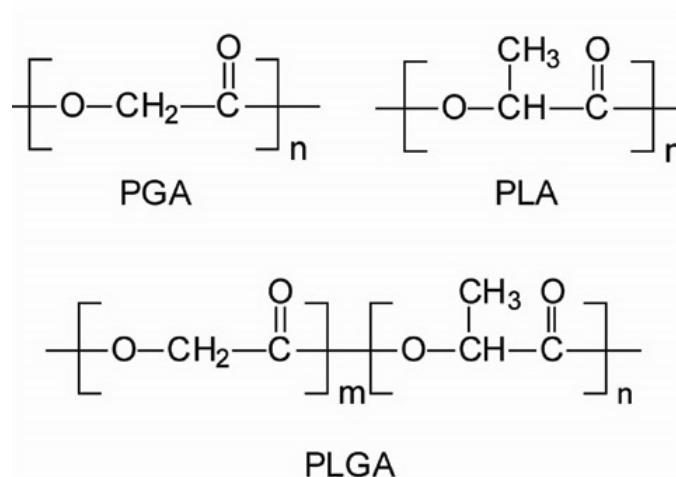
### 1.4.3 Scaffolds for nano-carrier systems

Tissue engineering is defined as “the application of the principles and methods of engineering and life sciences toward the fundamental understanding of structure-function relationships in normal and pathological mammalian tissues and the development of biological substitutes that restore, maintain, or improve tissue function” [53]. The marriage of biosciences, engineering and clinical application synergistically has the goal to enhance grafts which are supposed to substitute tissues and organs. Scaffolds and grafts to replace skin, cartilage or bone tissue have already been successfully applied in clinical trials but structures like nerves, muscles, intestine or even blood vessels are desired, as well [54]. The combination of tissue engineering and transcript therapy could therefore be a powerful synthesis as surrounding cells around a graft or implant could be induced to differentiate to enhance tissue growth and scaffold replacement. Furthermore, such bio-functional implants have the potential to lower costs of therapy due to lower rehabilitation times.

There are two types of scaffolds designed to incorporate nucleic acids. They are either designed to release the nucleic acid complexes at site after implantation or to keep the cargo on the surface of the graft [55]. Additionally scaffolds have been created which carry transfected progenitor cells into the implants' surrounding areas which potentially regenerates lost tissue [56]. Hence, the approach of combining nucleic acid delivery with the possibility to load nanocarriers or already transfected cells to specific sites, where protein production of any kind could be enhanced, can be combined with the ability of the tissue graft to physically support and template new tissue formation [57]. One example for a tissue engineering product which could be functionalized by nucleic acid complexes is injectable calcium phosphate cements. Those present a promising alternative to polymer based bone filling products because of their similarity to endogenous bone and high biocompatibility [58].

## 1.5 Poly (lactic-co-glycolic acid) (PLGA)

The copolymer poly(lactic-co-glycolic acid) or PLGA is one of the most investigated and versatile polymers in biomedical engineering mainly because of its biocompatibility and adjustable biodegradability *in vivo*. The versatility of the polymer is displayed best in the variety of its usage. In Scheme 4 the chemical structures of both monomers and the polymer is displayed.



**Scheme 4 – Chemical structure of poly(lactic-co-glycolic acid) (PLGA) co-block polymer and its pure constituents poly(glycolic-acid) (PGA) and poly(lactic-acid) (PLA) [59].**

PLGA coatings, nano- or microparticles, implants or even as surgical thread are only a few examples where the intrinsic features of PLGA is beneficial [60-62]. Physicochemical features like biodegradation velocity or hydrophobicity can be adjusted by the molecular weight, the ratio of glycolic- to lactic acid monomers and by the choice of head-groups on the polymer ends. If used as a carrier device, release kinetics is substantially influenced by the pH-level of surrounding fluids, drug type and the method PLGA is being processed [63, 64]. For pharmaceutical purposes the main topic of interest is the adjustability of drug release profiles. Depending on the hydrophobicity and the choice of PLGA composition, there are generally three distinguished release profiles which all have their appropriate field of application. In Fig. 1 A, three characteristic release profiles are shown where drug release can exhibit one or multiple phases. Type I shows a steady and monophasic release behavior in contrast to Type II where an initial burst is schematically displayed, followed by a saturation plateau. Type III displays a triphasic profile where an initial burst is followed

by a steady slow release until polymer erosion onset leads to a second burst. A burst release can be caused by particle swelling, crack formation or the hydration of drug particles on the surface of the polymer matrix. This is substantially influenced by the solubility of the drug as can be depicted from Fig. 1 B. Hence, hydrophilic drugs which get hydrated much easier than hydrophobic ones get released initially in a more prominent and faster way [65]. Furthermore, the velocity of this process can be influenced by the molecular weight of PLGA as small chains increase diffusion. The slow release phases which can occur between burst releases are mainly driven by drug diffusion out of the polymer matrix. In this phase the velocity is highly dependent on the density and porosity of the polymer matrix. Also drug-polymer and drug-drug interactions can be decisive [61].

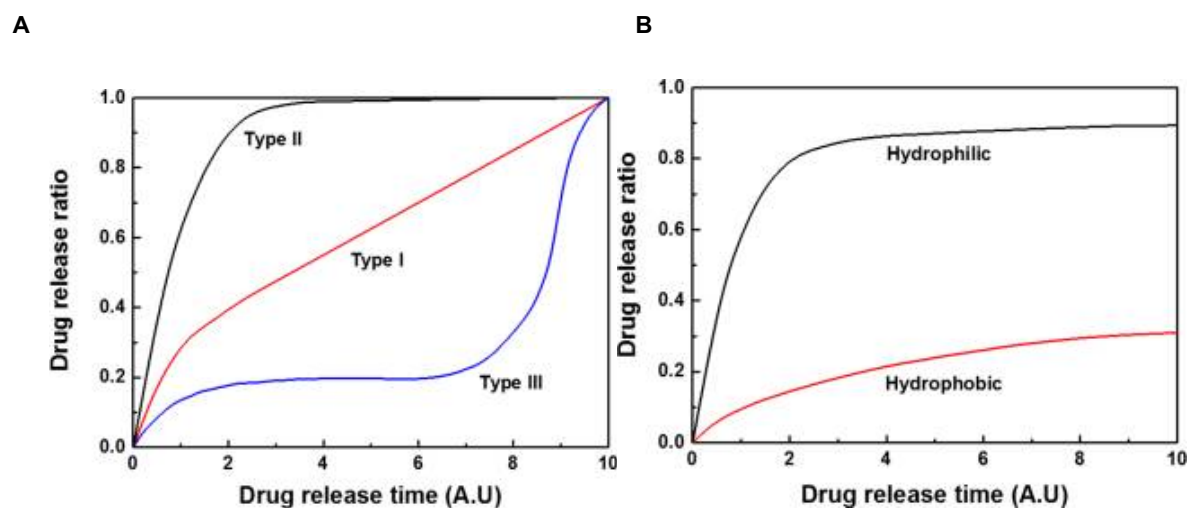
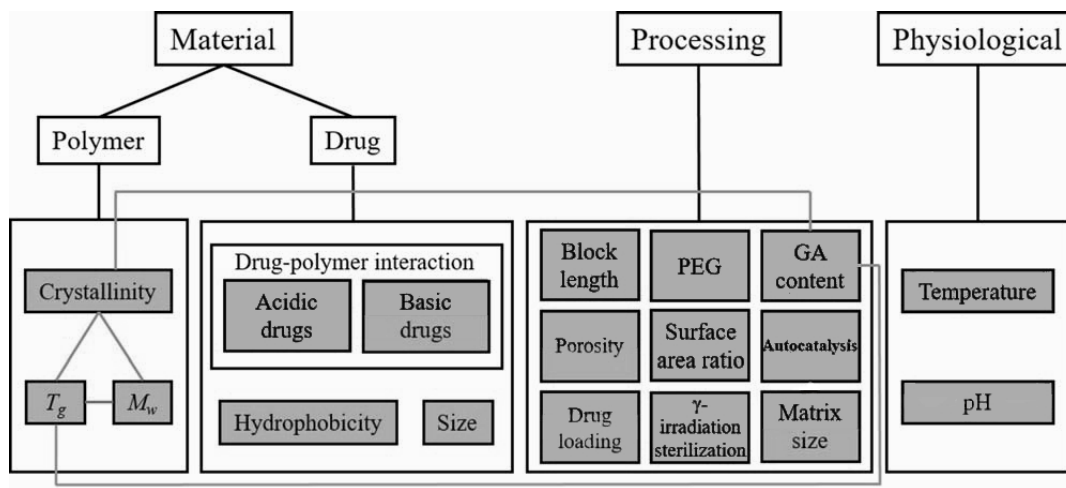


**Fig. 1 A):** Typical release profiles for different drug/polymer compositions in PLGA drug release kinetics. **B) Typical burst release drug release profiles of hydrophilic and hydrophobic drugs out of PLGA carriers. (A.U. was used as an arbitrary unit used for drug release time) [63].**

Crystallinity of PLGA is another factor which defines the degradation and drug release. Lower crystallinity generally improves faster drug release especially if diffusion is the main release type at hand. The composition of lactic acid (LA) to glycolic acid (GA) and the choice of LA isomer determine whether the copolymer turns out amorphous or semi-crystalline [66]. Hydrophobicity is another feature which can be easily adjusted by the ratio of LA to GA, because of the methyl group which is incorporated in the LA monomer [63].

To summarize, PLGA can be viewed as a chemical “construction kit” which can be formed for specified needs in drug delivery. All the various modification possibilities

like molecular weight or monomer block ratios can be chosen individually for each drug and application route. An overview with all the modification options for PLGA production is displayed in Scheme 5. This, and the fact that many medical products and carrier systems made of PLGA are approved by the FDA make the polymer to one of the most used carrier matrix agents nowadays [60, 61, 63, 64].



**Scheme 5 - Summary of all the set screws which can be altered for individual polymer matrix production for each drug and application route [63].**

## 1.6 Aim of the thesis

Successful expression of proteins derived from applied nucleic acids without activating the immune system is today as much a challenge as it has been in the first successful transfection trials *in vivo* made by Wolff *et al.* in 1990 [67]. Nowadays, the modification of nucleic acids complexing agents, has been extensively studied and improved to better reach this goal. To this day very few products based on this technology survive clinical trial testing because of their lack in functionality or limits-exceeding toxicity and immunogenicity [68, 69]. Especially the field of chemically modified mRNA delivery for protein production *in vivo* provides a rather new and promising approach of transcript therapy, with all its challenges in terms of complexation, specific cell targeting, cell uptake, endosomal escape and translation in the cytosol [70]. The task at hand for this thesis was not only to develop alternative complexing agents for the direct delivery of cmRNA but also to find strategies which enhance already established delivery systems by the help of tissue engineering techniques. The common basis for all the efforts here

has been the biocompatible polymer poly (lactic-co-glycolic acid). This work is divided in two main projects which contributed to this thesis.

Aim of the first project was the development, analysis and optimization of an intermediate phase which allows the incorporation and release of cmRNA comprising lipoplexes into calcium phosphate cements (CPC). Injectable CPCs are self-hardening cements, which have been in clinical use for the last years and have the potential to replace polymethylmethacrylate (PMMA) bone fillings in applications like kyphoplasty or vertebroplasty [71-75]. Due to the similarity to the ceramic phase of endogenous bone, hydroxyapatite and calcium phosphate mixtures comprise a substantially better biocompatibility than PMMA, but the relatively long periods of biodegradation hinder fast cell-ingrowth and the replacement of such implants by endogenous bone. Hence, to imitate natural bone, fiber or microparticle-based calcium phosphate composites have been of interest to enhance mechanical elasticity and to decrease degradation times significantly. PLGA- based microparticles mixed to these injectable cements are just one possibility to enhance these products for a faster degradation *in vivo* [58, 76, 77]. In this project, the possibility of encapsulating cmRNA bearing lipoplexes into such microparticles for a fast release of lipoplex after contact with physiological media was desired. First, the incorporation procedure of lipoplexes into such PLGA-based microparticles was developed and optimized for initial lipoplex release, leading to immediate transfection efficiency *in vitro*. After the development and investigation of the standard operating procedure for microparticle formation the microparticles were incorporated into calcium phosphate cements and tested *in vitro* for their transfection potential as part of a composite structure.

The aim of the second project was to find a cmRNA complexation agent and delivery system for potential applications to tissue types where mucus is present. Deacetylated chitin or chitosan is well known for its advantageous properties in crossing mucus barriers and is able to complex other nucleic acids, like siRNA or DNA, because of primary amine groups on the polymer backbone [38, 41, 42, 78]. Hence, the idea was to establish and develop a chitosan-based cmRNA complex as a functional polyplex for cell transfection. Here, a thorough analysis of chitosan/cmRNA polyplexes in terms of physicochemical properties, biocompatibility and transfection efficiency *in vitro* was planned and performed. Due to lacking colloidal stability of chitosan-based nanoparticles, the next step in polyplex development and optimization for transfection

efficiency *in vitro* was a co-formulation process with PLGA. PLGA polymers in nanoparticles are known to increase polyplexes' capacity to compact the cargo for the prevention of premature degradation in physiological conditions and furthermore enhance the colloidal stability of such systems [79, 80]. After the optimization of the co-formulation process a comparison of chitosan- and co-formulated PLGA/chitosan polyplexes was performed. Features like of physicochemistry, colloidal stability in physiological simulations, transfection efficiency and cytotoxicity on mouse fibroblasts were analyzed for their potential of being a potential candidate for future *in vivo* testing.

## 2 Materials and methods

In the following chapter all chemicals, devices and methods, which were used for both projects, are listed and described.

### 2.1 Materials

#### 2.1.1 Chemicals - microparticle project

##### *Lipoplex formation:*

Ethanol, HPLC grade	Carl Roth, Karlsruhe, Germany
C12-(2-3-2)	Ethris, Planegg, Germany
1,2-dioleoyl-sn-glycero-3-phos-phoethanolamine	Avanti Polar Lipids, Alabastar, USA
1-palmitoyl-2-[11-(dipyrrometheneboron difluoride)-undecanoyl]-sn-glycero-3-phosphoethanolamine	Avanti Polar Lipids, Alabastar, USA
Plant derived cholesterol	Avanti Polar Lipids, Alabastar, USA
1,2-Dimyristoyl-sn-glycerol, methoxypolyethylene Glycol	NOF America, White Plains, USA
Water for injection	B.Braun, Melsungen, Germany
Citric acid ≥ 99,5 %	Carl Roth, Karlsruhe, Germany
Sodium chloride ≥ 99,5 %	Carl Roth, Karlsruhe, Germany
Sodium hydroxide solution 5N	Carl Roth, Karlsruhe, Germany

##### *Microparticle formation:*

Resomer® RG 750 S	Evonik, Darmstadt, Germany
Resomer® RG 752 S	Evonik, Darmstadt, Germany
Resomer® RG 755 S	Evonik, Darmstadt, Germany
Resomer® RG 858 S	Evonik, Darmstadt, Germany
Resomer® RG 502 H	Evonik, Darmstadt, Germany
Resomer® RG 503 H	Evonik, Darmstadt, Germany
Resomer® RG 504 H	Evonik, Darmstadt, Germany
Dichloromethane, for peptide synthesis	Carl Roth, Karlsruhe, Germany
Poly (vinyl alcohol) 31.500-50.000 Mw	Sigma Aldrich, St. Louis, USA
Phosphate saline buffer (1x)	Gibco, Eggenstein, Germany

##### *Microparticle Analysis:*

Heparin sodium salt from porcine mucosa	Sigma Aldrich, St. Louis, USA
Dimethylsulfoxide, BioScience grade	Carl Roth, Karlsruhe, Germany
Coelenterazine, native ≥ 95 %	Synchem, Grove Village, USA
Methanol, HPLC grade	Carl Roth, Karlsruhe, Germany

*Ceramic/polymer composition:*

Calcibon® paste BioMet, Munich, Germany

*Cell Culture:*

Dulbecco's modified eagle medium GlutaMax, Low Glucose Gibco, Eggenstein, Germany

Trypsin-EDTA (0,05%), phenol red Gibco, Eggenstein, Germany

Accutase Cell Detachment Solution Gibco, Eggenstein, Germany

Phosphate saline buffer (1x) Gibco, Eggenstein, Germany

Penicillin-Streptomycin (10000 U/ml) Gibco, Eggenstein, Germany

Fetal Bovine Serum, qualified, E.U.-approved Gibco, Eggenstein, Germany

*cmRNA (encoding proteins):*

*Metridia Luciferase* Ethris, Planegg, Germany

*Firefly Luciferase* Ethris, Planegg, Germany

Erythropoietin Ethris, Planegg, Germany

Green Fluorescent protein Ethris, Planegg, Germany

Td Tomato Ethris, Planegg, Germany

*Dyes:*

Label IT® TM-Rhodamine Labeling Kit (Mirus Bio, Madison, USA)

*Water:*

Water for injection B.Braun, Melsungen, Germany

Aqua bidest. Kerndl, Weissenfeld, Germany

**2.1.2 Chemicals - nanoparticle project**

*Polymers for particle formation:*

Protasan UP CL 113, Mw <150 kDa FMC BioPolymer AS, Oslo, Norway

Polyethylenimine, branched 25.000 Mw Sigma Aldrich, St. Louis, USA

*Poly (lactic-co-glycolic acid) (PLGA):*

Resomer® RG 750 S Evonik, Darmstadt, Germany

Resomer® RG 502 H Evonik, Darmstadt, Germany

Resomer® RG 858 S Evonik, Darmstadt, Germany

*Surfactants:*

Poly (vinyl alcohol) 31.500-50.000 Mw Sigma Aldrich, St. Louis, USA

Poly (vinyl alcohol) 9.000-10.000 Mw Sigma Aldrich, St. Louis, USA

*Organic solvents:*

Dichloromethane, for peptide synthesis Carl Roth, Karlsruhe, Germany

Ethyl acetate Sigma Aldrich, St. Louis, USA

*Gel electrophoresis:*

Agarose Standard	Carl Roth, Karlsruhe, Germany
TRIS-acetate-ethylenediaminetetraacetic acid (EDTA)	Carl Roth, Karlsruhe, Germany
peqGREEN®, RNA/DNA dye	VWR, Pennsylvania, USA

*Cell Culture:*

Dulbecco's modified eagle medium GlutaMax, Low Glucose	Gibco, Eggenstein, Germany
Trypsin-EDTA (0,05%), phenol red	Gibco, Eggenstein, Germany
Phosphate saline buffer (1x)	Gibco, Eggenstein, Germany
Penicillin-Streptomycin (10000 U/ml)	Gibco, Eggenstein, Germany
Fetal Bovine Serum, qualified, E.U.-approved	Gibco, Eggenstein, Germany

*Cytotoxicity assay*

3-(4,5-Dimethylthiazol-2-yl)-2,5-diphenyltetrazoliumbromid (MTT)	Trevigen, Gaithersburg, Germany
$\alpha$ -D(+)-Glucose Monohydrat	Carl Roth, Karlsruhe, Germany
Triton® X-100	Carl Roth, Karlsruhe, Germany
2-Propanol, HPLC grade	Carl Roth, Karlsruhe, Germany
Hydrochloric acid, 1N	Carl Roth, Karlsruhe, Germany
Phosphate saline buffer (1x)	Gibco, Eggenstein, Germany

*cmRNA (encoding proteins):*

<i>Metridia Luciferase</i>	Ethris, Planegg, Germany
<i>Firefly Luciferase</i>	Ethris, Planegg, Germany
Green Fluorescent protein	Ethris, Planegg, Germany

*Dyes:*

RNA Gel Loading Dye	Thermo Fisher, Waltham, USA
DBCO-Sulfo Cyanin 3	Jena Biosciences, Jena, Germany
DBCO-Sulfo Cyanin 5	Jena Biosciences, Jena, Germany

*In Vivo test:*

D-Luciferin sodium salt	Synchem, Grove Village, USA
-------------------------	-----------------------------

*Water:*

Water for injection	B.Braun, Melsungen, Germany
Aqua bidest.	Kerndl, Weissenfeld, Germany

## 2.2 Methods – general protocols

Some of the analysis methods conducted in this thesis were both used in the nanoparticle and microparticle projects. Those general methods are described in the next chapter.

### 2.2.1 Measurement of nanoparticle size

Nanoparticle dispersions were measured by dynamic light scattering method (DLS) *via* a Zetasizer Nano ZS (Malvern, Worcestershire, United Kingdom). Here, a cumulant mean or Z-average size is defined as the harmonic intensity averaged particle diameter and certified under ISO 13321/ ISO 22412. This parameter is a hydrodynamic value and therefore only applicable to particles in dispersion or solution. Cumulants analysis results in a mean size value and a polydispersity index which is dimensionless and provides information about the homogeneity in size of the particles in dispersion [81]. For every measurement the refractive index was adjusted to each solvent, the particles were synthesized in. 100  $\mu\text{l}$  of dispersion was measured in a disposable cuvette in triplicates with at least 10 measurements, each. For each measurement particle dispersion concentrations of at least 10  $\mu\text{g cmRNA/ml}$  were used.

### 2.2.2 Measurement of nanoparticle zeta potential

Particles were analyzed for their surface charge *via* Zetasizer Nano ZS (2.2.1), as well. The Zeta potential in mV is defined as the potential at the boundary of particles dispersed in a fluid and gives insight into colloidal stability *via* ionic repulsion. The higher a particle is charged the faster those particles will repulse themselves from each other which can be measured *via* light scattering of a set laser beam. The electrophoretic mobility when a certain electric field is applied to the dispersion is proportional to certain frequencies, detected by light scattering and can therefore be recalculated to a surface charge or Zeta potential [82]. For every measurement 750  $\mu\text{l}$  of particle dispersion were added to a special reusable cuvette where electrodes were attached on the sides to apply the electric current for measurement. Every sample was

conducted in triplicates with at least 10 measurements, each. As for size measurements particle dispersion concentrations of at least 10  $\mu\text{g cmRNA/ml}$  were used.

### **2.2.3 Cell culture**

In the two projects depicted here, three different cell lines for *in vitro* assays of various kinds were used. The pre-screening for microparticle synthesis analysis was completely done with rat derived bone marrow stem cells (rBMSCs), the general bio-functionality and cytotoxicity tests for both nano- and microparticles were conducted on mouse fibroblasts (NIH3T3) and the composite calcium phosphate/PLGA bio-functionality tests were done on (C2C12) mouse myoblasts with the potential for differentiation to osteoblasts [83]. All of those cell lines were cultivated with the same media and conditions:

After thawing frozen cell (in DMSO) vials from an in-house cell bank, cells were cultivated in Dulbeccos's modified eagle medium (DMEM) containing 10 % fetal bovine serum (FBS) and 1 % Penicillin/Streptomycin (Pen/Strep). After confluency was reached the cells were washed with PBS and subsequently trypsinated (accutase treatment for rBMSCs) and passaged up to 20 times for *in vitro* assays. Cell counting was done by an automated cell counter (Countess II, Thermo Fisher Scientific, Waltham, USA) and seeding into standardized 96, 48 and 24 well plates (Corning, New York, USA).

### **2.2.4 Scanning electron microscopy**

For the visualization of nanoparticle- and microparticle surfaces and their subsequent analysis a Scanning electron microscope (SEM) (Zeiss-Leo DSM 982 Gemini, FELMI-ZFE, Graz, Austria) was utilized. Images were taken at a chamber current of 5 kV. Sputtering was done with a mixture of 60/40 gold/palladium by a sputter coater (Edwards S150B, HHV Ltd, West Sussex, UK) for 1 min at 40 W and 7.5 mbar. Nanoparticles were analyzed without sputtering at the same conditions.

---

## 2.3 Methods - microparticle project

### 2.3.1 Lipoplex formation

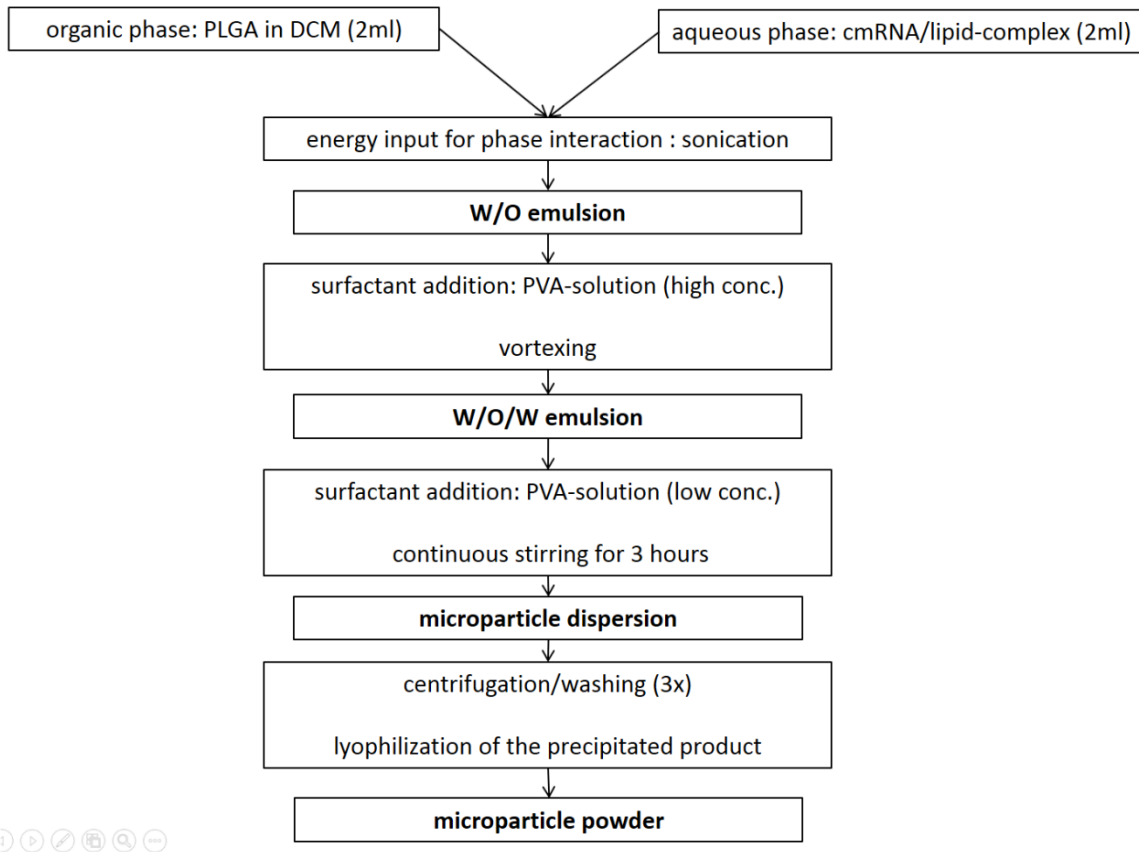
Nano-sized lipoplexes were prepared by a simplified method as described in Jarzebinska *et al.* [47]. In brief, an ethanol phase containing the oligoalkylamine N,N'-Bis(2-aminoethyl)-1,3-propanediamine modified with C12 alkylchains (C12-(2-3-2), (1,2-dioleoyl-sn-glycero-3-phos-phoethanolamine (DOPE), plant derived cholesterol and 1,2-dimyristoyl-sn-glycerol methoxypolyethylene glycol (DMG-PEG-2k) at molar ratios of 8/5.29/4.41/0.88, was complexed with cmRNA (dissolved in a 10 mM citrate/150mM sodium chloride buffer solution; pH 4.5) by a solvent exchange method in a volume to volume ratio of 0.2 ethanol to aqueous phase. Both phases were equilibrated for 10 min, before the ethanol phase was injected into the water phase using an insulin syringe with subsequent vortexing for 15 s. The subsequent nanoparticle dispersion was equilibrated for 30 min at room temperature before it was ready to use. The final concentration of cmRNA was 0.2 mg/ml at an N/P (nitrogen to phosphate) ratio of 17. Lipoplex dispersion were stored at 4 °C and could be used for at least four weeks without significant loss of functionality.

### 2.3.2 Fluorescence labelling for fluorescence microscopy

cmRNA was labelled by two different routes in this study. First of all, cmRNA coding for erythropoietin (EPO) was labelled with a TM-Rhodamine dye for detection by fluorescence microscopy. The dye consists of a fluorophore connected to a linker unit which is responsible for electrostatic interaction with the nucleic acids and a reactive alkylating group which covalently attaches to heteroatoms in the RNA strands [84]. Labelling was conducted with a ready-to-use label-IT<sup>®</sup> TM-Rhodamine dye (Mirus Bio, Madison, USA) as recommended by the manufacturer. 50 µg of EPO cmRNA were treated and a theoretical coupling of 7.85 labels per nucleic acid was calculated. cmRNA was detected *via* a fluorescence microscope (Leica DMI8) with an external laser source for excitation (Leica EL 6000). TM-Rhodamine has its excitation maximum at 546 nm and emits best at 576nm.

### 2.3.3 Microparticle formation

PLGA microparticles were synthesized by an adjusted water/oil/water solution double emulsion solvent evaporation technique [85-87]. An outline of the procedure can be seen in Scheme 6. An organic phase was prepared by dissolving PLGA in 2 ml dichloromethane (DCM). The first aqueous solution consisted of freshly prepared lipoplex dispersion (0.2 mg cmRNA/ml), diluted with PBS to a total volume of 2 ml. The aqueous phase in particle formations where no lipoplexes were encapsulated consisted of 2 ml PBS. The lipoplex dispersion was dispensed dropwise into the organic phase and the mixture was sonicated by an ultrasonic probe (Branson Digital Sonifier 250-D, Dansbury, USA) for varying pulse lengths and at different sonication intensities. The resulting emulsion was subsequently given dropwise into a second aqueous solution consisting of 6 ml 4 % poly (vinyl alcohol) (PVA) (30-55kD) in water. This emulsion was vigorously vortexed for at least 10 s and added dropwise to a second PVA solution in water (8 ml; 1 % PVA) while mixing on a magnetic stirrer. After the organic solvent evaporated completely (emulsion turned from milky to slightly transparent), the resulting microparticle dispersion was centrifuged at 3000 x g and washed three times with water. After resuspension with 5 ml of water the particles were snap-frozen in liquid nitrogen and lyophilized (Christ Alpha 2-4; Osterode am Harz, Germany) overnight. The dry powder was weighed to determine the yield and stored at -20 °C.



**Scheme 6 - Schematic representation of the PLGA microparticle preparation process. A water-in-oil-in water emulsion solvent evaporation technique was used for the synthesis of encapsulating lipoplexes in the polymer matrix**

### 2.3.4 Measurement of microparticle size

For the measurement of mean diameter and standard deviation of the PLGA microparticles, powders were suspended in water and investigated under the light microscope (Carl Zeiss, Axiovert 25, Jena, Germany) on a standard glass microscope slide. Three images at different fractions of the slide were captured at a magnification of 10 by a microscope camera (Carl Zeiss, AxioCam ERc 5s, Jena, Germany) (Fig. 2). A macroinstruction programmed for ImageJ was used to convert the image to a binary state (Fig. 3). Particles were subsequently counted and measured for particle areas, ferrets and amounts of particles (Fig. 4). From this data set the mean diameter, and its deviation for one microparticle batch was determined in triplicates. A copy of the macroinstruction can be found in the appendix (7.3)

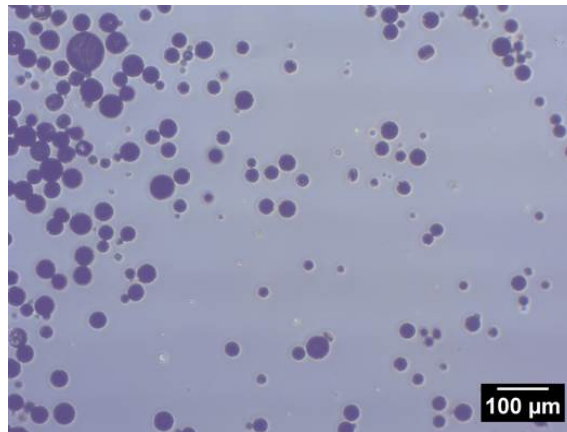


Fig. 2 – Exemplary image of PLGA microparticles taken by light microscopy at a magnification of 10

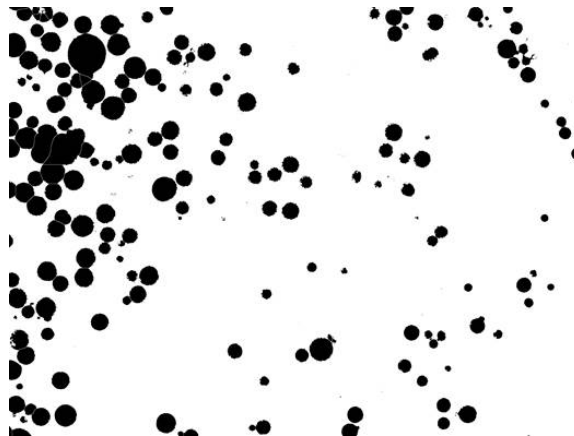


Fig. 3 - Binary image of Fig. 2 after image post processing by ImageJ. Microparticles are indicated in black color

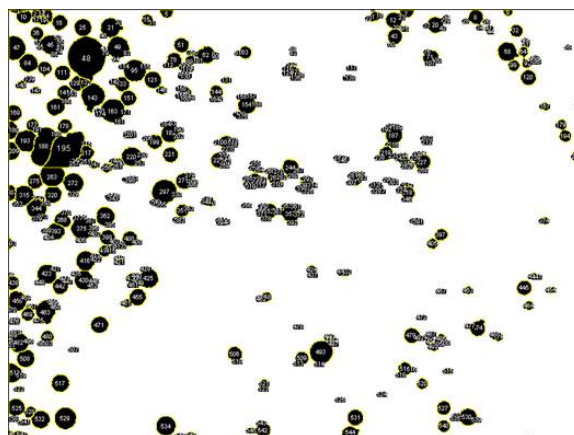


Fig. 4 - post processed image of Fig. 3. Particle analysis *via* particle detection with programmed criteria. Only particles with a round shape and certain size were detected and analyzed

### 2.3.5 cmRNA quantification protocol in microparticles

To determine how much cmRNA was encapsulated in how much microparticle polymer the PLGA matrix had to be dissolved first without destroying the cargo. Microparticle dissolving was achieved by dimethyl sulfoxide (DMSO) addition and shaking. Depending on size and porosity of the microparticles the time for dissolving deviated from a few seconds to 2 h while shaking on a Thermomixer (Eppendorf ThermoMixer® 5436, Hamburg, Germany) at room temperature. cmRNA displacement from the lipoplexes dissolved in DMSO was done by the addition of heparin sodium salt from porcine mucosa. As the salt is not soluble in DMSO, it was dissolved in water prior to mixing with DMSO in a concentration of 10 mg/ml. Water to DMSO ratio was 3/7. cmRNA displacement *via* heparin interaction with the cationic lipids was done at 70°C and shaking at 7000 rpm on a Thermomixer. Encapsulation efficiency of cmRNA in microparticles could be subsequently measured by Quant-iT RiboGreen® Assay. Nucleic acids react with the dye which leads to a shift in its emission behavior. This was quantitatively detected by a multilabel plate reader (Wallac Victor, Perkin-Elmer Life Sciences, Waltham, USA) at an excitation/emission maximum of 500/525 nm.

### 2.3.6 Surface topology investigation

Particle powders were attached on a graphene sheet and coated with gold and palladium at a ratio of 60/40 with a sputter coater (Edwards sputter coater S150B, HHV Ltd., West Sussex, UK) for 1 min at 40 W and 7.5 mbar. The sputtered particles were subsequently scanned by a Zeiss-Leo DSM982 Gemini (FELMI-ZFE, Graz, Austria) scanning electron microscope at 5 kV and investigated by ImageJ (Fig. 5). A macroinstruction (appendix 7.3) programmed for ImageJ was used to analyze the porous areas divided by the total surface area on the microparticles. Here, well defined particle surface areas with low differences in brightness were chosen manually for further examination. Those areas were defined as indicated in Fig. 6. These areas were converted into a binary state, in which the black pore areas could be quantified and divided by the total area which is visible on the raw data images. This form of measurement is an artificial quantification of surface pore areas which does not reflect any 3-dimensional porosity volume values. A quotient of black to grey areas from the

raw data images (Fig. 5) was calculated as a dimensionless measure of porosity (Fig. 7). Three images of each batch of microparticles were investigated to obtain a mean value and standard deviation of detected pore areas divided by total surface areas.

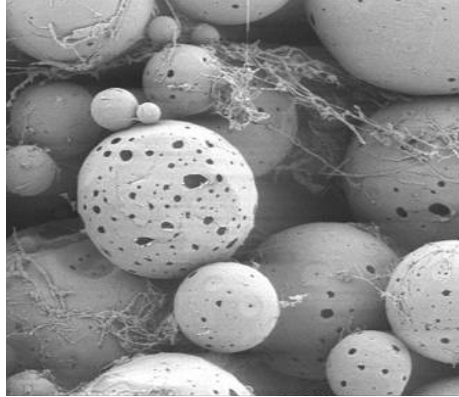


**Fig. 5 - Exemplary images of PLGA microparticles taken by scanning electron microscopy at a magnification of 1000.**

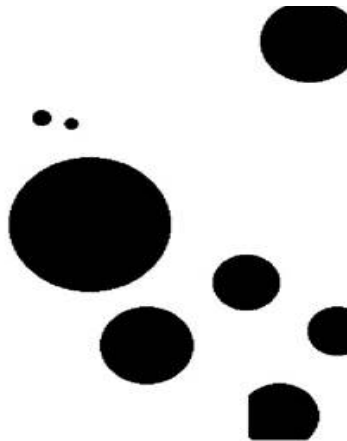


**Fig. 6 - selected areas of Fig. 5 where smooth surface area is distinguishable with pore areas.**

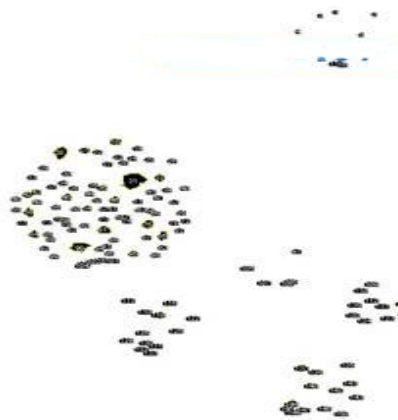


**Fig. 7 - pore area quantification in the areas detected in Fig. 5**

### 2.3.7 *In vitro* transfection efficiency

The expression of the cmRNA encoded protein (*metridia luciferase*) after transfection of murine fibroblasts/myoblasts was used to determine lipoplex efficiency and functionality after release from the microparticle matrix [88]. Cells were cultivated in Dulbecco's modified eagle medium (DMEM-GlutaMax Low Glucose) containing 10 % fetal bovine serum (FBS), 1 % Penicillin/Streptomycin (Pen/Strep) and were freshly trypsinated before seeding onto 24/48-well plates at a density of 50000/30000 cells/well with 500/250  $\mu$ l, respectively. Microparticles were subsequently added to the cell/medium mix at various dosages of cmRNA on a defined number of cells before cell adhesion. In CPC/PLGA composite trials a dosage of 20 pg cmRNA/cell was used. After the addition of coelenterazine buffer, containing a 50 mM PBS-buffer (pH 7.0) to 100  $\mu$ l of the supernatants, collected 24, 48, 72 and 96 h after transfection, luminescence was measured in triplicates using a luminescence reader (Wallac Victor, Perkin-Elmer Life Sciences, Waltham, USA). Most of the microparticles adhered to the cell monolayer after 24 h which enabled simple medium exchange after supernatant investigation. Hence, the protein production between each time point of measurement was investigated independently.

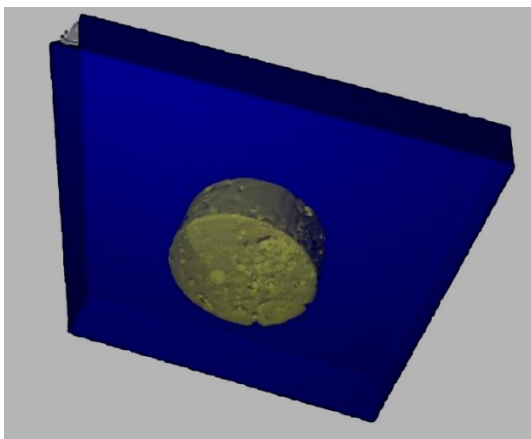
### 2.3.8 Composite mixing with bone substitute materials

Polymer/cement composites were prepared by direct mixing of powders in weight-to-weight (w/w) ratios from 100:0, 90:10, 80:20 to 70:30 Calcibon<sup>®</sup> (BioMet, Munich, Germany) to PLGA microparticles after freeze drying. The powders were mixed *via* a dental shaker for 30 s to obtain a homogeneous product. Curing was initiated by disodium hydrogen phosphate ( $\text{Na}_2\text{HPO}_4$ , 2.5 mg/ml) which was delivered with the Calcibon<sup>®</sup> powder as a ready-to-use kit. All the specimens were cured with a powder to liquid ratio of 2.5 % (w/v) and the mixture was prepared as recommended by the distributor. For transfection, powder mixes were prepared directly in a 48-well plate and shaped by a spatula where approximately half of the well bottom was covered with the hardened composite and the other half kept free for cell attachment. For the  $\mu$ -CT investigation the powders were cured and formed to cylindrical shapes.

### 2.3.9 $\mu$ -CT analysis of composites

Composite specimens were analyzed by a non-invasive 3D CT examination (CT  $\mu$ 40; Scanco Medical AG, Bassersdorf, Switzerland). The increment was set to 157  $\mu\text{m}$  with an angle of  $0^\circ$ . Scanning was done at an isotropic voxel size of 10  $\mu\text{m}$  (55kVp, 145 mA; ICT 40). The voxel size of the images was set to 8000  $\mu\text{m}$  with a total number of 500 slices. The integration time of the beam was set to a maximum of 300 ms and two data sets for each slice were recorded. The raw data was processed by ImageJ/BoneJ [89]. Each specimen was examined as a whole and a fraction in the sample was chosen randomly for density comparisons by ImageJ. Virtual discs of a diameter of 2 mm and 99 slices were analyzed (Fig. 8 A). The greyscale threshold to distinguish between dense and high-crystalline cement phases and low-crystalline/density phases were determined individually for each specimen. In Fig. 47 (supplementary information) a schematic description of the analysis is depicted. A triplicate of greyscale measurements at areas outside of the composites in a  $\mu$ -CT slide was done to determine the threshold for the high-density cement phase. The maximum level of the greyscale (100 % white) inside the composites was defined as the upper limit of the high-density cement phase. Volume to volume ratios of CPC/PLGA composites were calculated and illustrated *via* a greyscale threshold method. Due to substantial density differences between polymer and cement phase, the threshold could be set manually. The cement phase could be qualitatively identified as red pixels (Fig. 8 B).

A



B

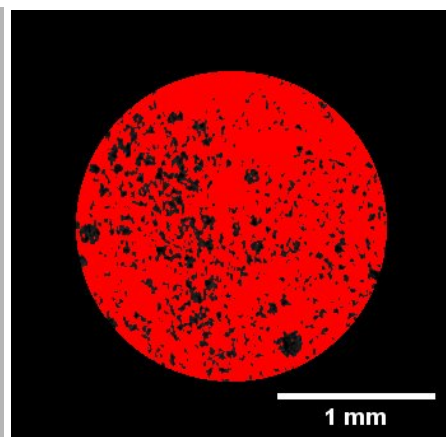


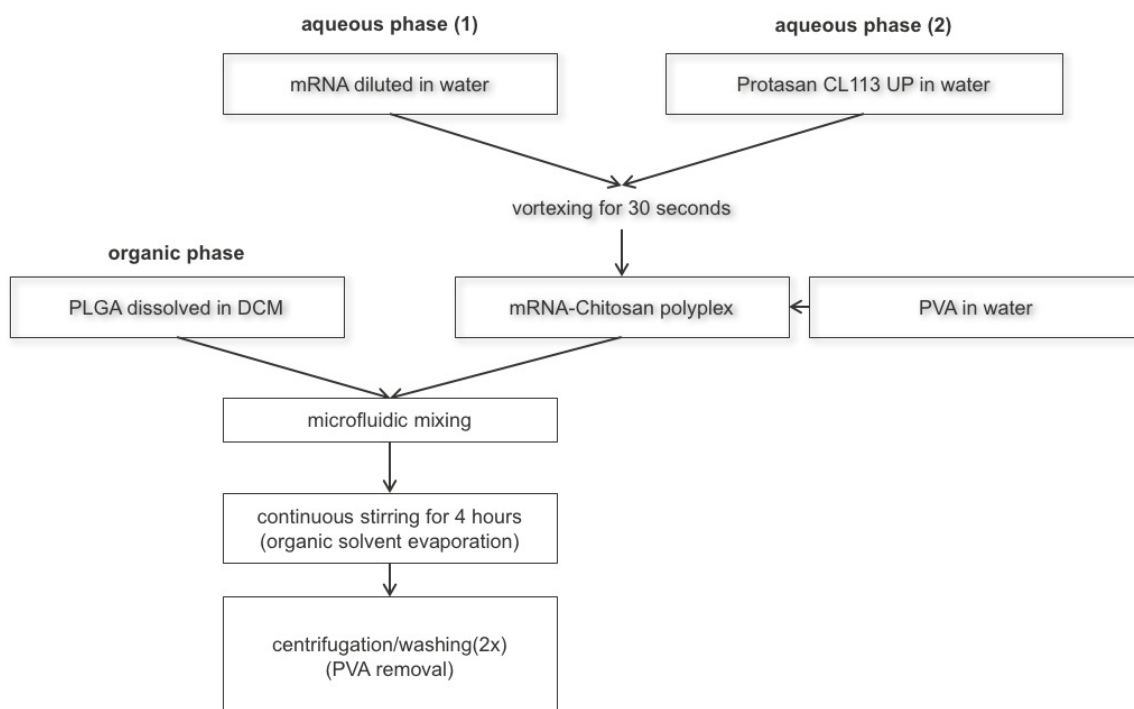
Fig. 8 – A) Exemplary image of a volume disc virtually cut out of a composite specimen, the blue box indicates the defined volume which was analyzed and the yellow masses represent the ceramic fraction of the disc. B) Exemplary slice of a volume disc displaying random parts of a CPC/PLGA specimen. The cement phase is marked in red color.

---

## 2.4 Methods – nanoparticle project

### 2.4.1 Preparation of chitosan and co-formulated PLGA/chitosan polyplexes

In Scheme 7 the formation of nanoparticles with and without PLGA is displayed. Chitosan/cmRNA complexes were formed by one-pot mixing of different amounts of chitosan (Protasan UP CL 113), and cmRNA at different concentrations and constant volume to volume ratios of 1/1 for each N/P ratio. As described below, nitrogen from primary amines on chitosan, and phosphates, from cmRNA backbones define N/P ratios which were used as a guideline to investigate the interaction of the cargo and its encapsulating agent. Here, the amount of substance (mol) of the chitosan's deacetylated fraction which carries one free primary amine on each monomer was divided by the amount of substance (mol) of the phosphates in a typical cmRNA. A mean molecular weight of 340 g/mol was defined per cmRNA base. For N/P 1, 2, 4, 8, 10, 15, 20 a volume of 60, 120, 240, 480, 560, 900, and 1200  $\mu\text{l}$  of chitosan solution (2.5 mg/ml) was mixed to 300  $\mu\text{l}$  of cmRNA (1 mg/ml) solution, respectively. The resulting dispersion was vigorously vortexed for 30 s. After equilibration for 10 min at room temperature chitosan polyplexes were ready to use. For the co-formulation with PLGA (Resomer<sup>®</sup> RG 750 S), 200  $\mu\text{l}$  of dissolved poly (vinyl alcohol) (PVA, 10%) were added to 2 ml of the chitosan nanoparticle dispersion after equilibration and was diluted with water to 4 ml. The subsequent aqueous phase was mixed with 20 mg of poly (lactic-co-glycolic acid) (PLGA) dissolved in 6 ml dichloromethane (DCM) *via* a microfluidic syringe pump. The resulting emulsion was stirred for 4 h. Two centrifugation steps at 15000x g for 5 min and 110000x g for 1 h, were utilized for agglomeration filtering and nanoparticle washing [90].



**Scheme 7 - Schematic representation of the Chitosan/PLGA/cmRNA-complex preparation process. Self-assembling of chitosan/cmRNA particles takes place before co-formulation with PLGA by a water-in-oil emulsion solvent evaporation technique was conducted.**

## 2.4.2 Fluorescence labelling for FRET analysis

For FRET analysis a chemically modified firefly *luciferase*-encoding cmRNA where all uridines bear an azide was utilized for coupling *via* copper-less click-chemistry. Both Cyanin-3 (Cy3) and Cyanin-5 (Cy5) fluorophores are attached to a DBCO group with a labile triple bond. DBCO and the azides covalently bond in a one pot reaction at 4°C for 2 h. A coupling of 10 % of free azide for both dyes was conducted in each 50 µg of cmRNA by using 2,455 nmol of dye (quantity of substance was calculated via the ratio of azide bearing bases and the molecular weight of cmRNA). The excitation maximum of Cy3/Cy5 is at 553/646 nm and emits best at 563/661 nm. FRET signal was quantified by a Tecan microplate reader Infinite® 200 PRO (Tecan, Männedorf, Switzerland).

### 2.4.3 cmRNA quantification in polyplexes

To determine the encapsulation efficiency and the yield after co-formulation with PLGA, the cmRNA concentration in a freshly formed PLGA/chitosan polyplex dispersion was conducted *via* Quant-iT RiboGreen<sup>®</sup> assay. 200 µl of polyplex dispersion was used for displacement by 50 µl of heparin (40 mg/ml) interaction including 50 µl of Triton X-100 (2%) at 70°C and shaking at 7000 rpm on a Thermomixer. Encapsulation efficiency of cmRNA in co-formulated particles could be measured subsequently by the addition of 100 µl Quant-iT RiboGreen<sup>®</sup> working solution to 100 µl of the specimen described above. For cmRNA quantification after copolymerization unbound cmRNA was used for defining calibration curves. The fluorescence shift of the dye to higher wavelengths after reaction with cmRNA was quantitatively detected by a multilabel plate reader (Wallac Victor, Perkin-Elmer Life Sciences, Waltham, USA) at an excitation/emission maximum of 500/525 nm.

### 2.4.4 Agarose gel electrophoresis

For gel formation, 150 ml of TRIS-acetate-ethylenediaminetetraacetic acid (TAE) buffer containing 1 % (w/v) agarose and 5 % peqGREEN<sup>®</sup>, RNA/DNA dye was used. The mixture was heated shortly in a microwave oven until agarose was completely dissolved. The fluid was poured into a gel template and hardened for approximately 0.5 h. Before the samples were added, the gel was given into an electrophoresis template containing TAE buffer to cover the gel completely with fluid. The samples were treated with a loading dye 20 µl were subsequently added into the pockets of the gel. For cmRNA displacement in samples where cmRNA had to be freed from their carrier, 10 µl of cmRNA complex dispersion was mixed with 2 µl of heparin (100 mg/ml) solution and 3 µl Triton<sup>®</sup> X-100 (2 %). As a next step the mix was equilibrated at 70 °C for 30 min, and subsequently added to 10µl of loading dye. Gel electrophoresis was performed at 150 V for 0.5 h. Analysis of the gels was executed by ChemiDoc XRS+ system and the images were post processed by ImageJ.

### 2.4.5 Fluorescence resonance energy transfer (FRET)

For FRET studies nanoparticles were prepared (as described in 2.4.1 and 2.4.2) with 10% of labelled cmRNA (80/20 % of Cy3/Cy5) and 90 % of green fluorescent protein (eGFP) encoding cmRNA. Here, cmRNA encoding for firefly *luciferase*, where all uridines were linked with an azide group, was labelled with DBCO-sulfo-Cyanin 3/5 (Cy3/Cy5) and mixed to unlabeled cmRNA encoding for green fluorescent protein (eGFP) in a ratio of 1/9. Labelling was executed according to the instructions of the manufacturer with slight modifications to allow a loading of 10 % of the azide bearing uridines. The excitation maximum of Cy3/Cy5 is at 553/571 nm and emits best at 646/662 nm, respectively. The FRET signal could be calculated as follows:

$$\text{FRET} [\ ] = \text{Cy5 (679 nm) intensity} / \text{Cy3 (517 nm) intensity} [91-93].$$

The emission levels of both dyes were measured simultaneously by a Tecan® Infinite Pro 200 (Tecan, Männedorf, Switzerland) multimode reader 8, 15, 20, 30, 60, 90 and 120 min after mixing the nanoparticle dispersions with different ratios to water, PBS, DMEM, FBS and 10 % of dissolved mucin.

### 2.4.6 *In vitro* transfection efficiency

NIH3T3 cells were cultivated in DMEM containing 10 % FBS and 1 % Penicillin/Streptomycin (Pen/Strep). 24 h before transfection, cells were trypsinated before seeding onto standard 96-well plates at a density of 10.000 cells/well. After cell attachment over night the cell culture medium was removed and different amounts of PBS or DMEM were mixed with the nanoparticle dispersions which were analyzed and added to the cell monolayer for different amounts of incubation time. The nanoparticle dispersions were exchanged with cell culture medium and the samples were incubated at 37 °C and 5 % CO<sub>2</sub> for another 24 h. After the addition of coelenterazine buffer, containing a 50 mM PBS-buffer (pH 7.0) to 100 µl of the supernatants, collected 24 and 48 h after transfection, bioluminescence was measured in triplicates using a luminescence reader (Wallac Victor, Perkin-Elmer Life Sciences, Waltham, USA).

#### **2.4.7 *In vitro* cell viability assay (MTT)**

Cell viability was investigated by 3-(4,5-Dimethylthiazol-2-yl)-2,5-diphenyltetrazolium-bromide (MTT) assay. Here, by a colorimetric method based on the cleavage of yellow tetrazolium to insoluble crystalline formazan, the mitochondrial activity of living cells could be quantified [94]. Transfection prior to MTT testing was conducted as described in chapter 2.4.6. 24 h after transfection cell culture medium was replaced by 100  $\mu$ l of MTT buffer consisting of 1 mg/ml MTT reagent and 5 mg/ml D-(+)-glucose dissolved in PBS. After 2 h of incubation at 37 °C and 5 % CO<sub>2</sub> solubilisation of the crystals was achieved by the addition of 100  $\mu$ l of 10 % Triton<sup>®</sup> X-100 in anhydrous isopropanol and 0.1 N hydrochloric acid (HCl). Dissolved formazan was detected and quantitatively measured *via* a multiplate reader at a wavelength of 590 nm. As a reference, 8 wells were treated with water instead of nanoparticle dispersions while transfection on each plate.

### 3 Results

The central subject of this thesis is the investigation of how PLGA as a biodegradable polymer can be utilized in different cmRNA delivery applications. One of those possibilities was the development of an intermediate cmRNA carrier for the enhancement of bone substitute materials. Initial experiments showed that ceramics like calcium phosphates, which are commonly used in bone defect filling, could not be utilized as functional scaffolds for cmRNA delivery on its own. Therefore, the idea emerged to include a bioactive composite, basically consisting of PLGA. The strategy to enhance the ceramic pastes by insertion of PLGA-based microspheres was already tested by other researchers in the field of calcium phosphate based bone substitutes, especially for introducing a fast-degrading composite to increase cell ingrowth and implant degradation [58, 76, 77]. However, the microparticles, desired in this project, were not only supposed to increase the porosity of such ceramics, but to release functioning cmRNA vehicles which are able to enhance bone growth by triggering *i.e.* growth factors like BMP-2.

#### 3.1 Optimization of the microparticle formation process

PLGA-based microparticle formation for various applications has been described extensively over the last decades [85, 86, 95-99]. By simple reproduction of some of those described encapsulation routes, rather big (Fig. 9 A) or damaged spheres (Fig. 9 B) resulted as products after first formation trials. As the lipid nanoparticles have never been described as the cargo for encapsulation *via* an emulsion solvent evaporation technique with PLGA, optimization of these formulation routes was necessary. For this purpose, a scheme (Scheme 8) with all the critical steps was defined and each stage of the formation process was screened for its effect on the product.

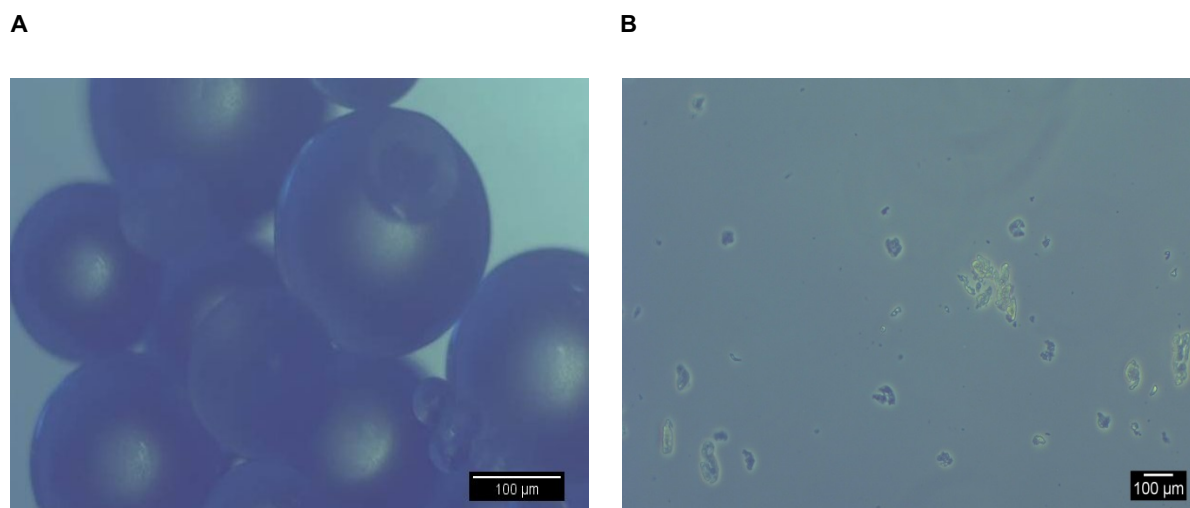
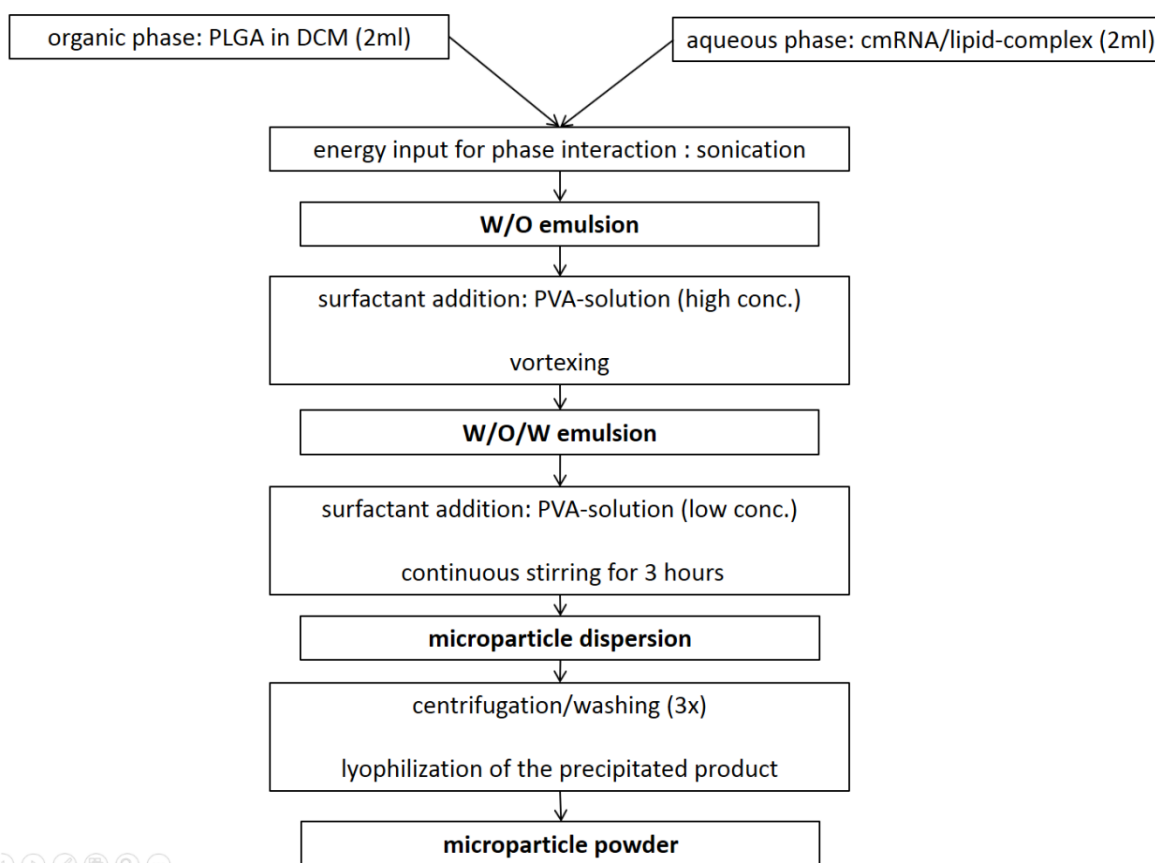


**Fig. 9 – A) PLGA microparticles with a diameter of 150-500  $\mu\text{m}$ ; B) shredded PLGA microparticles. Spherical shape could not be achieved without optimizing the formulation process for lipoplex encapsulation.**



**Scheme 8 -Schematic representation of the PLGA microparticle preparation process with the main factors for formation investigation in bold and the (intermediate) products in italic. For the investigation of parameter change impact factors, only one of the parameters was changed at a time, for each analysis.**

Here, first and foremost, the reproducibility in shape and size, and the transfection efficiency of the microparticle powders were defined as key properties. In a pre-screening, the organic phase, the aqueous phase, the surfactants and the energy intake for interphase mixing were investigated for their impact on the properties mentioned above. For all the following results three independently produced batches were formulated for each experimental setting to collect independent triplicates for analysis.

### 3.1.1 Influence of the organic phase: PLGA (Resomer<sup>®</sup>)

Seven different types of PLGA (Resomer<sup>®</sup>) with three different grades of hydrophobicity and varying chain lengths have been investigated to define the optimal carrier properties for the purpose of lipoplex encapsulation. Resomer<sup>®</sup> was chosen because these polymers have already been tested and used in various approved medical products [100]. A full list of all the different PLGA types is displayed in Table 1.

**Table 1 - Overview of the different Resomer<sup>®</sup> types which were used in this study. Properties like the ratio between glycolic acid and lactic acid monomers, the endgroup, degradation timeframe after implantation and the inherent viscosity (directly proportional to molecular weight) are depicted for each [100].**

Resomer <sup>®</sup> name	502 H	503 H	504 H	750S	752 S	755 S	858 S
Glycolic-/ Lactic Acid (GA/LA)	1:1	1:1	1:1	1:3	1:3	1:3	1:6
Endgroup	Acid	Acid	Acid	Ester	Ester	Ester	Ester
Degradation timeframe	< 3 months	< 3 months	< 3 months	<6 months	<6 months	<6 months	9 months
Inherent viscosity [dl/g]	0.16 - 0.24	0.32 - 0.44	0.45 - 0.60	0.8 - 1.2	0.14 - 0.22	0.5 - 0.7	1.3 - 1.7

The polymers can be grouped into two different families of polymers. 502 H, 503 H and 504 H are polymers where the ratio between glycolic acid and lactic acid monomers is 1:1. The H indicates carboxyl groups on the polymers' ends. 750 S, 752 S, 755 S and 858 S are PLGA polymers with an ester termination and a monomer ratio of 3:1 and 6:1, respectively, in favor of lactic acid. As shown in scheme 4 (chapter 1.5) the only difference of the monomers is an additional methylene group on the lactic acid monomer. Due to this small difference, chemical, physical and mechanical properties, including crystallinity, differ substantially between all the different types of PLGA used in this study. In Fig. 10 the effect of Resomer<sup>®</sup> type on microparticle formation is

depicted concerning size and transfection efficiency of the microparticles after lyophilization.

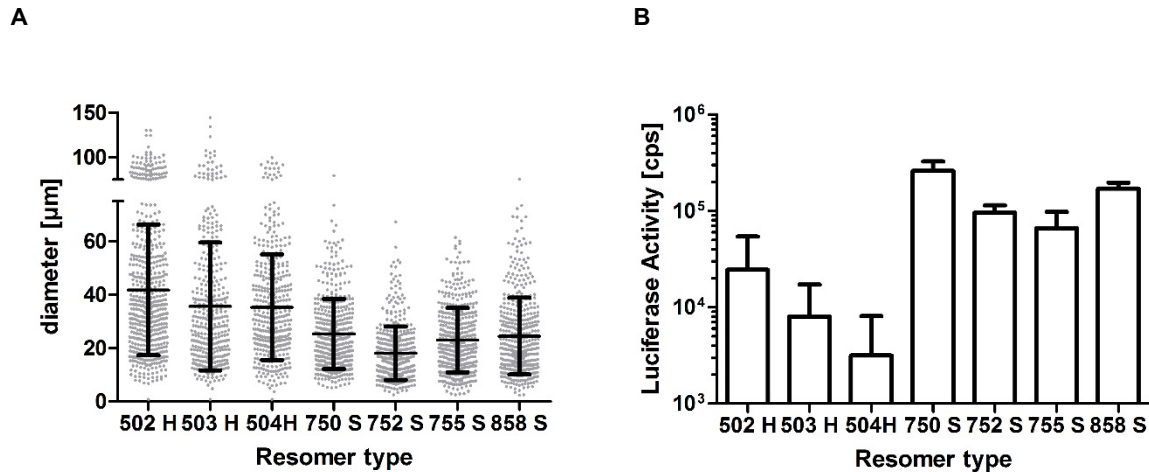
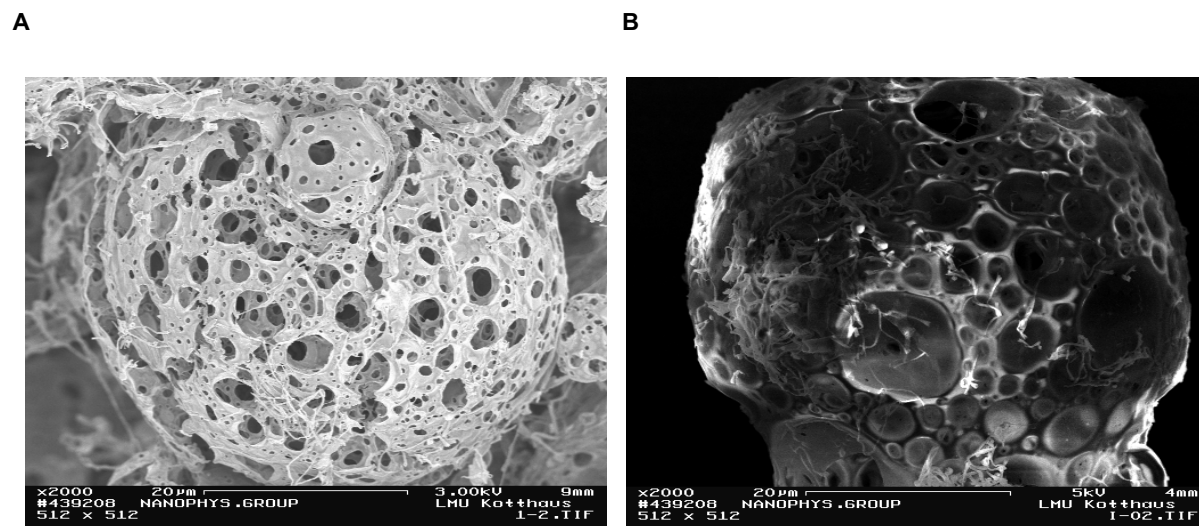


Fig. 10 – A) Particle size measurement of microparticles formed with different PLGA/Resomer<sup>®</sup> types B) Transfection efficiency of microparticles formed with different PLGA/Resomer<sup>®</sup> types on mesenchymal rat bone marrow stem cells (rBMSCs). The reporter protein (*metridia luciferase*) activity was determined after 24 h post transfection by measuring bioluminescence expressed in counts per second (cps)

The results for particle size measurements and transfection efficiency revealed biggest differences between polymers containing a lactic acid to glycolic acid (LA/GA) ratio of 1:1 and polymers containing more lactic acid than glycolic acid. In general, particles made of Resomer<sup>®</sup> 502 H, 503 H and 504 H were approximately double in mean size than the particles made of the other tested polymers. Furthermore, a decline in mean size with increasing inherent viscosity for could be observed (Table 1). The same trend in size analysis was observed with the microparticles which were made of ester-terminated PLGA types from 750 S to 858 S. Concerning transfection efficiency *in vitro* the trends within polymers with higher and lower lactic acid content were similar to the size measurements. From 502 H to 504 H, and therefore from low to high inherent viscosity, protein production decreased substantially. Bioluminescence was approximately one magnitude lower for all particles made of low LA content polymers than the particles made of polymers from 750 S to 858 S. Here 750 S was the best performing carrier polymer. Due to these results Resomer<sup>®</sup> 750 S was chosen for further optimization. In Fig. 11 and 12, exemplary images of microparticles reveal the main differences in particle topology, which were observed between particles made of

lower (GA:LA = 1:1) (Fig. 9) and higher (GA:LA  $\leq$  1:3) (Fig. 10) lactic acid monomer containing polymers and between acid- and ester terminated PLGA types, respectively.



**Fig. 11 – A) Exemplary image of hydrophilic Resomer<sup>®</sup> 503 H and B) Resomer<sup>®</sup> 504 H-based microparticles taken by scanning electron microscopy at a magnification of 2000**

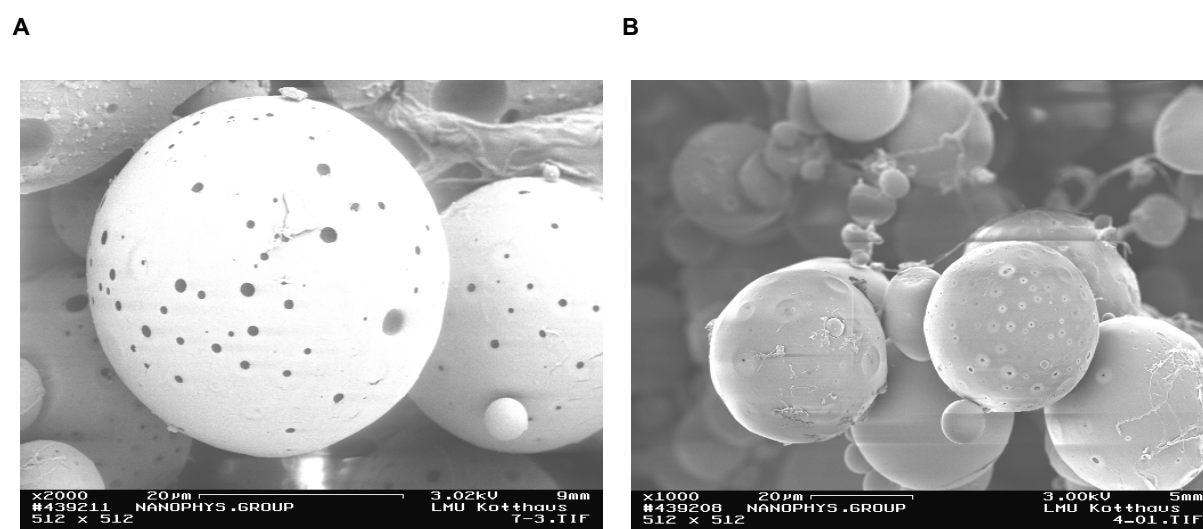


**Fig. 12 – A) Exemplary image of hydrophobic Resomer<sup>®</sup> 858 S and B) Resomer<sup>®</sup> 752 S-based microparticles taken by scanning electron microscopy at magnifications of 1000 and 2000, respectively**

Representative for the polymers with lower lactic acid content and acid-termination, particles in Fig. 9 present sponge-like, highly porous spherical structures under the electron microscope. In contrast, particles made of PLGA types with higher lactic acid content and ester-termination (Fig. 10) exhibit a smoother surface with defined and smaller surface pores.

### 3.1.2 Influence of the surfactant: poly (vinyl alcohol) (PVA) solutions

The stabilization of the emulsion, in which the evaporation of the organic solvent takes place, is crucial for the spherical shaping and hardening in the microparticles' formation process. The effect of surfactant concentrations was investigated and results are shown in Fig. 13 for the first- and Fig. 14 for the second aqueous solution. Below the PVA concentration levels shown, the emulsion collapsed and no particles could be obtained.

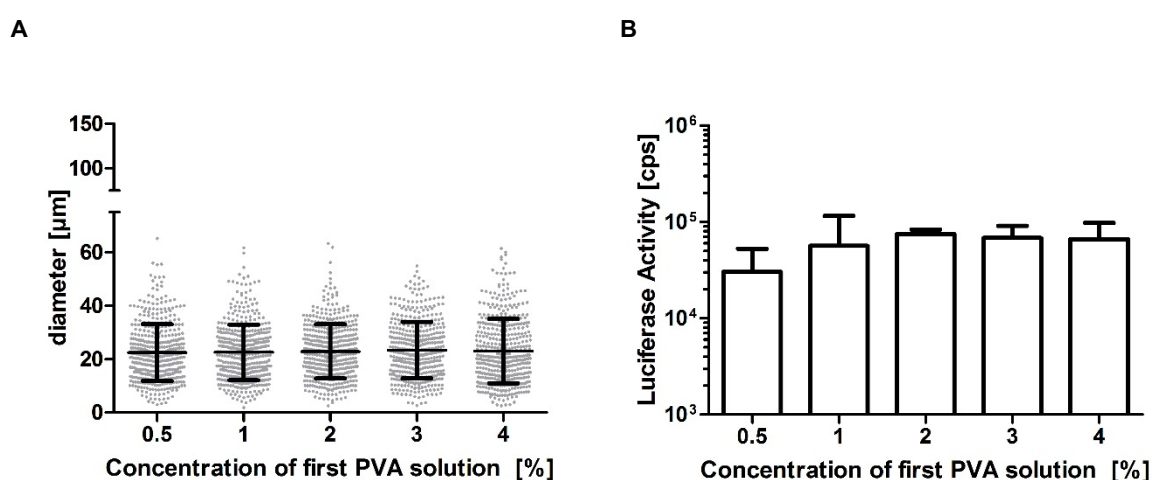


Fig. 13 – A) Particle size measurement of microparticles formed with different PVA concentrations in the first aqueous solution of the particle formation process. B) Transfection efficiency on rat bone marrow stem cells of microparticles formed with different PVA concentrations in the first aqueous solution of the particle formation process. The reporter protein (*metridia luciferase*) activity was determined after 24 h post transfection by measuring bioluminescence expressed in counts per second (cps)

The critical surfactant concentration for spherical particle formation was found at 0.5 % PVA for the first and 0.2 % PVA for the second solution. The influence of higher surfactant concentrations than needed for emulsion stabilization on particle size and transfection efficiency in the first aqueous solution is negligible. No differences in size between 0.5 and 4 % PVA could be observed. Only the particles with the lowest PVA concentration showed lower transfection efficiency than all the other tested specimens. Hence, 4 % PVA in the first aqueous solution was used as a standard to guarantee stable emulsions until the particle hardening process was completed to gain microparticles with optimal transfection efficiency.

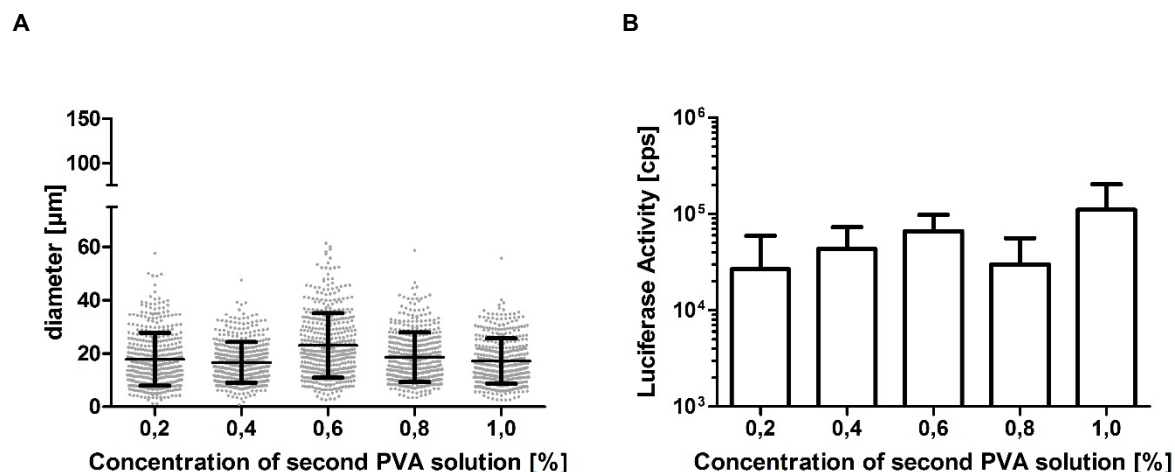


Fig. 14 – A) Particle size measurement of microparticles formed with different PVA concentrations in the second aqueous solution of the particle formation process. right: Transfection efficiency on rat bone marrow stem cells of microparticles formed with different PVA concentrations in the first aqueous solution of the synthesis process after 24 h post transfection. The reporter protein (*metridia luciferase*) activity was determined after 24 h post transfection by measuring bioluminescence expressed in counts per second (cps)

An increase of PVA concentrations over the minimum for spherical particle formation did not lead to any trends in mean particle size either. Only particles made with 0.6 % PVA were slightly bigger in size than all other specimens. Protein production showed no significant trends for microparticles equilibrated in higher concentrations in the second aqueous solution. Particles formulated in 1 % PVA concentration in the second aqueous solution exhibited highest protein production. Hence, 1% PVA was used for further investigations and optimizations.

### 3.1.3 Influence of the energy input for phase interaction: sonication

The interaction between the immiscible organic and aqueous phase is the basic requirement for microparticle formation based on a W/O/W solvent evaporation technique and therefore the encapsulation of the cargo. Sonication of the immiscible phases with a sonifier probe lead to reproducible particle formation and was chosen as energy source for phase interaction. In Fig. 15 results of size and transfection efficiency measurements for microparticles formed with different sonication energy input levels are depicted.

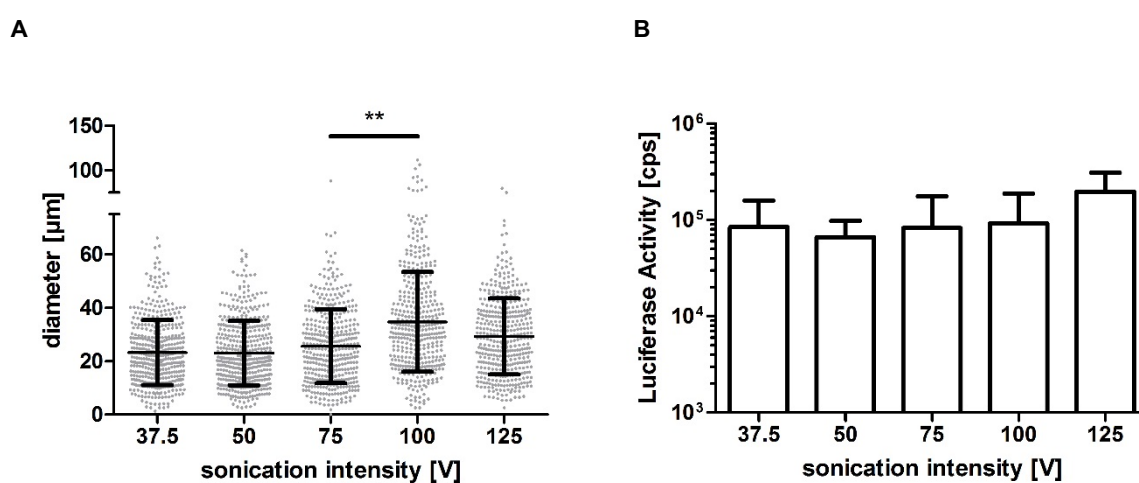


Fig. 15 – A) Particle size measurement of microparticles formed with different levels of sonication energy intensities. B) Transfection efficiency on rat bone marrow stem cells of microparticles formed with different levels of sonication energy intensities. The reporter protein (*metridia luciferase*) activity was determined after 24 h post transfection by measuring bioluminescence expressed in counts per second (cps)

Microparticle size analysis showed hardly any differences between different sonication intensities from 37.5 to 125 V, except for one outlier result at 100 V where the particles turned out to be approximately 10 μm bigger in the mean. The mixing with different sonication intensities showed no substantial trends in transfection efficiency when in the same range of sonication intensities. The best performing particles in terms of transfection efficiency were formulated with 125 V. Hence, this setting was used for further investigations.

Next to the intensity of the sonication at constant times of pulsing, the pulse length itself was investigated. Results for size and transfection efficiency measurements of particles formulated with pulses from 5 x 0.1 s to 1 x 5 s are displayed in Fig. 16.

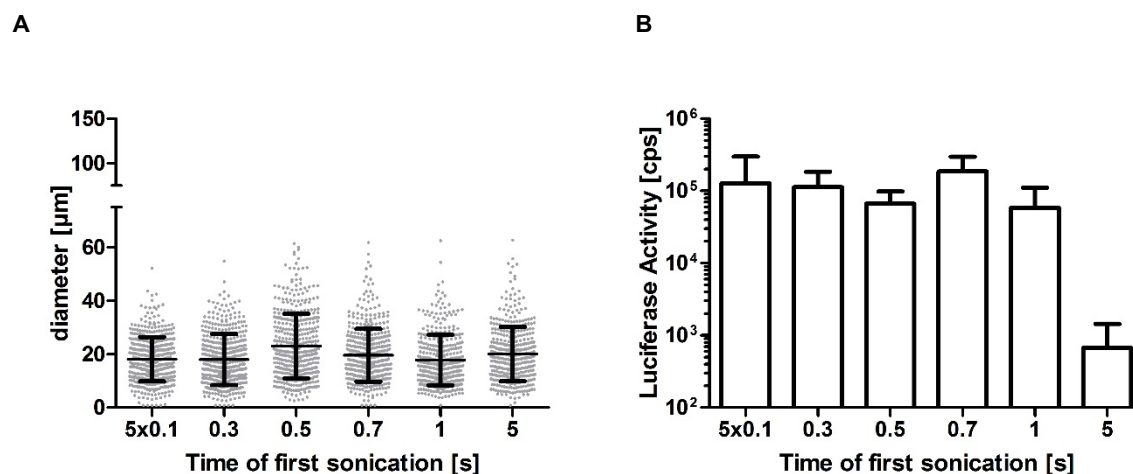
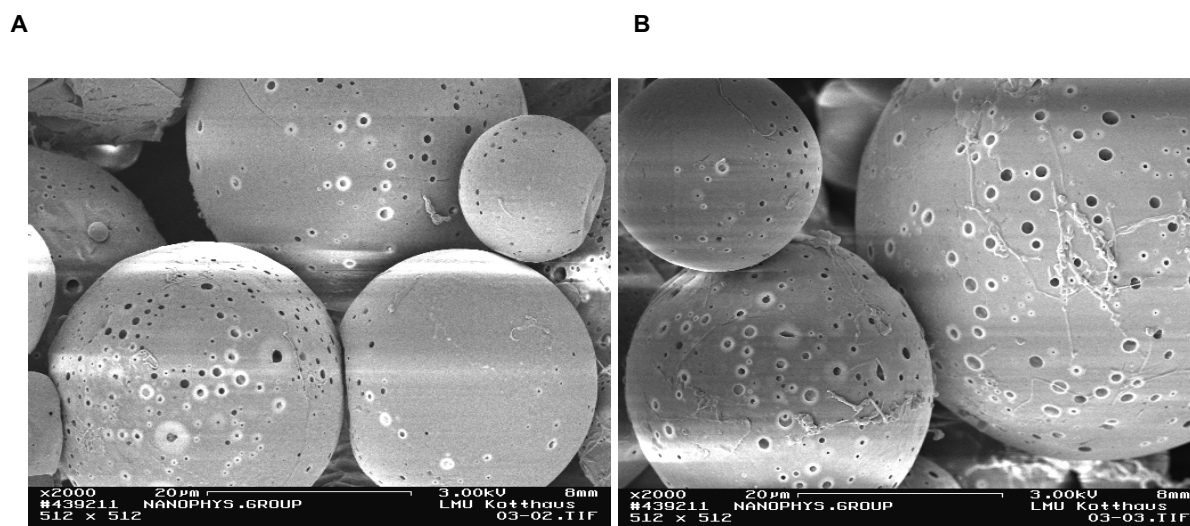


Fig. 16 – A) Particle size measurement of microparticles formed with different times of sonication pulses. B) Transfection efficiency on rat bone marrow stem cells of microparticles formed with different times of sonication pulses. The reporter protein (*metridia luciferase*) activity was determined after 24 h post transfection by measuring bioluminescence expressed in counts per second (cps)

No substantial size differences or trends were observed between particles made with sonication pulses from 5 x 0.1 s to 1 x 5 s but transfection efficiency dropped drastically after increasing the pulse up to 5 s. Best protein production after 24 h post transfections was observed for particles made with 0.7 s pulses which is why this setting was used for further experiments.

Additionally, exemplary particles exhibiting rather high and no transfection efficiency *in vitro* after their respective sonication process were scanned by SEM for potential visible damaging due to the process. Fig. 17, shows microparticles formulated with a sonication pulse time of 1s at 75 V representing well transfecting spheres and Fig. 18 depicts microparticles formulated with a sonication pulse of 5 s at 75 V, representing spheres where no protein activity could be measured 24 h after transfection.



**Fig. 17 - Exemplary images of PLGA microparticles taken by scanning electron microscopy at a magnification of 2000. Microparticles were emulsified with a pulse time of 1 s at 75 V.**

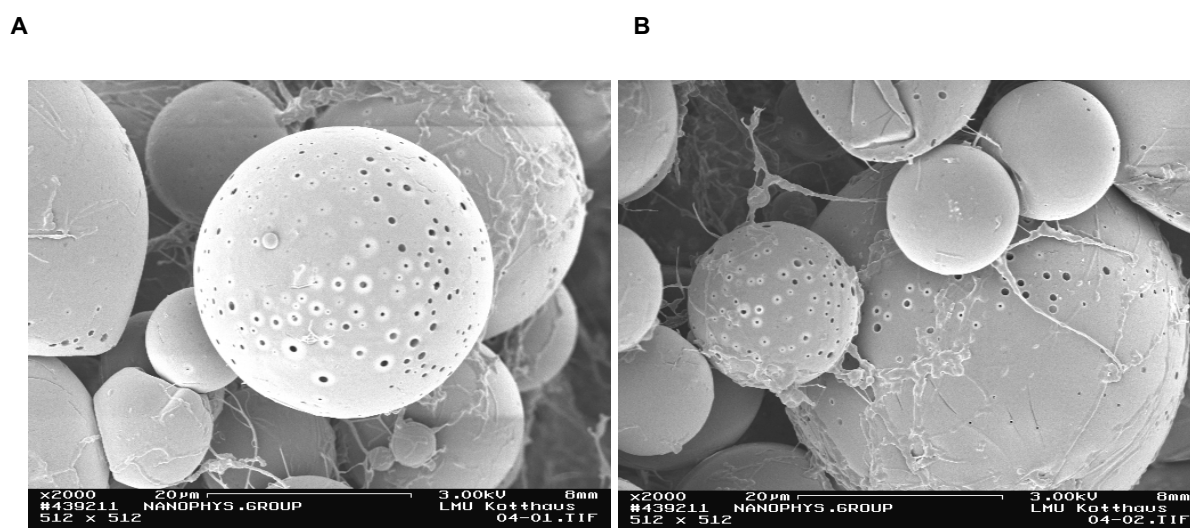


**Fig. 18 - Exemplary images PLGA microparticles taken by scanning electron microscopy at a magnification of 2000. Microparticles were emulsified with a pulse time of 5 s at 75 V.**

All images displayed in both Fig. 17 and Fig. 18 disclose no considerable differences in topology, surface porosity or overall appearance. All particles display the typical porous surface and a spherical shape. Hence, the lack of transfection efficiency for particles emulsified with a 5 s pulse at 75 V intensity of sonication, cannot be explained by the shaping process of the microspheres. String-like structures can be observed in all SEM images.

### 3.1.4 Aqueous phase: cmRNA/lipid-complex

The lipoplex loading of PLGA microparticles by emulsion solvent evaporation technique and its effects on the outcome of the product has not been described, so far. This is why lipoplex loading into the polymer matrix was investigated thoroughly in terms of possible effects on encapsulation efficiency, microparticle shape, size, surface topology and bio-functionality at different ratios of lipoplex to PLGA. Here, the lipoplex itself and its composition were kept constant which means that cmRNA to lipid contents is directly proportional. Hence, a new unit was introduced where the ratio of lipoplex to PLGA in microparticle formation could be described as  $\mu\text{g RNA/mg PLGA}$ .

#### *Lipoplex encapsulation efficiency in microparticles*

Encapsulation efficiency defines how much cmRNA was encapsulated during microparticle formation at different process parameters compared to a theoretical 100 % loading. For measurement, it was crucial to release the RNA safely out of the polymer matrix without harming the cargo after the microparticles were lyophilized and in the form of a white powder. DMSO was used as the dissolving agent for the polymer matrix premixed with heparin sodium salt in water to displace the cmRNA out of the cationic lipids. The subsequent dispersion contained the free cmRNA, which could be quantified subsequently *via* RiboGreen Assay. Results of Table 2 and Fig. 19 show the results of encapsulation efficiency measurements of microparticles loaded between 0.2 and 4  $\mu\text{g cmRNA/mg PLGA}$ . For a better comprehension of this experiment a dotted line representing a theoretical 100 % encapsulation of the lipoplexes during microparticle formation, is shown.

**Table 2 - encapsulation efficiency of cmRNA in microparticles after formation, including theoretical loading parameters from 0.2 to 4  $\mu\text{g cmRNA/mg PLGA}$ .**

encapsulation efficiency:					
100 % encapsulation [ $\mu\text{g cmRNA/mg PLGA}$ ]	0.2	0.5	1	2	4
measured encapsulation [ $\mu\text{g cmRNA/mg PLGA}$ ]	0.064	0.190	0.390	0.673	0.842
Standard deviation [ $\mu\text{g cmRNA/mg PLGA}$ ]	0.002	0.021	0.019	0.007	0.040
lipoplex loading efficiency [%]	32.10%	37.98%	38.96%	33.66%	21.06%

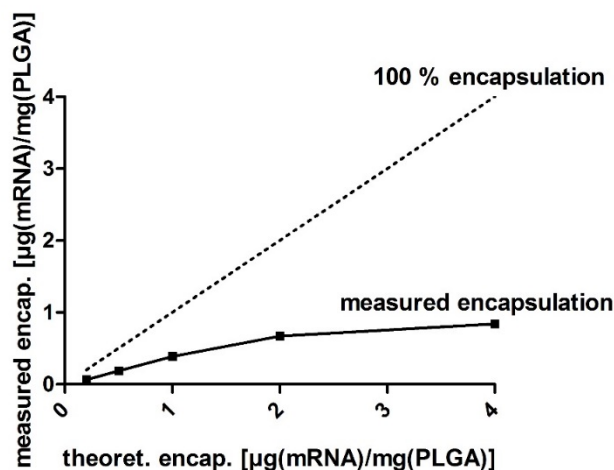


Fig. 19 – Encapsulation efficiency of cmRNA in PLGA microspheres of batches produced with different nanoparticle to polymer ratios of 0.2 to 4  $\mu\text{g RNA/mg PLGA}$ . The dotted line indicates a theoretical encapsulation of 100%.

The measured results and the theoretical encapsulation at 100 % increasingly diverge from each other the more lipoplex was used for microparticle formation. Hence, the more lipoplex, which was initially used, the more lipoplex/cmRNA was eventually not encapsulated and lost in the washing process before lyophilization. The graph for the measured results increases logarithmically and plateaus between loading parameters of 2 to 4  $\mu\text{g RNA/mg PLGA}$ . Here, a lipoplex saturation concentration could be indicated for these loading parameters.

#### *Microparticle size distribution by light microscopy and image analysis*

All microparticle mean sizes shown in this thesis were measured and analyzed *via* light microscopy image post-processing. It was possible to filter out broken, non-spherical particles from the analysis, which would not have been possible by *i.e.* light scattering methods. In Table 3 and Fig. 20. the comparison of the mean sizes of differently loaded microparticles discloses that from low to high loading ratios (0.2 to 4  $\mu\text{g cmRNA/mg PLGA}$ ) the particle mean becomes significantly smaller. The standard deviation for 0.2  $\mu\text{g cmRNA/mg PLGA}$  was rather high compared to all other examined microspheres with some particles exceeding the size of 120  $\mu\text{m}$ .

**Table 3 - mean particle size of PLGA microparticles with loading parameters from 0.2 to 4  $\mu$ g cmRNA/mg PLGA.**

microparticle size:					
loading parameters [ $\mu$ g cmRNA/mg PLGA]	0.2	0.5	1	2	4
Mean particle size [ $\mu$ m]	28.90	23.04	20.53	19.07	14.10
Standard deviation [ $\mu$ m]	16.83	6.27	5.11	8.75	8.05

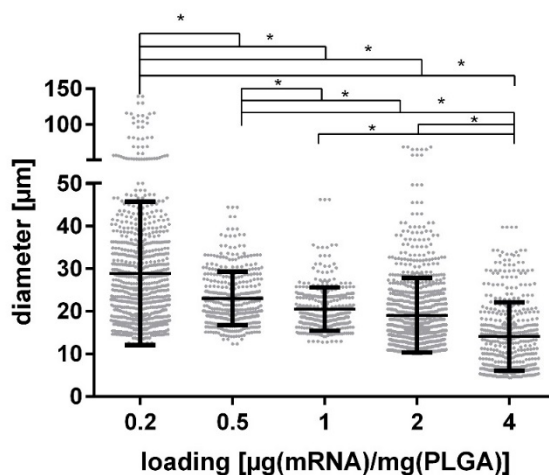


**Fig. 20 - Particle size measurement of microparticles loaded with different nanoparticle to polymer ratios from 0.2 to 4  $\mu$ g RNA/ mg PLGA. Diameters of particles were determined *via* post processing of images taken by light microscopy.**

Additionally, the particles made with loading parameters 0.5 and 1  $\mu$ g cmRNA/mg PLGA exhibited lowest polydispersity with hardly any outlier particles above 40  $\mu$ m. Here, the encapsulation of lipoplexes and the effect on the specific surface *via* mean particle size is similar to the effect, which certain surfactants can have on PLGA microparticle formation [63].

#### *Surface topology investigation by SEM and image analysis*

Further analysis of particle powders revealed that besides the mean size of the microparticles, their surface topology is affected by nano-complex loading, as well. Examination of particles with a cmRNA loading of 0  $\mu$ g - 4  $\mu$ g cmRNA/mg PLGA by scanning electron microscopy (SEM) as displayed in Fig. 21, disclosed increased surface pore areas with decreased loading levels.

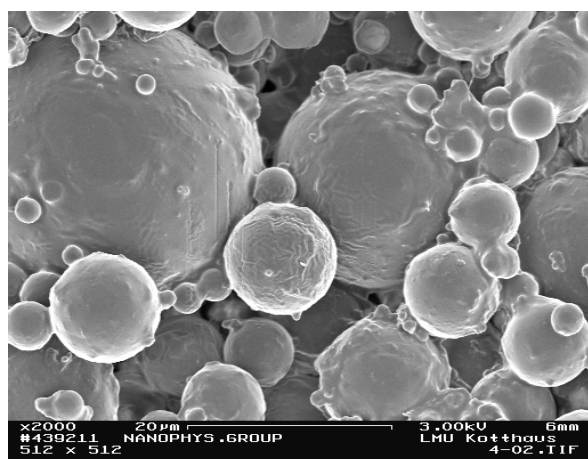
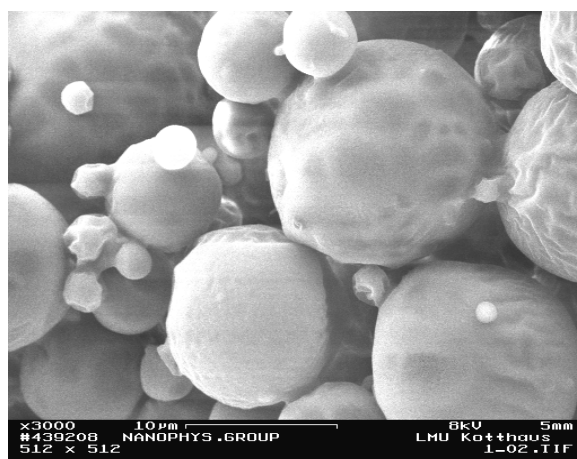
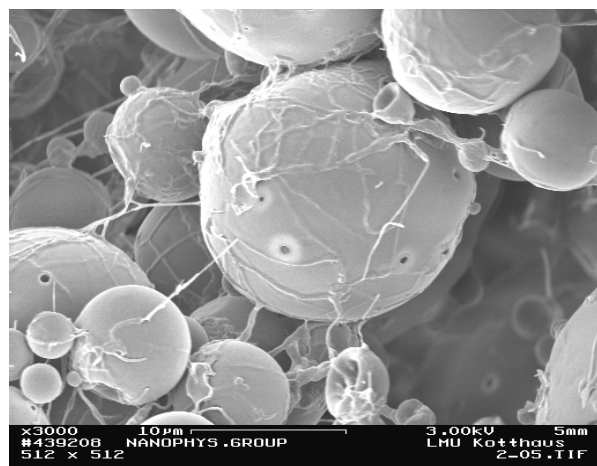
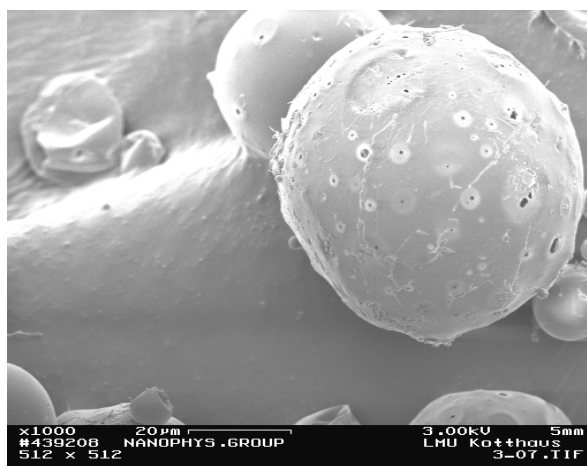
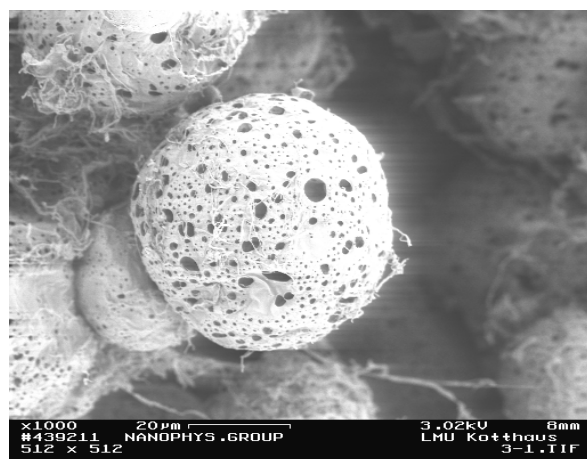
A – 4  $\mu\text{g/cmRNA/mg PLGA}$ B – 2  $\mu\text{g/cmRNA/mg PLGA}$ C – 1  $\mu\text{g/cmRNA/mg PLGA}$ D – 0.5  $\mu\text{g/cmRNA/mg PLGA}$ E – 0.2  $\mu\text{g/cmRNA/mg PLGA}$ F – 0  $\mu\text{g/cmRNA/mg PLGA}$ 

Fig. 21 – Exemplary images of PLGA microparticles taken by scanning electron microscopy at magnification of 3000, 2000 and 1000, respectively, for lipoplex loadings of A) 4, B) 2, C) 1, D) 0.5, E) 0.2 and F) 0  $\mu\text{g cmRNA/mg PLGA}$ .

At 4 and 2  $\mu\text{g}$  cmRNA/mg PLGA no surface porosity was visible. When no lipoplexes were used in the microparticle formation process, the spheres resemble sponge-like structures, which can be compared to microparticles made of Resomer<sup>®</sup> 502 H, 503 H or 504 H. The qualitative analysis of SEM images taken of particles with loadings between 0.2 and 1  $\mu\text{g}$  cmRNA/PLGA showed string-like structures around the spheres. These cannot be found on the closed surfaces of microparticles loaded with 2 or 4  $\mu\text{g}$  cmRNA/ mg PLGA. As a next step the black pore areas on the surfaces of the particles were quantified and divided by the total surface area visible on the images. The quantification results of the surface topology analysis are depicted in Fig. 22.

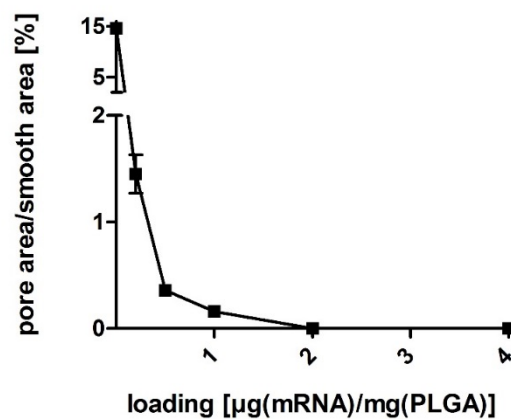


Fig. 22 – Porosity measurement of microparticles loaded with different nanoparticle to polymer ratios from 0 to 4  $\mu\text{g}$  cmRNA/mg PLGA. Pore areas were divided by total particle surface area on scanning electron microscopy images to gain porosity quantification.

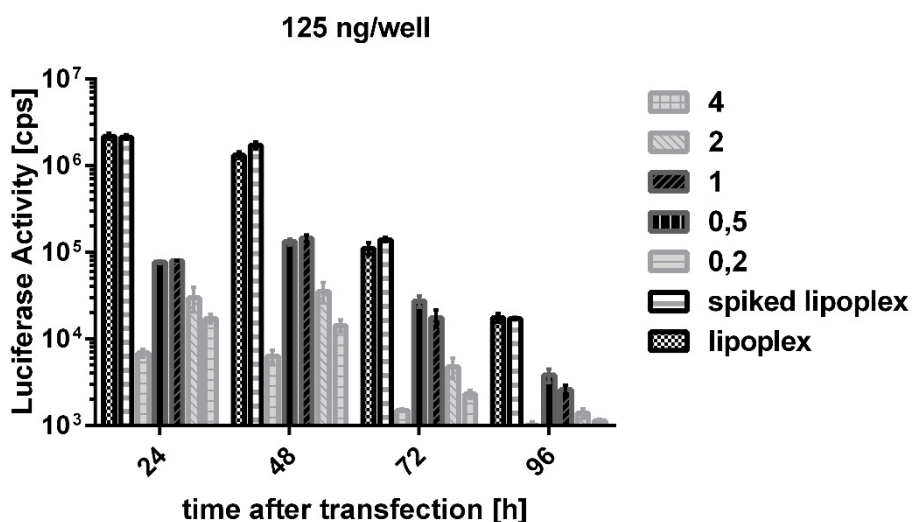
Quantitative analysis of three SEM images for each loading parameter between 0.2 and 4  $\mu\text{g}$  cmRNA/mg PLGA show exponentially decreasing pore-to-total surface area ratios. No surface pores were measured for 2 and 4  $\mu\text{g}$  cmRNA/mg PLGA in any of the images taken for surface topology analysis.

#### *Transfection efficiency investigation by metridia luciferase assay*

After the determination of the particles' encapsulation efficiency, surface topologies and mean sizes, the spheres with different lipoplex loadings were compared for their transfection efficiency *in vitro*. In Fig. 23 transfection efficiency analysis of microparticles loaded with 0.2, 0.5, 1, 2 and 4  $\mu\text{g}$  cmRNA/mg PLGA at two different

dosages, is displayed. Luminescence levels in supernatants were measured after 24, 48, 72 and 96 h for 125 and 250 ng/well. The dose was determined by microparticle encapsulation efficiency analysis prior to the transfection.

A



B

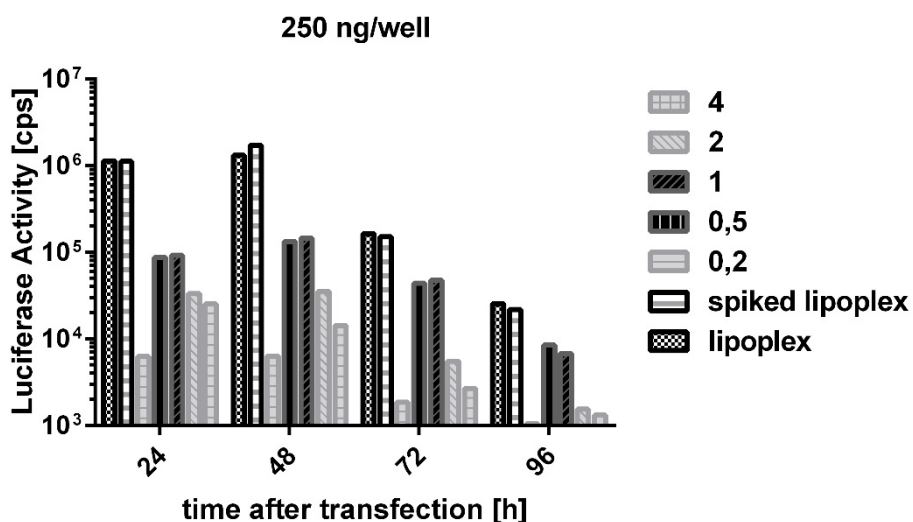


**Fig. 23 - Transfection efficiency of microparticles loaded with different nanoparticle to polymer ratios from 0.2 - 4 $\mu$ g cmRNA/mg PLGA on NIH3T3 mouse fibroblasts with different dosages for dosages of 2.5 and 5 pg cmRNA/cell (125 ng and 250 ng/well). As controls, free lipoplexes and lipoplexes spiked to non-loaded microparticles were added to the cells at the same dosages. The reporter protein (*metridia* luciferase) activity was determined 24, 48, 72 and 96 h post transfection by measuring bioluminescence expressed in counts per second.**

Generally, microparticle transfection efficiency is approximately one magnitude lower than those of free lipoplexes and free lipoplexes spiked on non-loaded microparticles at the same cmRNA dosages. Highest transfection efficiencies for free lipoplexes were measured at a dose of 125 ng/well after 24 h post transfection. At higher doses cytotoxicity may already have an effect on protein production. Only microparticles which were loaded with concentrations of 0.5 to 1  $\mu\text{g}$  cmRNA/mg PLGA showed substantial transfection efficiency after 24 and 48 h for all dosages. Both levels dropped after a peak expression at 48 h after transfection. The luminescence trends over time are similar for both free lipoplexes and microparticles.

In combination with the results from encapsulation efficiency experiments, a loading of 0.5  $\mu\text{g}$  cmRNA/ mg PLGA was chosen for further experiments. Although, those particles depict best transfection efficiency next to particles with a loading of 1  $\mu\text{g}$  cmRNA/mg PLGA, a loading of 0.5 is beneficial due to its higher efficiency in lipoplex encapsulation.

### **3.2 Visualization of release of lipoplexes *in vitro***

After having accomplished an optimized process for reproducible microparticle synthesis with subsequent transfection efficiency in the first days post transfection, the next goal was to investigate the lipoplex's release behavior out of their polymer matrix in physiological fluids. For this purpose, spheres with 0.5  $\mu\text{g}$  cmRNA/mg PLGA were formulated to qualitatively investigate the release mechanisms of the lipoplex bound in its matrix at different time points post transfection. The lipid component as well as cmRNA, were fluorescence labelled and encapsulated into microparticles for transfection on C2C12 mouse myoblasts. Those were utilized for this experiment, because they resemble later target cells as they are able to differentiate into osteoclasts [83]. The results of the fluorescence microscopy analysis are exhibited in Fig. 24. Here, images of microspheres (column A) and treated cells (column B) after transfection at time points from 0 to 96 h are displayed.

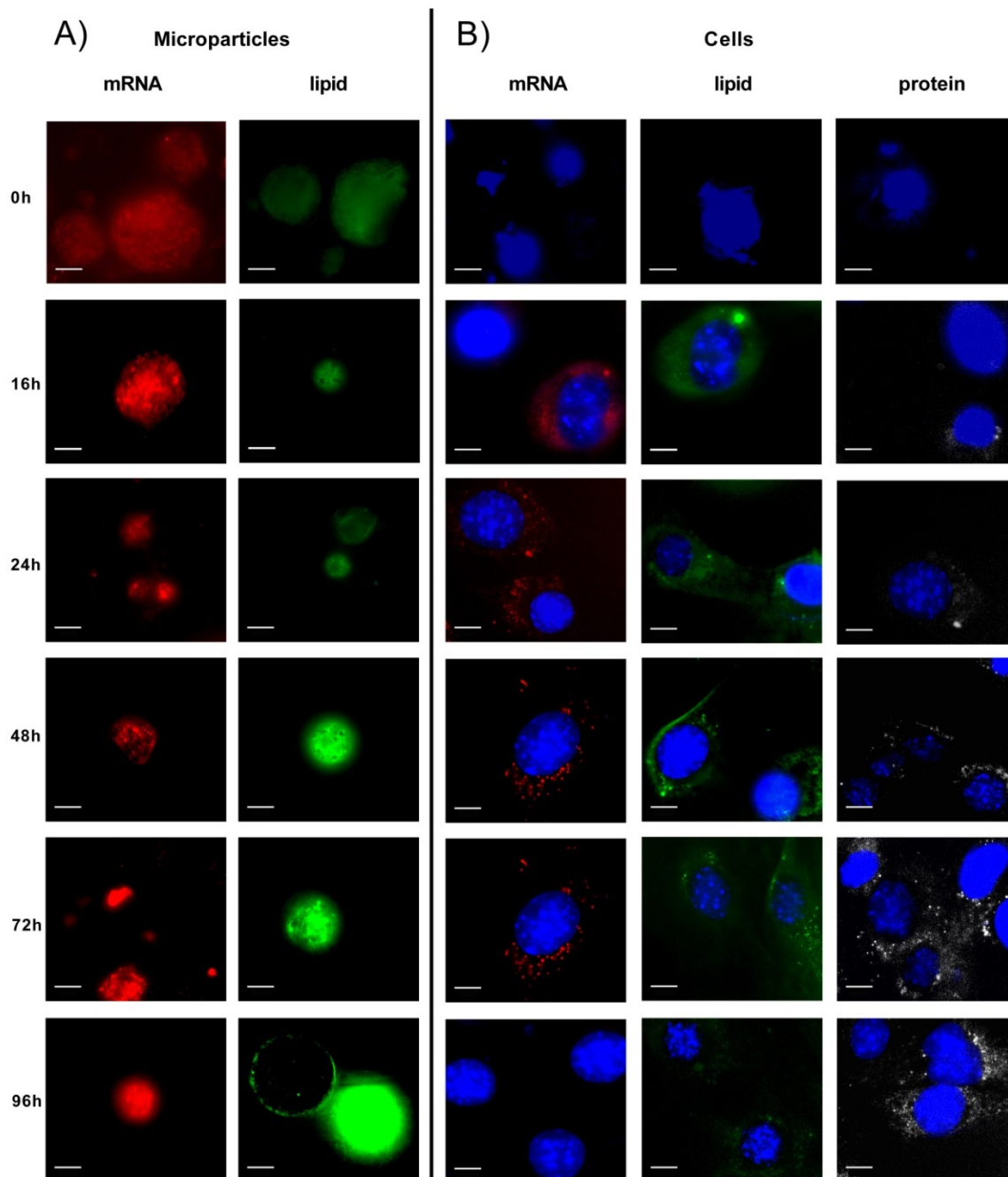


**Fig. 24 - Exemplary images of microparticles on C2C12 murine myoblasts taken by fluorescence microscopy for qualitative mRNA (red pixels) and lipid (green pixels) release and protein (white pixels) production visualization during the first four days after transfection. The scale bars represent a length of 10 $\mu$ m. a) From top to bottom, the two columns show microspheres at time points from 0 to 96 h after transfection. The “mRNA” titled column displays encapsulated labeled mRNA in microspheres in red pixels. The “lipid” titled column displays encapsulated labeled DOPE in microspheres in green pixels. b) From top to bottom, the three columns display cells where the nucleus was stained and visualized by blue pixels at time points from 0 to 96 h after transfection. The “mRNA” titled column displays internalized labeled mRNA around the cell nucleus in red pixels. The “lipid” titled column displays internalized labeled DOPE around the cell nucleus in green pixels. The “protein” titled column displays recombinant protein produced in the cytosol accumulating over time in white pixels.**

---

The distribution of cmRNA (red pixels) and lipid (green pixels) in microparticles over time reveals that a fraction of both components remains in the polymer matrix, even after four days of incubation under physiological conditions. Partial release and transfection of cmRNA could be observed *via* detection of labelled cmRNA (red pixels) in cells (blue pixels) starting as early as 16 h and lasting until 72 h. After that time point, no further cmRNA signal in cells could be found. Lipids (green pixels) were detected from 16 h to 96 h, mostly distributed around the cell nuclei. Recombinant protein (white pixels) accumulated in the cells from 16 h to 96 h with increasing signals during the first 72 h. To conclude, the transfection process from lipoplex release out of the microparticle matrix could be visualized, where not the microparticles themselves, but their cargo is taken up by the cells. After three days for cmRNA and four days for the lipids none of the signals could be detected in the cells, which indicates the end of an initial lipoplex release, where the rest of the cargo remains entrapped in the polymer matrix.

### **3.3 Development of a composite ceramic/polymer bone substitute**

As the bioactive microparticles were developed for the enhancement of injectable bone substitute materials, the next step was to mix both the optimized polymer powder and the ceramic calcium phosphate (CaP) phase of an injectable bone substitute material. A well-established bone filling product (Calcibon<sup>®</sup>) was used for the experiments. In this chapter results for porosity enhancement and transfection efficiency of composite CPC/PLGA specimens, are presented. Ceramic to microparticle ratios were investigated *via*  $\mu$ -CT analysis, followed by a transfection efficiency *screen in vitro* on mouse myoblasts.

### 3.3.1 $\mu$ -CT analysis of composite specimens for porosity analysis

Optimized microspheres loaded with a lipoplex concentration of 0.5  $\mu\text{g cmRNA/mg}$  PLGA were incorporated into injectable calcium phosphate cements. Here, the ability of the microparticles to increase the ceramic porosity after specimen curing was tested. Four specimens with four different weight-to-weight ratios of CPC to PLGA of 100:0, 90:10, 80:20 and 70:30 were prepared. Those specimens were irregularly shaped, which made it necessary to determine defined volume fragments for each specimen to perform density comparison tests. Here, virtual discs with a diameter of 2 mm and the depth of 99 slices were determined and defined for analysis. Exemplary slices of the virtual discs, which were analyzed, can be seen in Fig. 25. From left to right specimens are depicted with an increase of microparticle phase to cement phase and a steady decrease in red pixels (cement phase) can be observed qualitatively. 3D rotational models after post processing *via* ImageJ are depicted in Fig. 26. Qualitatively the decline of ceramic phase (yellow fractions) from 0 % (w/w) of microparticles to 30 % (w/w) is apparent.

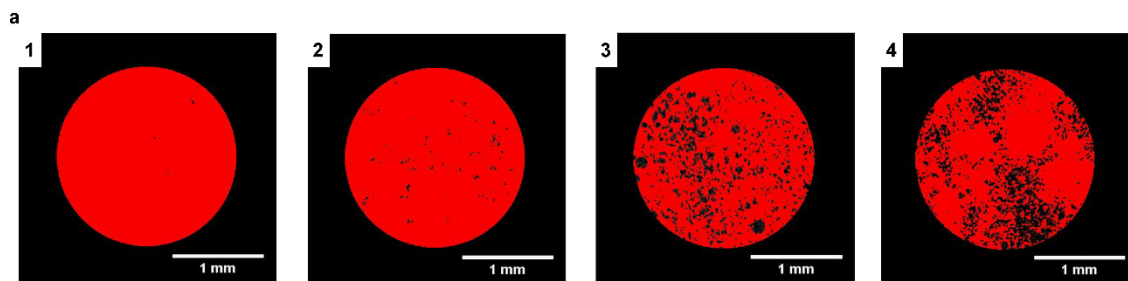


**Fig. 25 - Exemplary images of  $\mu$ -CT slices displaying random parts of CPC/PLGA specimens of different weight to weight ratios. The weight to weight ratios depicted in A to D are 100/0, 90/10, 80/20 and 70/30 calcium phosphate phase to pore phase (air and incorporated polymer microspheres), respectively. The cement phase is marked in red color.**

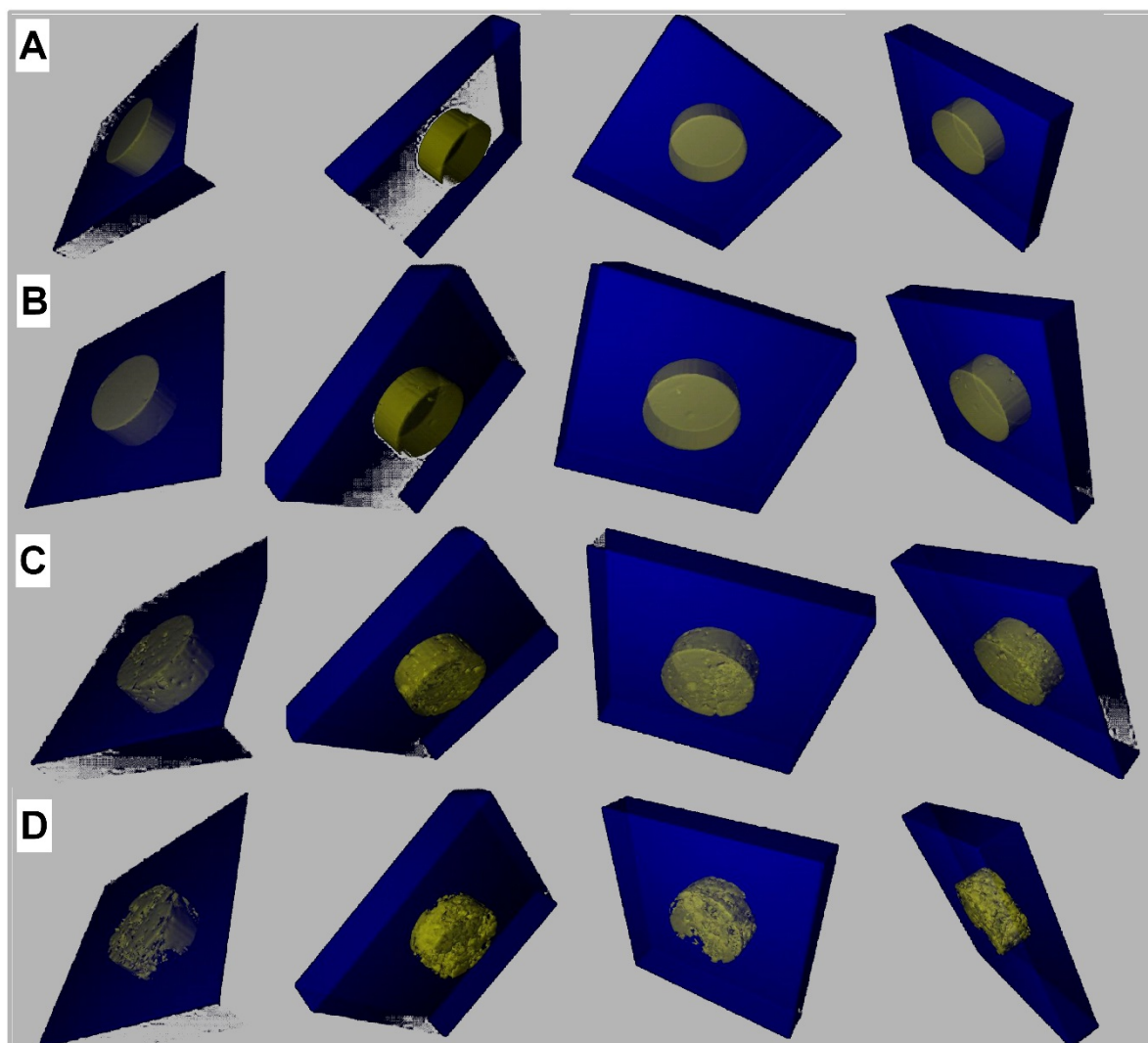


**Fig. 26 - Exemplary images taken from 3D rotation visualizations after the determination of a defined volume for density investigation. Ceramic high density parts are depicted in yellow for four different specimens: A) 100 w% CPC. B) 90/10 w% CPC/PLGA. C) 80/20 w% CPC/PLGA. D) 70:30 w% CPC/PLGA**

In Fig. 27. the results of the greyscale analysis are depicted. Here volumes of cement phase divided by lower density volumes were quantified in the defined discs, which are illustrated in Fig. 26.

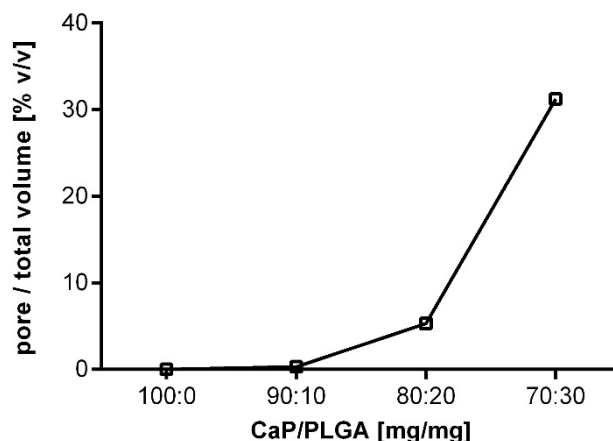
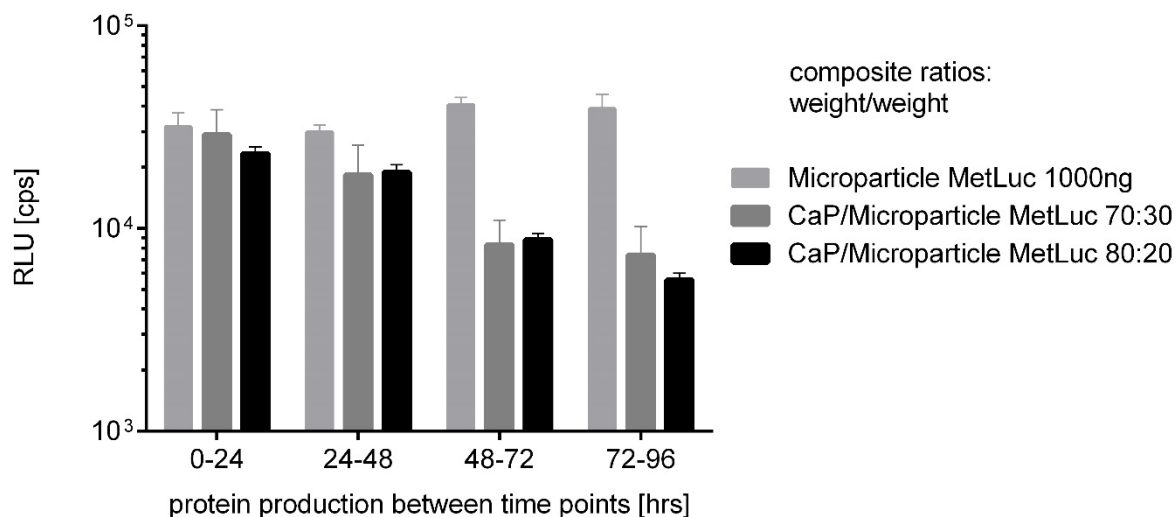


Fig. 27 - Pore volume to calcium phosphate cement volume ratio of four different CPC/PLGA weight to weight ratios. The ratio was calculated by macro programming of  $\mu$ -CT voxels slides as can be seen in Fig. 25

The calculated volume to volume ratios between the cement phase and the microparticle phase in the four different composites displayed an exponentially shaped increase in PLGA volume after the stepwise increase of CPC to PLGA weight to weight ratios. The non-linear course of the graph can be explained by the substantial difference in density between PLGA and cement.

### 3.3.2 Transfection efficiency of composite and microparticle specimens

Four CPC/PLGA composites as described above were additionally tested for their transfection efficiency *in vitro*. Protein production was measured over four days after transfection. Fig. 28 displays the results of those specimens, where bio-functionality was detected, and free PLGA microparticles with the same loading parameters were added to the experimental setup as a positive control.



**Fig. 28 - Transfection efficiency of microparticles loaded with a nanoparticle to polymer ratio of 0.5  $\mu$ g cmRNA/mg PLGA encapsulated in CPC in different weight to weight ratios on C2C12 mouse myoblasts. The doses for both free microparticles and components was 20  $\mu$ g cmRNA/cell (1000 ng/well). The reporter protein expression (*metridia luciferase*) activity was determined 24, 48, 72 and 96 h post transfection by measuring bioluminescence expressed in counts per second (cps).**

Transfection efficiency analysis of the composite specimens with CPC/PLGA %(w/w) between 80:20 to 70:30 exposed similar bioluminescence levels as free microparticles in the first two days after transfection. After 3 days, protein production decreased for the composites compared to pure PLGA microspheres. In contrast to the transfection efficiency tests on mouse fibroblasts (Fig. 21), the protein production on mouse myoblasts (Fig. 26) after free microparticle transfection showed no significant drop after 4 days and peak expression was observed after 72 h.

### 3.4 PLGA in nanoparticle carriers

PLGA, as versatile as it is in various therapeutic approaches, is also known to stabilize and enhance polyplexes on a nanosize-level, *i.e.* in chitosan complexes [41, 42, 101]. In the second project of this thesis a novel polyplex containing chitosan for potential targets where mucosa barriers have to be crossed was developed. After successful nanoparticle formation with cmRNA and chitosan alone, co-formulation with PLGA was established, examined and optimized to gain possible polyplex enhancement in terms of biocompatibility, stability and transfection efficiency by this process. The goal of the

---

second part of this thesis was to explore the potential of chitosan-based cmRNA complexes, with and without PLGA, for their applicability in potential future *in vivo* trials. The reason for co-formulation with another polymer as an alternative to pure chitosan-based polyplexes, is their lack of colloidal stability in physiological fluids, which challenged many chitosan-based nano-carrier related efforts in the last years [99-101]. For various different cargos, which have already successfully been encapsulated in chitosan-based nano-carriers, stabilizers like PEG or PLGA were additionally needed for successful *in vivo* functionality [102-104]. In this thesis, a comparison between chitosan- and co-formulated PLGA/chitosan polyplexes was conducted to determine the impact of co-formulation in physicochemical properties, especially the colloidal stability in a simulated physiological environment after optimizing the co-formulation itself.

### 3.4.1 Chitosan nanoparticle development and characterization

For this study Protasan<sup>®</sup> CL 113 UP, which is a water-soluble chitosan-chloride salt with a degree of deacetylation between 75 to 90 %, was used as the complexing agent for cmRNA, as it has already proven its potential as a complexing agent for DNA and other non-nucleic acid cargos [105, 106]. In a first trial, chitosan polyplexes with cmRNA coding for *metridia luciferase* were formed by pipetting and subsequent vortexing in N/P ratios of 0.5 to 10. In Fig. 29 size and zeta potential results for these particles, dispersed in water, are displayed.

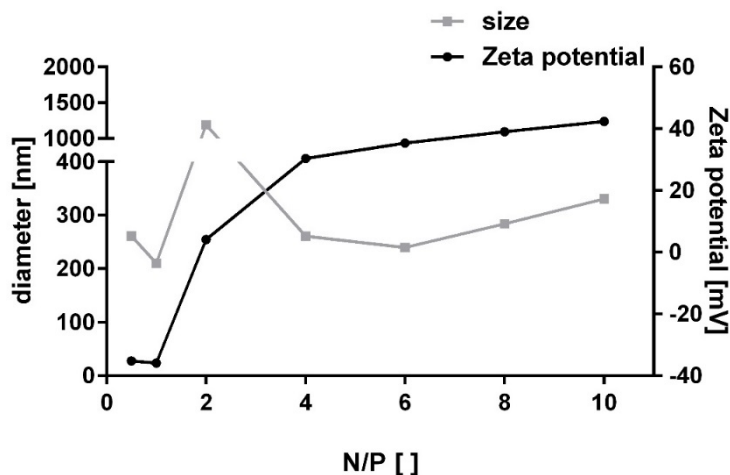


Fig. 29 – Nanoparticle size and Zeta potential of chitosan polyplexes at N/P ratios of 0.5 to 10. The particles were mixed by pipetting and subsequent vortexing.

The results of size analysis after 30 min of equilibration at room temperature show stable nanoparticles between 200 and 300 nm, except for N/P 2 where agglomeration was observed. Zeta potential analysis showed negatively charged particles at N/P ratios lower than 2 and a steady increase of surface charge in the range of 30 to 40 mV for N/P ratios between 4 and 10. At N/P ratio of 2 no charge was observed.

To investigate the polydispersity of the chitosan-based polyplexes the shapes of the size measurement graphs were examined, as well. Fig. 30 depicts the results of the size distribution measurements of all N/P ratios between 0.5 and 10.

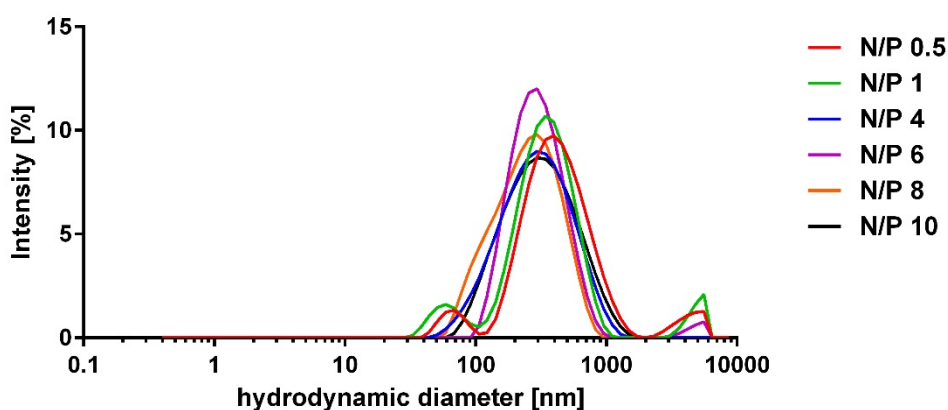
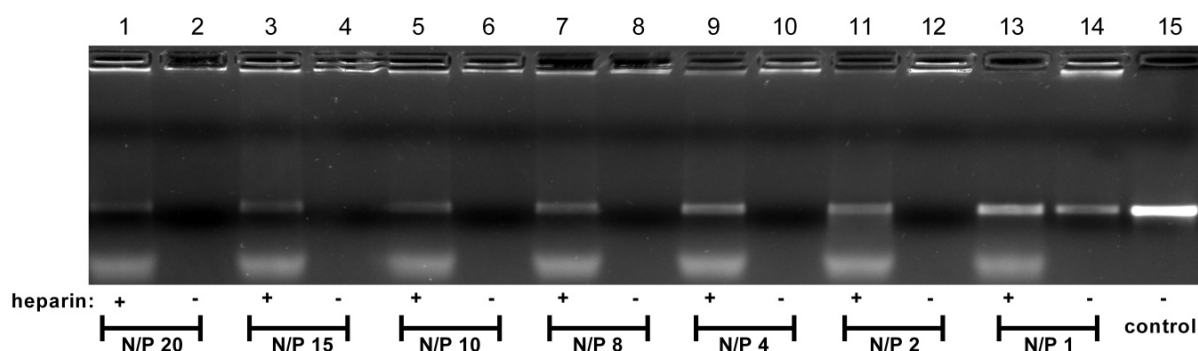


Fig. 30 - size distribution results from dynamic light scattering measurements in water of polyplexes characterized in Fig. 27.

Here, measurements for N/P 2 could not be detected as the agglomerates were either above the detection limit or no particles were formed in these conditions. All other specimens show a main peak at approximately 200 nm. Additionally, agglomeration peaks at sizes bigger than 1  $\mu\text{m}$  and low sized peaks at sizes between 30 and 100 nm can be observed for specimens, with an N/P ratio higher than 6.

Furthermore, gel electrophoreses was performed for polyplexes with N/P ratios from 1 to 20, to investigate the chitosan's ability to fully bind cmRNA at different polymer to nucleic acid ratios. An image of the gel is depicted in Fig. 31.



**Fig. 31 - Analysis of complex formation of chitosan (Protasan<sup>®</sup> CL UP 113) with cmRNA at N/P ratios of 1, 2, 4, 8, 10, 15 and 20. Uncomplexed cmRNA (control) is displayed in lane 15. From right to left two lanes were reserved for one N/P ratio where the right lane (-) shows the results of untreated samples and the left lane (+) the results of complexes treated with heparin for 30 min at 70°C on a shaker.**

Only at N/P 1 unbound cmRNA was detected in line 14, where no heparin was applied to the sample. At higher N/P ratios no band of free cmRNA could be detected in the untreated samples indicating that all cmRNA is complexed with chitosan. After complexation, the interaction between carrier and cargo could be reversed by the addition of heparin to the dispersion in lanes 1, 3, 5, 7, 9, 11 and 13.

### 3.4.2 Screening of O/W emulsion mixing techniques

As a next step the chitosan-based polyplexes were co-formulated with PLGA. In this project three different techniques were used for O/W emulsion formation. The first approach was a combination of osmotic mixing while the emulsion was stirred for 4 to 24 h with subsequent emulsion mixing by an Ultra Turrax homogenizer. This approach was tested, using different organic solvents like ethyl acetate and dichloromethane at different homogenizer settings for 2 to 15 min. Here, all products lead to similar results in particle size distribution after organic solvent evaporation. In Fig. 32 an exemplary size distribution of a product after emulsification *via* Ultra Turrax homogenization is displayed.

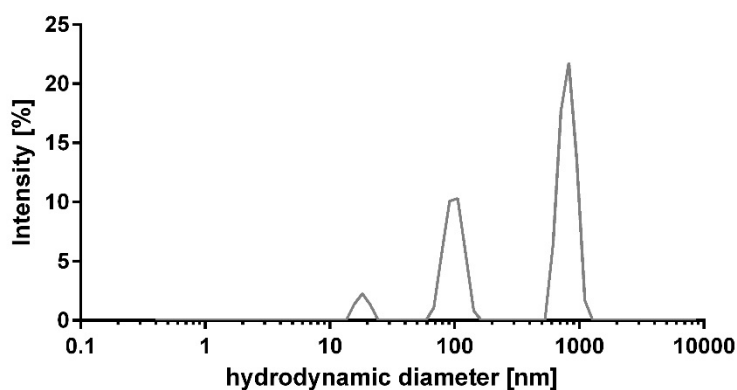


Fig. 32 - Exemplary size distribution of a PLGA/chitosan co-formulation polyplex after using an Ultra Turrax homogenizer for O/W emulsion formation.

The particle distribution shows three particle size families where one peak is in the range of 1  $\mu\text{m}$ , one in the range of approximately 100 nm and a small peak in the range of 20 nm.

As it was not possible with this technique to form homogeneous particles, a second approach was anticipated where the interaction between the immiscible phases is triggered by sonication. Here, the parameters of pulse intensity, their repetition and the times between pulsing were screened. By using sonication techniques for emulsification, the reproducibility of the co-formulated PLGA/chitosan particle formation increased substantially and the product became homogenous in size as displayed in Fig. 33.

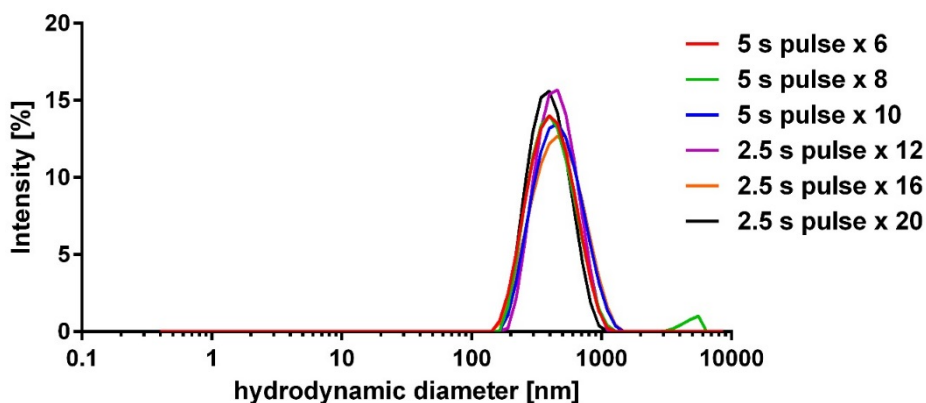


Fig. 33 - Exemplary size distribution of co-formulated PLGA/chitosan polyplexes after using a sonicator for emulsion formation.

In this experiment different pulse lengths and repetitions were screened for potential polyplex optimization in terms of homogeneity of the hydrodynamic diameter. As all of the co-formulation parameters used for this experiment resulted in the same homogeneous particle distribution after polyplex preparation, no further optimization steps were needed for this method of emulsification.

The results of the mean hydrodynamic diameter values and their respective zeta potential at different sonication pulses are shown in Fig. 34.

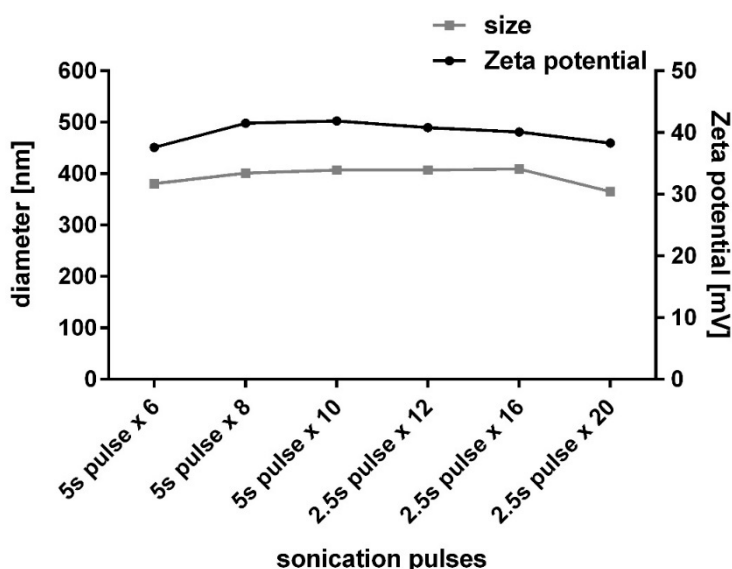
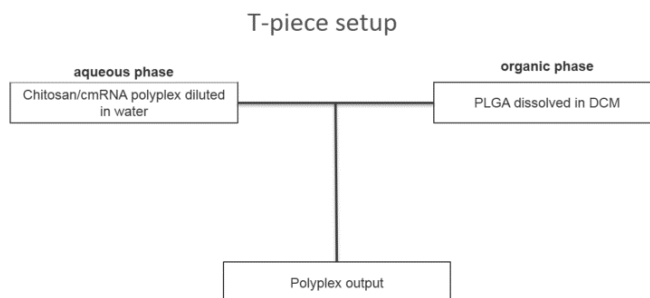


Fig. 34 - Nanoparticle size and zeta potential of co-formulated PLGA/chitosan polyplexes at an N/P of 10. The O/W emulsion was mixed by sonication with a pulsing of 5 s at 6, 8 and 10 pulses and 2.5 s at 12, 16 and 20 pulses, respectively.

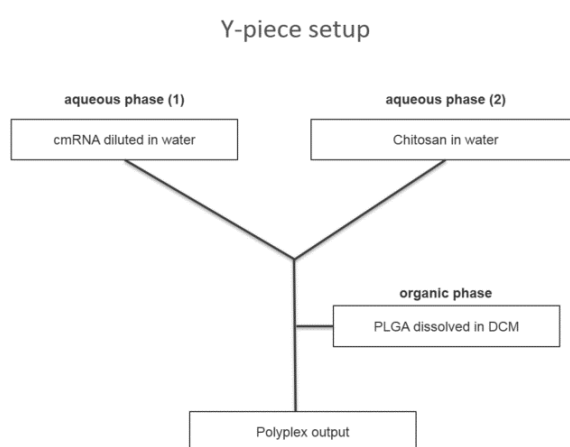
---

Size and zeta potential analysis showed hardly any differences in the outcome of the product due to variations in pulsing but the resulting polyplexes did not show any transfection efficiency (data not shown). One possible reason for the lack in functionality could be a degeneration or disruption of cmRNA during the sonication. Therefore, this method for co-formulation was abandoned for further experiments. Even higher reproducibility in particle size was achieved by emulsification *via* microfluidic mixing. An exemplary result of a screening is shown in Fig. 35 where two different mixing setups in microtube arrangements were investigated. Here, a T-piece setup (Scheme 9 A) represents a two fluid mixing arrangement where the premixed aqueous phase is mixed in one point with the organic phase and the emulsion is discharged in an angle of 90 °. A Y-piece setup (Scheme 9 B) splits the aqueous phase into two fluids where the chitosan and cmRNA is initially separated from each other.

A



B



**Scheme 9 – A) Schematic representation of the PLGA/chitosan/cmRNA-complex preparation process by microfluidic mixing in a “T-piece” setup. Chitosan polyplexes are mixed directly with the organic phase. B) Schematic representation of the PLGA/chitosan/cmRNA-complex preparation process by microfluidic mixing in a “Y-piece” setup. Chitosan polyplexes are mixed in a separate tubing before subsequently added to the organic phase.**

In a Y-piece setup the chitosan/cmRNA interaction and particle formation takes place immediately before the dispersion gets mixed to the organic phase. Both setups showed similar results in size and zeta potential as illustrated in Fig. 35. and first evidence of transfection efficiency *in vitro* (data not shown). The possibility of stabilizing the particle output by the addition of a buffer at a neutral pH was included into this pre-screening as well.

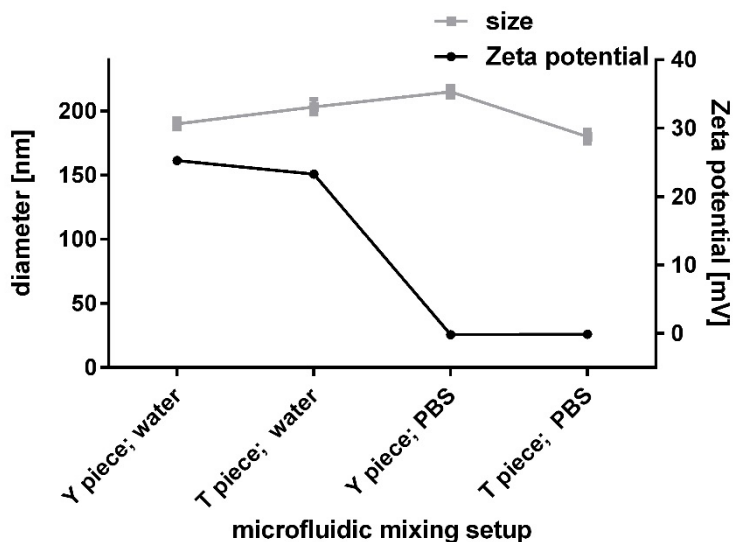


Fig. 35 - Nanoparticle size and zeta potential of co-formulated PLGA/chitosan polyplexes at an N/P of 10. The O/W emulsion was mixed by microfluidic mixings with either a T piece or a Y piece setup in either water or PBS as the diluent in the aqueous phase.

Apart from a zeta potential drop to almost no charge, the influence of a PBS-buffered aqueous solution can be neglected concerning particle formation. Furthermore, several different injection speeds and injection volumes were optimized before a standard operating protocol for the synthesis of PLGA/chitosan particles could be implemented. As the T-piece setup resulted in less effort in synthesis setup and the resulting particles could be reproduced at a defined injection speed, this mixing technique became the standard operating procedure for further experiments.

### 3.4.3 Screening of different PLGA polymers for the co-formulation

After being able to define optimized synthesis protocols in terms of emulsion mixing and gaining reproducibility in polyplex particle size and zeta potential, the influence of PLGA polymer ratios to chitosan and the type of PLGA was screened for highest transfection efficiency. Three different PLGA types representing different hydrophilic/hydrophobic behaviors, due to their chemical structure, were formulated in a constant polymer weight per weight ratio of 1:10 chitosan/PLGA. Here only three different polymers were tested as each of those represents a certain class of

hydrophobic behavior. (3.1.1) Transfection efficiency results after co-formulation with each one representative of a lactic- to glycolic acid ratios (LA/GA) are displayed in Fig. 36.

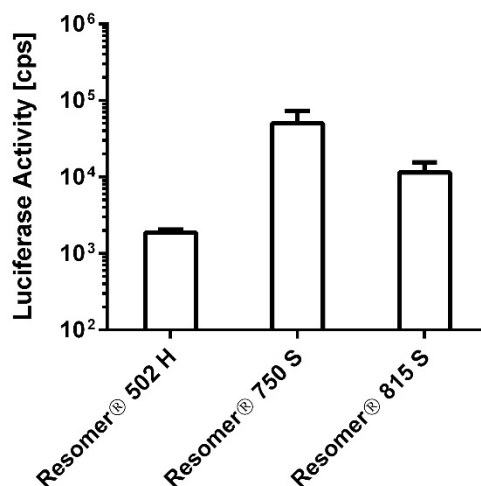


**Fig. 36 - Transfection efficiency of co-formulated PLGA/chitosan polyplexes at an N/P ratio of 8 on NIH3T3 mouse fibroblasts (600 ng cmRNA/well) formulated with different PLGA types. For all specimens the cmRNA encapsulation efficiency was determined before transfection. cmRNA dosage was kept constant for all specimens during the experiment. The reporter protein (*metridia luciferase*) activity was determined 24 h post transfection by measuring bioluminescence expression in counts per second (cps).**

Co-formulation with Resomer® 750 S, representing PLGA polymers with a LA/GA ratio of 7.5/2.5, resulted in particles with the highest protein activity after 24 h post transfection, followed by the more hydrophobic Resomer® 815 S and the rather hydrophilic Resomer® 502 H with an acid-terminated head-group.

Furthermore, different ratios of 1:1, 1:62.5 and 1:125 (w/w) of chitosan to Resomer® 750 S were tested for their influence on transfection efficiency after particle formation, as well. The results of this experiment are displayed in Fig. 37.

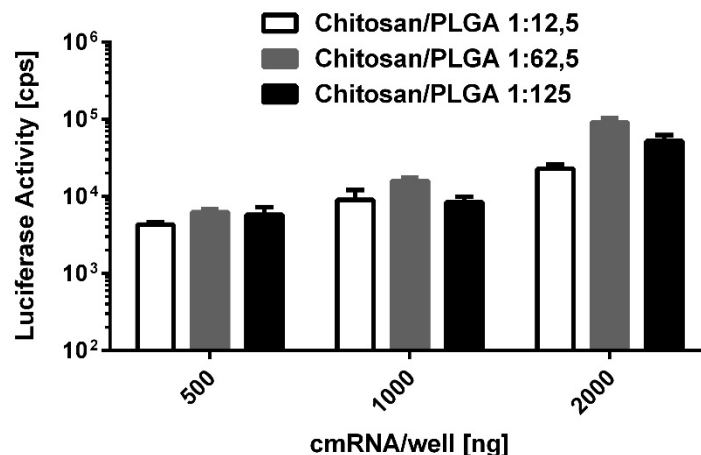


Fig. 37 - Transfection efficiency of co-formulated PLGA/chitosan polyplexes at an N/P ratio of 8 on NIH3T3 mouse fibroblasts formulated with different chitosan to Resomer<sup>®</sup> 750 S weight to weight ratios. The reporter protein (*metridia luciferase*) activity was determined 24 h post transfection by measuring bioluminescence expression in counts per second (cps)

In all dosages of cmRNA on cells from 500 to 2000 ng/well, highest protein activity could be measured for a polymer to polymer ratio of 1:62.5 (w/w). Hence, this polymer ratio was set as standard for further investigations.

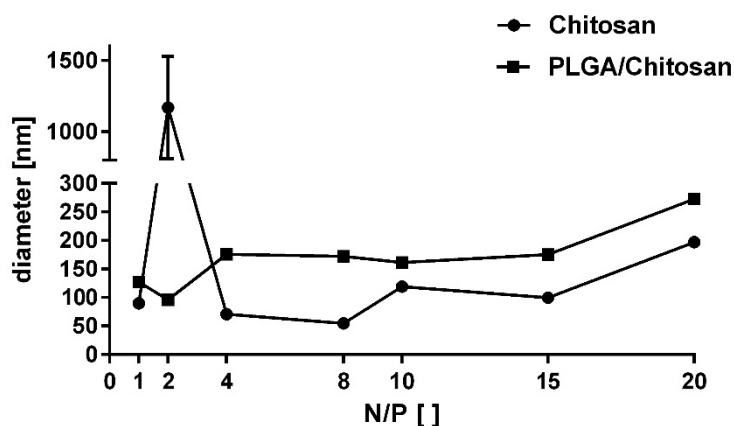
### 3.5 Investigation of co-formulation effects

As a next step after the pre-screening of chitosan/cmRNA polyplexes, the impact of co-formulation with PLGA was investigated in detail. Here, the main focus was on the analysis of possible stability enhancements in physiological fluids and a direct comparison for cytotoxicity *in vitro* between both polyplex types.

#### 3.5.1 Polyplex size and zeta potential comparison

First the effect of co-formulation with PLGA on the hydrodynamic diameter and zeta potential on the co-formulated particles was investigated. The results for size and zeta potential measurements are displayed in Fig. 38.

A



B

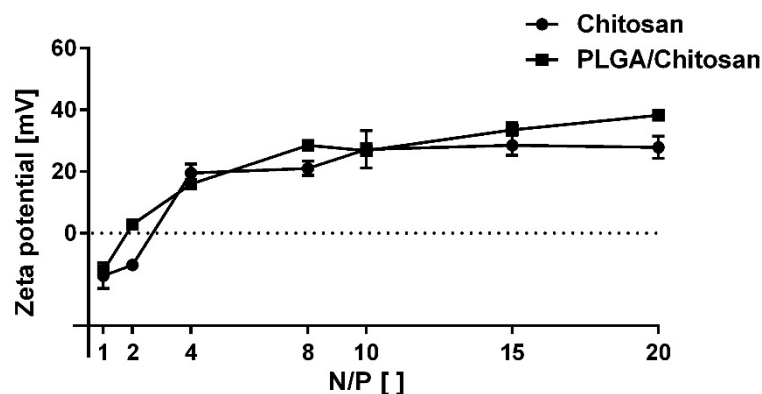


Fig. 38 – A) Hydrodynamic size and B) Zeta potential of chitosan- and PLGA/chitosan (62.5:1 w/w) polyplexes at N/P ratios of 1, 2, 4, 8, 10, 15 and 20.

No significant size difference was observed for N/P ratios between 1 and 20 for both pure chitosan- and PLGA/chitosan polyplexes. Chitosan polyplexes agglomerate at N/P 2 with resulting particle diameters  $1 \pm 0.5 \mu\text{m}$  and beyond detection limits. This effect could not be observed for co-formulated particles at the same N/P ratio where the surface charge is negative. In general, PLGA/chitosan particles were slightly bigger compared to chitosan polyplexes except particles at N/P 2.

In contrast to that, PLGA incorporation did not influence the surface charge of the nanoparticles. Generally, both chitosan-based and co-formulated PLGA/chitosan polyplexes, show a steady increase in surface charge from -11/-12 mV at N/P 1 to +25/+24 mV at N/P 10. From N/P 10 to 20 no further increase in zeta potential was measured for both polyplex types. The biggest difference between chitosan- and co-

formulated PLGA/chitosan polyplexes in zeta potential was observed at N/P 2, where co-formulated particles show a negative surface charge compared to almost no charge for chitosan particles.

### 3.5.2 Polyplex imaging *via* SEM

Along with the results from size and zeta potential experiments the topological shape of the nanoparticles was investigated for any irregularities and differences between chitosan and co-formulated PLGA/chitosan polyplexes. Here, scanning electron microscopy was performed and exemplary images are depicted in Fig. 39.

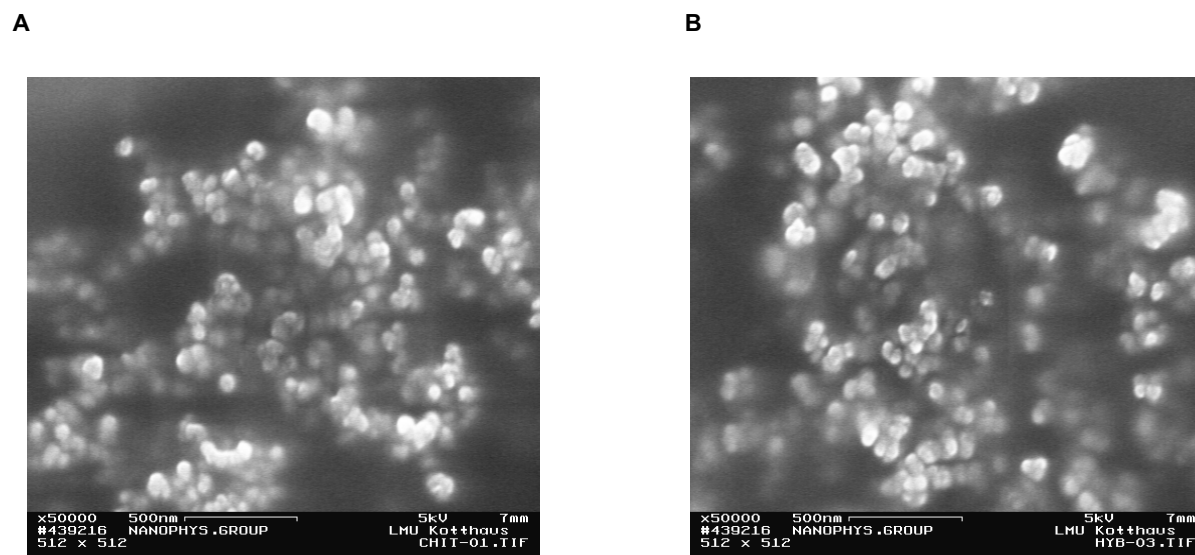


**Fig. 39 - Exemplary images of A) chitosan and B) co-formulated PLGA/chitosan nanoparticles taken by scanning electron microscopy at a magnification of 50000.**

After qualitative observation and analysis of the images no significant differences in shape or agglomeration behavior were perceived. Both chitosan- and PLGA/chitosan polyplexes form clusters of particles and appear in a spherical shape.

### 3.5.3 Influence on complexation and particle stability

The enhancement of colloidal stability and the ability to maintain integrity/compaction of the chitosan polyplexes in physiological fluids was one of the main goals of this project. The ability to protect the cargo in a physiological environment is critical for successful activity after transfection *in vivo*. Fluorescence resonance energy transfer (FRET) analysis was used as a measure for the compaction of cmRNA and therefore a good measure for particle stability. In Fig. 40 the compaction level of cmRNA complexed with either chitosan or co-formulated PLGA/chitosan polymer blends at N/P ratios of 8 and 15 in different amounts of PBS, is shown.

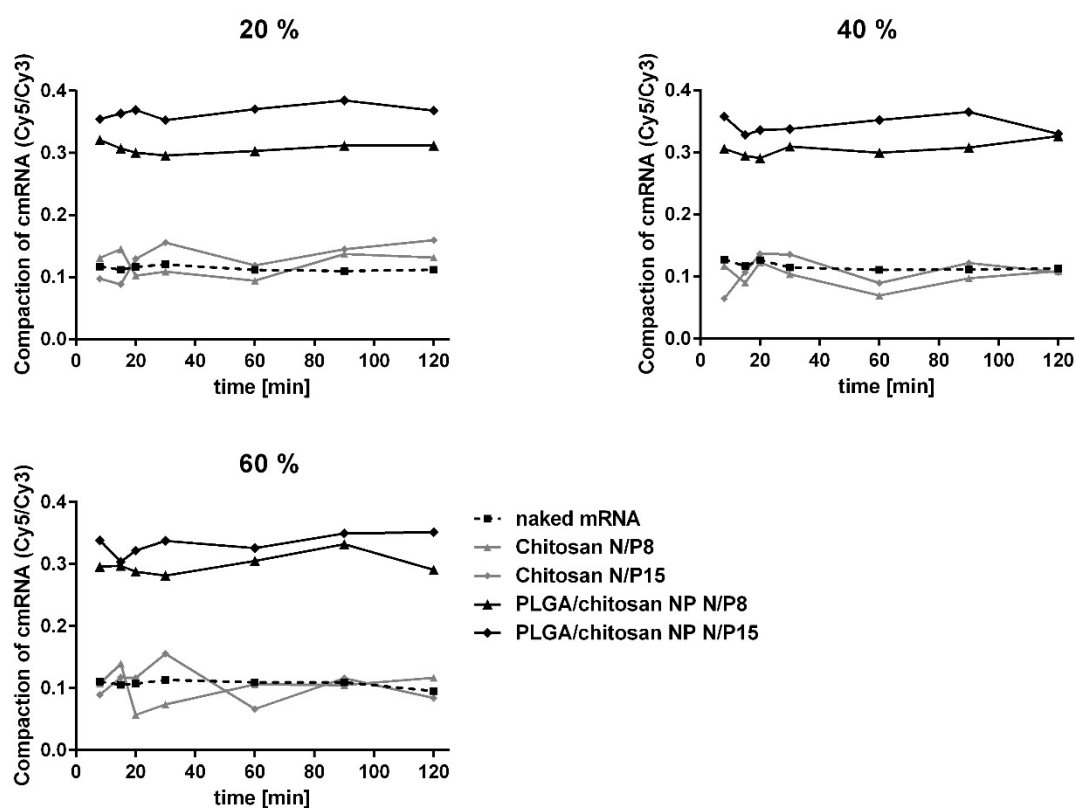
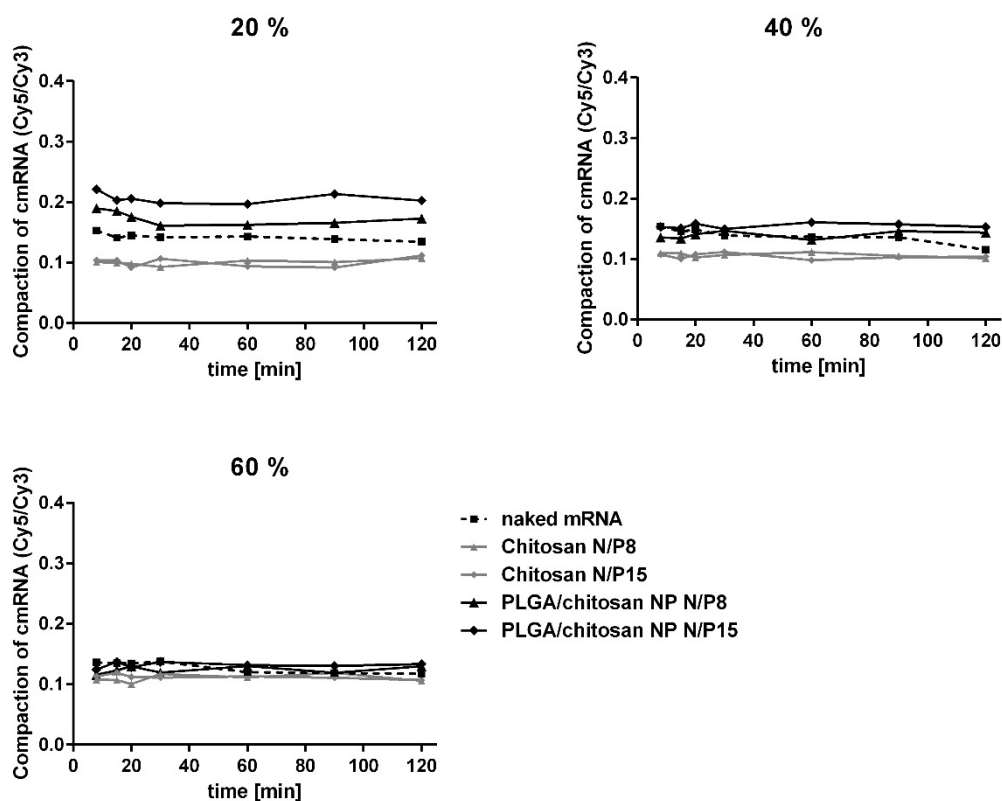


Fig. 40 – FRET analysis over time of chitosan- and co-formulated polyplexes mixed with PBS measured at multiple time points between 8 min and 2 h. Nanoparticle dispersions were mixed with 20 %, 40 % and 60 % of the test fluid.

Here, all three concentrations of polyplex dispersion in PBS showed no substantial differences in compaction levels for each specimens over time. In every setting both co-formulated polyplex samples show approximately 3 times the FRET signal than free

cmRNA or chitosan/cmRNA polyplexes. N/P 15 signal exceeds the signal of N/P 8 marginally in all settings.

After determining the specimens' stability in PBS the nanoparticles were analyzed after mixing with cell culture medium (DMEM). Results are shown in Fig. 41.



**Fig. 41 - FRET analysis over time of chitosan- and co-formulated polyplexes mixed with DMEM measured at multiple time points between 8 min and 2 h. Nanoparticle dispersions were mixed with 20 %, 40 % and 60 % of the test fluid.**

The stability was measured after mixing the nanoparticle dispersions to three different concentrations of DMEM, which was used for *in vitro* experiments. For all concentrations of DMEM no compaction change over time was detected for any of the test dispersions. At 20 % DMEM, uncomplexed cmRNA shows higher FRET signals than chitosan/cmRNA polyplexes. This could be due to partly compaction by the ingredients of DMEM, like amino acids or different sugars. The same can be seen for 40 % DMEM, as well. Both, in 20 and 40 % DMEM co-formulated PLGA/chitosan polyplexes showed stable but lower compaction over time, compared to the results measured for mixing with PBS. The compaction drops almost to the level of uncomplexed cmRNA at 40 % and cannot be distinguished at 60 %.

The third test fluid which was investigated was fetal calf serum (FCS) and stability results are depicted in Fig. 42.

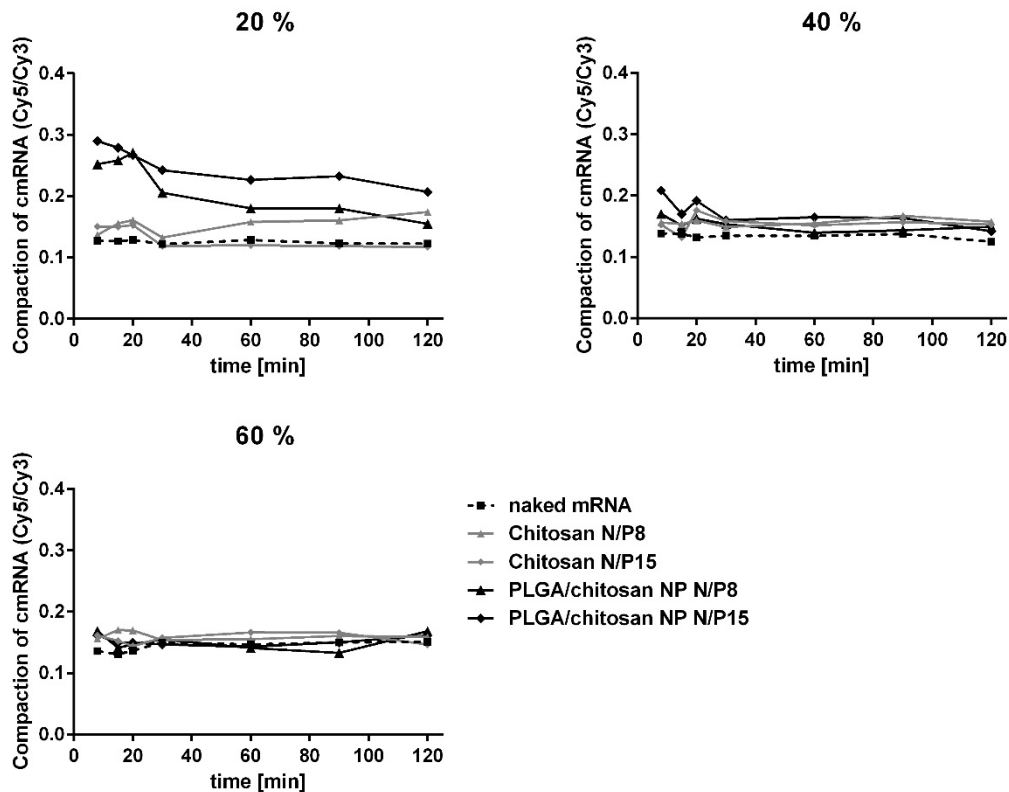


**Fig. 42 - FRET analysis over time of chitosan- and co-formulated polyplexes mixed with FCS measured at multiple time points between 8 min and 2 h. Nanoparticle dispersions were mixed with 20 %, 40 % and 60 % of the test fluid.**

Co-formulated PLGA/chitosan polyplexes showed again the best compaction levels at 20 % of FCS. In contrast to measurements in DMEM and PBS, the high level of compaction decreases steadily over 2 h. Chitosan polyplexes showed again hardly any compaction, but slightly bigger compaction levels than uncomplexed cmRNA in all test settings. At 40 % serum the stability of co-formulated polyplexes decreased to the level of uncomplexed cmRNA much faster within about 30 min post mixing. At 60 % FCS the compaction values drop immediately after mixing to the level of uncomplexed cmRNA. To conclude, serum has the potential to lower the co-formulated polyplexes' stability by steady erosion over time while chitosan/cmRNA complexes show hardly to any compaction in all settings.

To conclude, FRET analysis revealed that chitosan-based particles showed little complexation compared to uncomplexed cmRNA and no substantial stabilization in all tested media. In contrast, FRET analysis indicated a substantial increase in cmRNA compaction for co-formulated PLGA/chitosan particles for all N/P ratios in all test media. In general, complexation was higher for N/P 15 compared to N/P 8 in the case of co-formulated particles.

### 3.5.4 Influence of co-polymerization on cytotoxicity

Apart from being functional and stable in physiological fluids, carrier systems for nucleic acids are desired to be as non-toxic and biocompatible as possible to gain a relatively wide therapeutic efficacy. Therefore, biological functionality and cytotoxicity comparisons between chitosan- and co-formulated PLGA/chitosan polyplexes were conducted side-by-side. In Fig. 43 MTT assay measurements for chitosan-based polyplexes are shown.

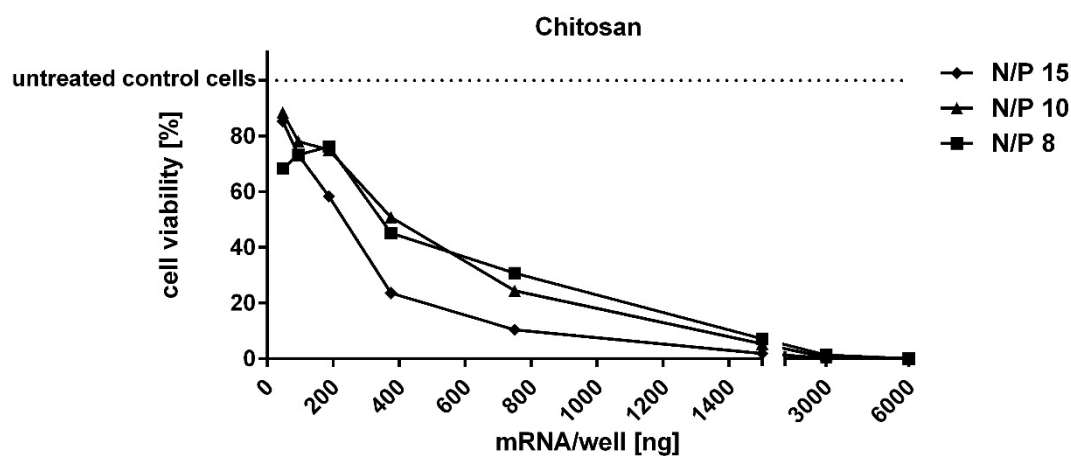


Fig. 43 - MTT assay results for chitosan polyplexes on NIH3T3 mouse fibroblasts. The results are normalized to untreated cells which were seeded on the respective plates. N/P ratios of 8, 10 and 15 were analyzed.

In the case of pure chitosan polyplexes toxicity is prominent already at very low doses. Almost no cell viability can be observed from 1.5  $\mu\text{g}$  cmRNA/well and higher. Below 1.5  $\mu\text{g}$  cmRNA/well the toxicity is proportional to the N/P ratio and therefore the polymer content. The more polymer which was added to the transfection media, the lower the cell viability was identified after 24 h.

In the same experiment co-formulated PLGA/chitosan polyplexes at the same N/P ratios were tested for their biocompatibility and the results are shown in Fig 44.

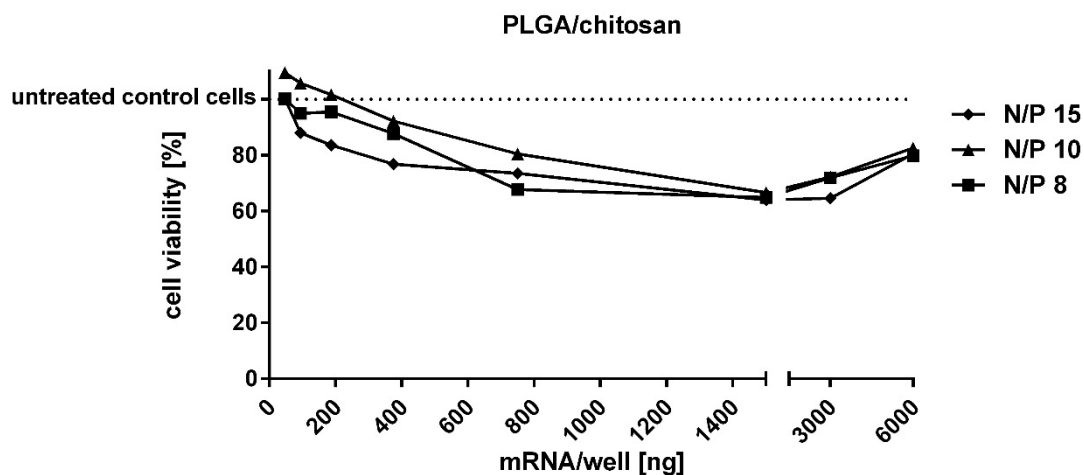


Fig. 44 - MTT assay results for co-formulated PLGA/chitosan polyplexes on NIH3T3 mouse fibroblasts. The results are normalized to untreated cells which were seeded on the respective plates. N/P ratios of 8, 10, and 15 were analyzed.

In contrast to chitosan/cmRNA complexes, cells transfected with co-formulated PLGA/chitosan polyplexes exhibit high cell viability, even at high doses after 24 h post transfection. Here, no trends in N/P ratio comparison can be observed and cell viability never declines below approximately 80 %. All in all, the PLGA/chitosan polyplexes can be labelled as non-toxic in the given experimental setup. The negligible decline in cell viability for all N/P ratios at 6000 ng cmRNA/well was accounted to fluctuations of MTT signal depending on the position of the respective well plate.

### 3.5.5 Influence on transfection efficiency

The high level of biocompatibility of co-formulated PLGA/chitosan polyplexes was observed in the experiment results of the transfection efficiency tests, as well. In Fig. 45 A, a visualization of the transfection process for co-formulated particles is displayed.

A

B

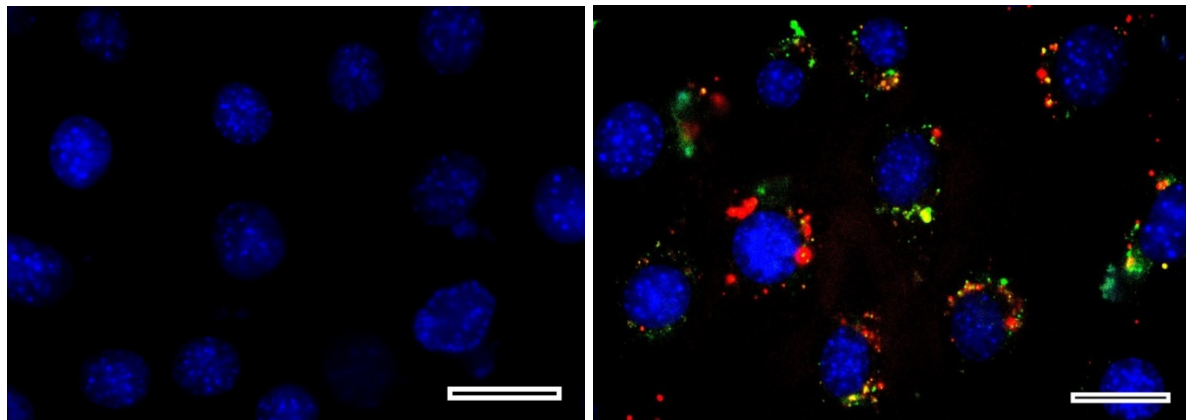


**Fig. 45 – Exemplary images of NIH3T3 mouse fibroblasts taken by fluorescence microscopy. The scale bar represents a length of 10  $\mu$ m. The nuclei are displayed in blue-, cmRNA in red- and recombinant protein developed *via* transfection in green color. A) The image was taken after 24 h post transfection and the cells were treated with water. B) The image was taken after 24 h post transfection and depicts cells transfected with co-formulated PLGA/chitosan polyplexes at an N/P ratio of 15. The dose was 1  $\mu$ g cmRNA/well.**

In the exemplary image of cells 24 h after transfection with co-formulated polyplexes the red dots indicate internalized cmRNA in the cytosol and the recombinant protein in green color after successful translation. The quantification of protein activity after 24 h post transfection of both chitosan- and co-formulated PLGA/chitosan polyplexes is depicted in Fig. 46. Here the *luciferase* activity was measured for dosages between 47 and 6000 ng cmRNA/well for both chitosan- and co-formulated PLGA/chitosan polyplexes at N/P ratios of A) 8, B) 10 and C) 15.

A

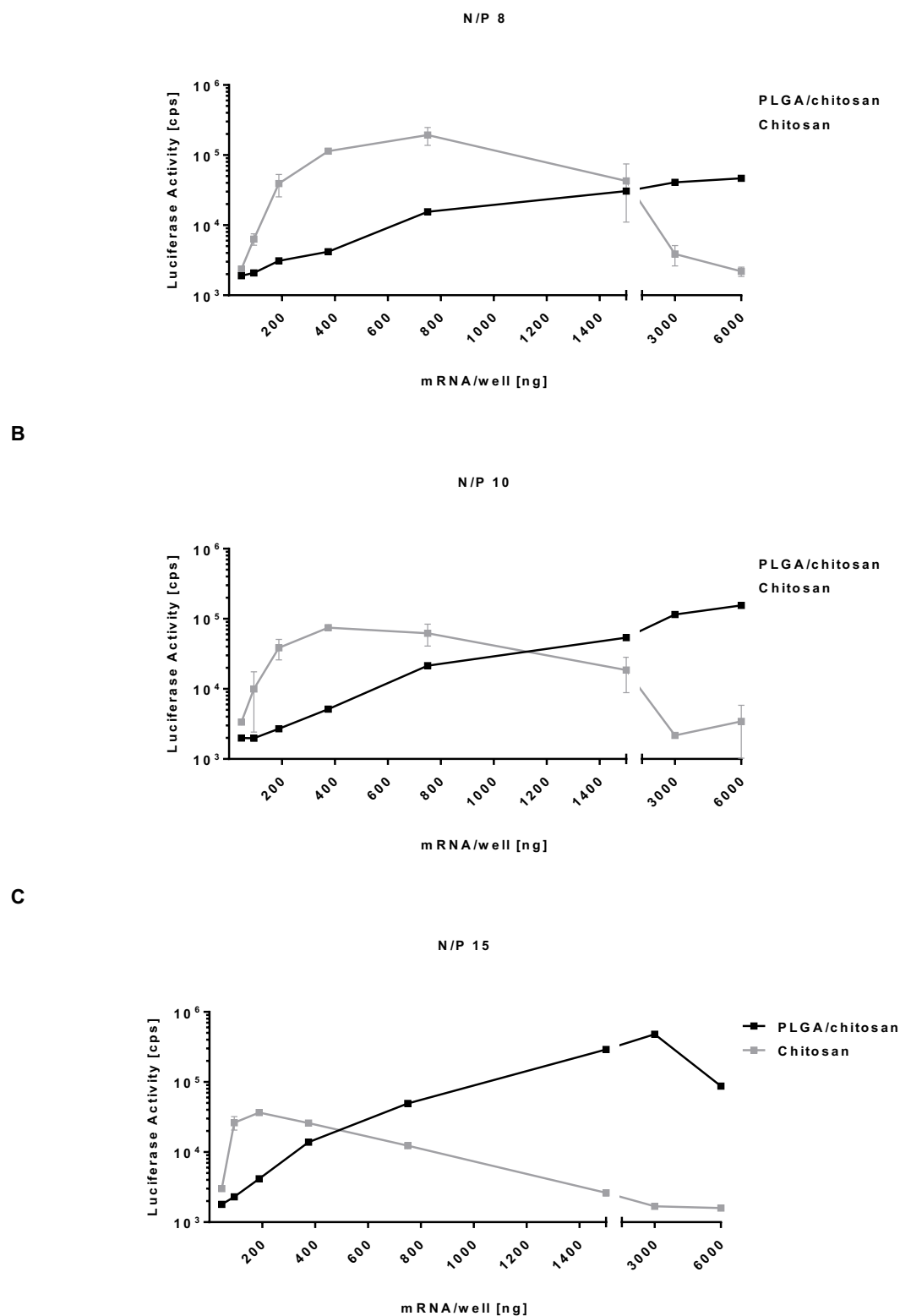


**Fig. 46 - Transfection efficiency of chitosan and co-formulated PLGA/chitosan polyplexes at N/P ratios of 8, 10, and 15 on NIH3T3 mouse fibroblasts. The reporter (*metridia luciferase*) activity was determined 24 post transfection by measuring bioluminescence expressed in counts per second (cps).**

Chitosan polyplexes exhibit peak expression at N/P 8 and decrease with increasing N/P ratio. The shift of peak expressions to lower dosages can be accounted to the efficiency and the toxicity of the chitosan. Peak expression with following decline in luminescence at higher dosages for co-formulated PLGA/chitosan nanoparticles was only perceived at N/P 15 where it exceeds the luminescence levels of chitosan polyplexes. In contrast to chitosan polyplexes the peak expression shifts to higher dosages with increasing N/P ratios.

## Discussion

The results of both micro- and nanoparticle experiments demonstrate the biocompatibility and the validity of poly (lactic-co-glycolic acid) as a carrier agent in the field of chemically modified messenger RNA delivery. On the one side, the polymer was successfully used as a matrix polymer for the incorporation and immobilization of lipoplexes containing cmRNA, with the ability to release its cargo when put into aqueous solutions. These functionalized microparticles were successfully incorporated into calcium phosphate (CaP) cements to form injectable composites with the potential of transfecting cells at site.

On the other side, PLGA enhanced chitosan/cmRNA polyplexes as a stabilizer with direct impact on cytotoxicity, transfection efficiency and the compaction ability of a chitosan-based polyplex.

### 3.6 PLGA microparticles as a lipoplex distribution system

In the first part of this thesis the incorporation of a functional cmRNA delivery system into injectable calcium phosphate-based cements was investigated. Early pre-screening results revealed a requirement for an intermediate phase between lipoplexes and calcium phosphate cement, as direct mixing did not result in any bio-functional activity. The lipoplexes were encapsulated into spherical PLGA matrices to provide the ability to immobilize the cmRNA carriers in the cements and release the bio-functional carrier at site. It was already discovered that the combination of CPC and PLGA microparticles conveys benefits in bone substitute degradation and cell in-growth into the implant in the healing process [58, 76, 77]. In this study the idea was to enhance this approach by the incorporation of a bio-functional agent in the form of cmRNA/lipoplexes into such microparticles with the potential of increasing faster bone healing by *i.e.* the introduction of growth factors, at site.

The formation process of the microparticles needed to be adjusted and optimized for an initial lipoplex release which leads to immediate transfection efficiency after contact with aqueous fluids. Results showed that it is possible to encapsulate lipoplexes into degradable polymer microspheres by a double emulsion solvent evaporation technique without destroying the complexes' functionality, but early experiments resulted in either

broken or too big microparticles. It was important to define a standard operating procedure for the formation process which provides reproducibility in size and efficiency. Using different Resomer<sup>®</sup> PLGA types for lipoplex encapsulation revealed the influence of the polymer's chemical properties on the ability to form appropriate microparticles. Resomer<sup>®</sup> 502H, 503 H, and 504 H which represent the most hydrophilic polymers used in these experiments, due to their GA/LA ratio of 1/1 and their acidic terminations, showed lowest transfection efficiency and biggest mean sizes with a sponge-like microparticle appearance. Their geometrical features resemble those of non-loaded particles, which indicated that these polymers were not able to successfully encapsulate the lipoplex cargo. Therefore, these polymers were excluded from any further experiments. An optimal encapsulation - to transfection efficiency balance was found by using polymers which presented comparably moderate to high hydrophobicity like Resomer<sup>®</sup> 750 S, 752 S, 755 S and 858 S. The hydrophobicity favors interaction of the lipoplex as proposed by the distributor [107]. Here, Resomer<sup>®</sup> 750 S was defined as the polymer of choice for further experiments due to best transfection efficiency results and a rather high reproducibility in particle formation.

Next, the influence of varying the surfactant concentrations in both the first and second aqueous phase of the particle formation protocol was investigated. For both aqueous solutions it was shown that as long as a minimum surfactant concentration for avoiding emulsion collapse was met, the surfactant concentration itself did not have any obvious effect on both size and transfection efficiency. In contrast, the emulsification process by different sonication protocols *via* a sonifier probe revealed a drastic drop in transfection efficiency, when the pulsing time of sonication and therefore the input power is exceeding an optimal process limit. As, in this case, no obvious effect on particle size and topology compared to particles made with lower sonication pulse times was detected, it is likely that the cargo itself was damaged or even destroyed by an excess of power input by sonication.

Varying the nanoparticle concentration during microparticle formation had the highest capacity to adjust the microparticles' size, topology and transfection efficiency. It was possible to optimize the ratio between lipoplex concentration in the first aqueous phase and a constant amount of PLGA in the organic phase to gain highest protein production levels after *in vitro* transfection. Here, a correlation between the specific surface of the microparticles and their ability to transfect cells was found. Highest protein production

---

occurred with particles, which exhibited relatively small particle sizes and rather high surface pore areas. The initial swelling of the microparticles which enables an initial diffusion of lipoplexes encapsulated on the surface, is favored at high specific surface areas. Hence, more lipoplex is initially released which leads to optimal transfection efficiency. This observation corresponds with literature about other PLGA-microparticle-based release systems, stating that controlling the specific surface of the microparticles is crucial for the control over release behavior of the cargo at hand [98, 99].

Consequently, an interval of lipoplex loading parameters between 0.5 and 1  $\mu\text{g cmRNA/mg PLGA}$  was determined where the product exhibited a maximum of transfection efficiency. Encapsulation efficiency analysis for these two loading parameters revealed higher loss of educt (lipoplex) during the formation process for 1  $\mu\text{g cmRNA/mg PLGA}$  with similar transfection efficiency as 0.5  $\mu\text{g cmRNA/mg PLGA}$ . Therefore, and with the aim of efficiently and economically optimizing particle formation parameters, the decision was made to continue the study with a particle loading parameter of 0.5  $\mu\text{g cmRNA/mg PLGA}$ .

*Via* fluorescence microscopy and lipoplex labelling it was possible to visualize the process of lipoplex release from the microparticle matrix during the first 4 days after transfection. The signal for both cmRNA and lipid contents was detected in the microparticles, as well as in the surrounding cells. In this experiment, a burst release of lipoplex which lead to the internalization of both lipids and cmRNA in cells was detected, while a second fraction of cargo was still entrapped in the polymer matrix after 4 days under simulated physiological conditions *in vitro*. The lipoplex fraction which was released was able to transport the cmRNA into the cytosol where it was successfully translated into the encoding protein. Different independent PLGA microparticle studies revealed similar patterns for an initial diffusion of cargo out of the matrix. Depending on the PLGA type and the physicochemical features of the cargo an initial burst release is often followed by a slow release *via* polymer erosion [97-99]. Furthermore, the results disclosed that cmRNA is cleared faster from the cytosol as their lipid counterparts which could be detected even after 4 days after transfection. As a next step the optimized particles were incorporated into CPCs to investigate their potential in combination with the injectable bone substitute.

---

### 3.7 PLGA microparticles as composite in injectable calcium phosphate cements

The incorporation of lipoplex loaded PLGA microspheres into calcium phosphate-based injectable cements resulted in composite specimens with an adjustable porosity. The weight to weight ratio of calcium phosphate (CPC) phase and PLGA polymer phase was adjusted successfully to control cement porosity in the composite after curing. As the densities between cement and polymer phases differ substantially, the impact of increasing polymer volume could be visualized *via* computer tomography. The porosity quantification results showed an exponential increase in low density polymer/air phase when the weight to weight ratio of PLGA to CPC was gradually increased. The exponential nature of the increase of polymer volume in the specimens is associated with the substantial differences in density between the two phases of the composite. At ratios lower than 70:30 (cement/polymer) % (w/w) the specimens lost their integrity after hardening which disqualified them from further investigations. Depending on the % (w/w) ratio of CPC to PLGA we could show that lipoplexes were still released out of the polymer/cement matrix which resulted in positive transfection of target cells *in vitro*. Transfection efficiency analysis *via* bio-luminescence measurements revealed similar results for particles compacted in the cement matrix and free microparticles at cement to polymer ratios lower than 90:10 % (w/w) after 24 h. The decline in protein production after 48 h could be explained by the limited surface area of microparticles which could directly swell at the presence of aqueous fluids.

### 3.8 The enhancement of chitosan/cmRNA complexes by co-formulation with PLGA

In the second part of this thesis the first aim was to investigate the capacity of chitosan for cmRNA compaction and complexation. We confirmed that chitosan is able to bind negatively charged cmRNA due to its deacetylated state, where free amines provide the positive charge. But the resulting polyplexes resulted in labile nanoparticles with hardly any compaction and stability in physiological fluids like DMEM or serum which was observed by FRET analysis. This lack of stability was observed in other studies

dealing with chitosan as a carrier system for nucleic acids [102] and could be due to its chemical structure. Compared to other well-investigated polyplex agents like branched polyethyleneimine (brPEI) the polymer itself is elongated and has only one primary amine per deacetylated monomer. In contrast brPEI exhibits a network of interacting primary-, secondary and tertiary amines which together form a dense network of positive charges (charge per weight for brPEI: 1:43 x 1/g/mol; for chitosan: 1:190 x 1/g/mol) [28, 108]. Hence, the focus was placed on the enhancement of chitosan/cmRNA polyplexes by the co-formulation with PLGA in terms of cmRNA compaction and stability in physiological fluids. For this purpose, PLGA was incorporated *via* a solvent evaporation technique again with interface interaction between the chitosan polyplex dispersion and an organic phase containing the polymer in the presence of PVA as the emulsion stabilizer. The adjustment of the co-formulation process in terms of the emulsification process and the optimal composition of chitosan to PLGA polymer led to reproducible polyplex formation. Especially using the highly controlled method of microfluidic mixing for interphase co-formulation showed high reproducibility in size and efficiency due to the controlled adjustability of process parameter [109, 110]. The main difference of both double emulsion solvent evaporation techniques in the microparticle formation as described above and the nanoparticle co-formulation was the optimization of the energy input to the respective emulsions. Here, it was possible to form nano-sized co-formulations with an incorporation of PLGA to the chitosan polyplex due to fine tuning of the microfluidic mixing. Due to these standard operating procedure modifications for PLGA co-formulation, an investigation of the effects of co-formulation on the nanoparticles' properties was made possible. It was not possible to confirm any incorporation of PLGA into chitosan polyplexes directly by chemical analysis but comparisons to chitosan polyplexes in terms of physicochemical properties, colloidal stability in physiological fluids, biocompatibility and transfection efficiency indirectly showed differences in particle behavior.

First size comparisons were conducted which revealed that co-formulation made the nanoparticles slightly bigger in hydrodynamic diameter, even though obvious differences in the surface or spherical shape could not be detected. Zeta potential analysis revealed no substantial differences between chitosan- and PLGA/chitosan polyplexes at different N/P ratios. Hence, in contrast to shielding processes such as PEGylation, the zeta potential could be maintained although another agent was

introduced to the nanoparticle structure [104, 111]. These results indicate that PLGA was incorporated into the nanoparticles without shielding the positive charges derived from chitosan.

Furthermore, it was demonstrated that the degree of compaction was considerably increased after co-formulation of chitosan/cmRNA complexes with PLGA. Co-formulation enabled protection from destabilization in physiological media comprising FCS, including increased stability in cell culture medium and PBS. Compaction of cmRNA analysis *via* FRET analysis also revealed a steady increase in stability in all test media from low to high N/P. FRET analysis revealed the PLGA's capacity to increase the colloidal integrity of chitosan/cmRNA complexes, which possibly prevents premature particle decomposition in future *in vivo* applications. In summary, chitosan/cmRNA composites can be successfully complemented by PLGA addition, which results in enhanced compaction and protection of the cargo without changing the surface charge. PLGA/chitosan polyplexes exhibit substantially higher colloidal stability in simulated physiological conditions than chitosan/cmRNA complexes alone. The effects of co-formulation were also observed in the analysis of transfection efficiency and cytotoxicity on mouse fibroblasts. The trends in cell viability in combination with transfection efficiency revealed a rather narrow dosing window for chitosan-based nanocomplexes. The decrease of protein production and therefore the transfection efficiency correlates with a decrease in cell viability, meaning an increase in toxicity. The higher the N/P ratios, the more the peak expression shifted to lower dosages of cmRNA on cells.

In contrast, no substantial cell toxicity at any dosage could be observed for PLGA/chitosan particles at all tested N/P ratios. The transfection results demonstrated functionality at high dosages with even higher peak luminescence levels as chitosan polyplexes. Therefore, the positive charge of chitosan polyplexes cannot be determined as the main reason for cytotoxicity, as the co-formulated particles with PLGA exhibited comparable charge properties. Hence, the increase in cell viability after transfection for co-formulated polyplexes is solely due to the properties of PLGA and its co-formulation to the polyplexes. The shift to higher dosages to achieve high levels of protein production for co-formulated particles could be attributed to the PLGA's chemical behavior in aqueous fluids, as well. Due to its rather hydrophobic character, delayed hydrolysis takes place over time [60]. This could lead to a delay in

cmRNA translation at a certain point during cell uptake or the release from the carrier in the cytosol. Similar delays could be observed in PLGA-based nanocomplexes encapsulating various other cargos [79, 112]. Although we could show a substantial enhancement of complexation *in vitro* by co-formulation with PLGA, which preserved functionality of chitosan-based polyplexes, further studies in more complex environment like body fluids will need to be addressed. Most likely, the full potential of the co-formulated polyplexes in terms of colloidal stability and bio-functionality in physiological conditions can only be evaluated in further detailed *in vivo* studies.

## Summary

Both projects in this thesis aimed at finding strategies which make cmRNA biologically available *via* different application routes, by using the biopolymer PLGA as either matrix- or stabilization agent. cmRNA as one of the most promising approaches in transcript therapy bears the potential of treating diseases which cannot be treated until today. Combining such a polymer with its versatility and adjustability, which has been proven in various trials in different fields of drug delivery with the rather new cmRNA technique was therefore the aim of this project.

In the first study the focus was set on the incorporation of cmRNA/lipid system into a calcium phosphate cement system to potentially improve bone healing using transcript therapy. The production of *i.e.* growth factors by cmRNA transfection at site for new bone formation in combination with an injectable stabilization agent was set as the main goal of this study. The ability to directly inject a transfecting product into bone defects which in itself resembles natural bone, while maintaining a certain mechanical strength, is highly desirable for patients in need of surgical treatments like *i.e.* kyphoplasty or even vertebroplasty. The main task was to find a strategy which enabled the incorporation of a cmRNA carrier system in the cement phase which is able to release the cargo after implantation. This was done by circumventing the direct incorporation of the lipoplex into the hardly biodegradable cement phase by adding a biodegradable polymer phase which enables lipoplex release in combination with a porosity increase in the cement matrix. After the proof of concept for lipoplex incorporation into the microparticle matrix, and the microspheres' synthesis optimization, it was possible to successfully incorporate the polymer phase into CaP-based injectable cements for bone defect filling simulation *in vitro*. Even though the cmRNA was compacted into a lipoplex which was incorporated into a polymer matrix which itself was incorporated into injectable cement, biological functionality was maintained and demonstrated. As a next step these specimens need to be tested for long-term release kinetics and biocompatibility before they can be tested *in vivo*.

In the second project PLGA was not used as a matrix for the nanocarriers of cmRNA but as the compaction agent itself in combination with the amine-bearing polymer chitosan. Next to lipid-based vectors, polyplexes are a valid and desirable alternative for the compaction and transfection of nucleic acids. Chitosan as a biopolymer itself was already used in many different approaches of drug- and nucleic acid therapy but lacked sufficient ability to compact and stabilize the cargo in physiological conditions. The idea at hand was combining the chitosan's ability to bind nucleic acids and the PLGAs stabilizing properties for cmRNA compaction and delivery, especially because both polymers show high biocompatibility. We showed that chitosan alone is, in fact, able to bind cmRNA successfully and to transfect fibroblasts *in vitro*, but high cytotoxicity and low colloidal stability lowered the material's potential for cmRNA delivery drastically. For co-formulation with PLGA the operating protocol was optimized before the impact of co-formulation could be analyzed and investigated. Co-formulation led to physicochemical changes in the polyplexes which eventually led to a higher complexation potential with reduced bio-functionality while showing hardly any cytotoxicity. These findings bear the potential for an alternative strategy to already well-established carrier systems like br-PEI polyplexes or lipoplexes in general, which are known to be toxic, immunogenic and are hardly biodegradable. On the other hand, the PLGA/chitosan polyplexes have only proven their potential *in vitro* so far. Only future *in vivo* trials in highly complex fluids and obstacles for successful cell transfection in lungs like mucus barriers can reveal the potential of this new approach for polyplex-based cell transfection.

#### 4 References

- [1] P. Midoux, C. Pichon, J.J. Yaouanc, P.A. Jaffrès, Chemical vectors for gene delivery: a current review on polymers, peptides and lipids containing histidine or imidazole as nucleic acids carriers, *British journal of pharmacology* 157(2) (2009) 166-178.
- [2] S. Hama, H. Akita, R. Ito, H. Mizuguchi, T. Hayakawa, H. Harashima, Quantitative comparison of intracellular trafficking and nuclear transcription between adenoviral and lipoplex systems, *Molecular Therapy* 13(4) (2006) 786-794.
- [3] P.E. Monahan, R.J. Samulski, Adeno-associated virus vectors for gene therapy: more pros than cons?, *Molecular medicine today* 6(11) (2000) 433-440.
- [4] S.L. Ginn, I.E. Alexander, M.L. Edelstein, M.R. Abedi, J. Wixon, Gene therapy clinical trials worldwide to 2012—an update, *The journal of gene medicine* 15(2) (2013) 65-77.
- [5] T.J.o.G. Medicine, Gene Therapy Clinical Trials Worldwide Database, 2016.
- [6] M.S. Kormann, G. Hasenpusch, M.K. Aneja, G. Nica, A.W. Flemmer, S. Herber-Jonat, M. Huppmann, L.E. Mays, M. Illenyi, A. Schams, Expression of therapeutic proteins after delivery of chemically modified mRNA in mice, *Nature biotechnology* 29(2) (2011) 154-157.
- [7] K. Kariko, H. Muramatsu, J. Ludwig, D. Weissman, Generating the optimal mRNA for therapy: HPLC purification eliminates immune activation and improves translation of nucleoside-modified, protein-encoding mRNA, *Nucleic acids research* (2011).
- [8] V.F. Van Tendeloo, P. Ponsaerts, Z.N. Berneman, mRNA-based gene transfer as a tool for gene and cell therapy, *Current opinion in molecular therapeutics* 9(5) (2007) 423-431.
- [9] K. Kariko, D. Weissman, Naturally occurring nucleoside modifications suppress the immunostimulatory activity of RNA: implication for therapeutic RNA development, *Current Opinion in Drug Discovery and Development* 10(5) (2007) 523.
- [10] C.E. Samuel, Antiviral actions of interferons, *Clinical microbiology reviews* 14(4) (2001) 778-809.
- [11] B.R. Anderson, H. Muramatsu, S.R. Nallagatla, P.C. Bevilacqua, L.H. Sansing, D. Weissman, K. Karikó, Incorporation of pseudouridine into mRNA enhances translation by diminishing PKR activation, *Nucleic acids research* 38(17) (2010) 5884-5892.
- [12] K. Karikó, M. Buckstein, H. Ni, D. Weissman, Suppression of RNA recognition by Toll-like receptors: the impact of nucleoside modification and the evolutionary origin of RNA, *Immunity* 23(2) (2005) 165-175.
- [13] E. Sochacka, K. Kraszewska, M. Sochacki, M. Sobczak, M. Janicka, B. Nawrot, The 2-thiouridine unit in the RNA strand is desulfured predominantly to 4-pyrimidinone nucleoside under in vitro oxidative stress conditions, *Chemical Communications* 47(17) (2011) 4914-4916.
- [14] E.R. Balmayor, J.P. Geiger, M.K. Aneja, T. Berezhansky, M. Utzinger, O. Mykhaylyk, C. Rudolph, C. Plank, Chemically modified RNA induces osteogenesis of stem cells and human tissue explants as well as accelerates bone healing in rats, *Biomaterials* 87 (2016) 131-146.
- [15] M.-K. Abraham, A. Nolte, R. Reus, A. Behring, D. Zengerle, M. Avci-Adali, J.D. Hohmann, K. Peter, C. Schlensak, H.P. Wendel, In vitro study of a novel stent coating using modified CD39 messenger RNA to potentially reduce stent angioplasty-associated complications, *PLOS one* 10(9) (2015).

- [16] L. Xu, T. Anchordoquy, Drug delivery trends in clinical trials and translational medicine: Challenges and opportunities in the delivery of nucleic acid-based therapeutics, *Journal of pharmaceutical sciences* 100(1) (2011) 38-52.
- [17] J.L. Fox, Gene-therapy death prompts broad civil lawsuit, *Nature biotechnology* 18(11) (2000) 1136-1136.
- [18] A. Akinc, A. Zumbuehl, M. Goldberg, E.S. Leshchiner, V. Busini, N. Hossain, S.A. Bacallado, D.N. Nguyen, J. Fuller, R. Alvarez, A combinatorial library of lipid-like materials for delivery of RNAi therapeutics, *Nature biotechnology* 26(5) (2008) 561-569.
- [19] S.-d. Li, L.-y. Huang, Nonviral gene therapy: promises and challenges, *Gene therapy* 7(1) (2000) 31-34.
- [20] F. Scherer, M. Anton, U. Schillinger, J. Henke, C. Bergemann, A. Kruger, B. Gansbacher, C. Plank, Magnetofection: enhancing and targeting gene delivery by magnetic force in vitro and in vivo, *Gene therapy* 9(2) (2002) 102-109.
- [21] T.M. Pertmer, M.D. Eisenbraun, D. McCabe, S.K. Prayaga, D.H. Fuller, J.R. Haynes, Gene gun-based nucleic acid immunization: elicitation of humoral and cytotoxic T lymphocyte responses following epidermal delivery of nanogram quantities of DNA, *Vaccine* 13(15) (1995) 1427-1430.
- [22] B. Draghici, M.A. Ilies, Synthetic nucleic acid delivery systems: present and perspectives, *Journal of medicinal chemistry* 58(10) (2015) 4091-4130.
- [23] H. Cao, R.S. Molday, J. Hu, Gene therapy: light is finally in the tunnel, *Protein & cell* 2(12) (2011) 973-989.
- [24] I.A. Khalil, K. Kogure, H. Akita, H. Harashima, Uptake pathways and subsequent intracellular trafficking in nonviral gene delivery, *Pharmacological reviews* 58(1) (2006) 32-45.
- [25] M. Amyere, M. Mettlen, P. Van Der Smissen, A. Platek, B. Payrastra, A. Veithen, P.J. Courtoy, Origin, originality, functions, subversions and molecular signalling of macropinocytosis, *International journal of medical microbiology* 291(6) (2001) 487-494.
- [26] K. Takei, V. Haucke, Clathrin-mediated endocytosis: membrane factors pull the trigger, *Trends in cell biology* 11(9) (2001) 385-391.
- [27] P.R. Cullis, M.J. Hope, C.P. Tilcock, Lipid polymorphism and the roles of lipids in membranes, *Chemistry and physics of lipids* 40(2) (1986) 127-144.
- [28] O. Boussif, F. Lezoualc'h, M.A. Zanta, M.D. Mergny, D. Scherman, B. Demeneix, J.-P. Behr, A versatile vector for gene and oligonucleotide transfer into cells in culture and in vivo: polyethylenimine, *Proceedings of the National Academy of Sciences* 92(16) (1995) 7297-7301.
- [29] A. El-Sayed, S. Futaki, H. Harashima, Delivery of macromolecules using arginine-rich cell-penetrating peptides: ways to overcome endosomal entrapment, *The AAPS journal* 11(1) (2009) 13-22.
- [30] C.E. Smull, E.H. Ludwig, Enhancement of the plaque-forming capacity of poliovirus ribonucleic acid with basic proteins, *Journal of bacteriology* 84(5) (1962) 1035-1040.
- [31] F.E. Farber, J.L. Melnick, J.S. Butel, Optimal conditions for uptake of exogenous DNA by Chinese hamster lung cells deficient in hypoxanthine-guanine phosphoribosyltransferase, *Biochimica et Biophysica Acta (BBA)-Nucleic Acids and Protein Synthesis* 390(3) (1975) 298-311.
- [32] U. Lächelt, E. Wagner, Nucleic acid therapeutics using polyplexes: a journey of 50 years (and beyond), *Chemical reviews* 115(19) (2015) 11043-11078.

- [33] S.C. De Smedt, J. Demeester, W.E. Hennink, Cationic polymer based gene delivery systems, *Pharm Res* 17(2) (2000) 113-126.
- [34] J.E. Duncan, J.A. Whitsett, A.D. Horowitz, Pulmonary surfactant inhibits cationic liposome-mediated gene delivery to respiratory epithelial cells in vitro, *Human gene therapy* 8(4) (1997) 431-438.
- [35] J. Haensler, F.C. Szoka Jr, Polyamidoamine cascade polymers mediate efficient transfection of cells in culture, *Bioconjugate chemistry* 4(5) (1993) 372-379.
- [36] A. Akinc, M. Thomas, A.M. Klibanov, R. Langer, Exploring polyethylenimine-mediated DNA transfection and the proton sponge hypothesis, *The journal of gene medicine* 7(5) (2005) 657-663.
- [37] K. Tahara, T. Sakai, H. Yamamoto, H. Takeuchi, N. Hirashima, Y. Kawashima, Improved cellular uptake of chitosan-modified PLGA nanospheres by A549 cells, *International journal of pharmaceutics* 382(1) (2009) 198-204.
- [38] S. Jain, N. Jain, Y. Gupta, A. Jain, D. Jain, M. Chaurasia, Mucoadhesive chitosan microspheres for non-invasive and improved nasal delivery of insulin, *Indian journal of pharmaceutical sciences* 69(4) (2007) 498-504.
- [39] K. Roy, H.-Q. Mao, S.-K. Huang, K.W. Leong, Oral gene delivery with chitosan–DNA nanoparticles generates immunologic protection in a murine model of peanut allergy, *Nature medicine* 5(4) (1999) 387-391.
- [40] G.D.P. Dai Lam Tran, X.P. Nguyen, D.H. Vu, N.T. Nguyen, V.H. Tran, T. Mai, H.B. Nguyen, Q.D. Le, T.N. Nguyen, T.C. Ba, Some biomedical applications of chitosan-based hybrid nanomaterials, *Advances in Natural Sciences: Nanoscience and Nanotechnology* 2(4) (2011)
- [41] C. Stigliano, S. Aryal, M.D. De Tullio, G.P. Nicchia, G. Pascazio, M. Svelto, P. Decuzzi, siRNA-chitosan complexes in poly (lactic-co-glycolic acid) nanoparticles for the silencing of aquaporin-1 in cancer cells, *Molecular pharmaceutics* 10(8) (2013) 3186-3194.
- [42] N. Nafee, S. Taetz, M. Schneider, U.F. Schaefer, C.-M. Lehr, Chitosan-coated PLGA nanoparticles for DNA/RNA delivery: effect of the formulation parameters on complexation and transfection of antisense oligonucleotides, *Nanomedicine: Nanotechnology, Biology and Medicine* 3(3) (2007) 173-183.
- [43] P.L. Felgner, T.R. Gadek, M. Holm, R. Roman, H.W. Chan, M. Wenz, J.P. Northrop, G.M. Ringold, M. Danielsen, Lipofection: a highly efficient, lipid-mediated DNA-transfection procedure, *Proceedings of the National Academy of Sciences* 84(21) (1987) 7413-7417.
- [44] G.Y. Wu, C.H. Wu, Receptor-mediated in vitro gene transformation by a soluble DNA carrier system, *Journal of Biological Chemistry* 262(10) (1987) 4429-4432.
- [45] I.S. Zuhorn, U. Bakowsky, E. Polushkin, W.H. Visser, M.C. Stuart, J.B. Engberts, D. Hoekstra, Nonbilayer phase of lipoplex–membrane mixture determines endosomal escape of genetic cargo and transfection efficiency, *Molecular therapy* 11(5) (2005) 801-810.
- [46] Y. Xu, F.C. Szoka, Mechanism of DNA release from cationic liposome/DNA complexes used in cell transfection, *Biochemistry* 35(18) (1996) 5616-5623.
- [47] A. Jarzębińska, T. Pasewald, J. Lambrecht, O. Mykhaylyk, L. Kümmerling, P. Beck, G. Hasenpusch, C. Rudolph, C. Plank, C. Dohmen, A Single Methylene Group in Oligoalkylamine-Based Cationic Polymers and Lipids Promotes Enhanced mRNA Delivery, *Angewandte Chemie International Edition* 55(33) (2016) 9591-9595.
- [48] C.T. de Ilarduya, Y. Sun, N. Düzgüneş, Gene delivery by lipoplexes and polyplexes, *European journal of pharmaceutical sciences* 40(3) (2010) 159-170.

- [49] T. Allen, A. Chonn, Large unilamellar liposomes with low uptake into the reticuloendothelial system, *FEBS letters* 223(1) (1987) 42-46.
- [50] Y. Liu, L.C. Mounkes, H.D. Liggitt, C.S. Brown, I. Solodin, T.D. Heath, R.J. Debs, Factors influencing the efficiency of cationic liposome-mediated intravenous gene delivery, *Nature biotechnology* 15(2) (1997) 167-173.
- [51] K. Remaut, B. Lucas, K. Braeckmans, J. Demeester, S. De Smedt, Pegylation of liposomes favours the endosomal degradation of the delivered phosphodiester oligonucleotides, *Journal of controlled release* 117(2) (2007) 256-266.
- [52] M.C. Deshpande, M.C. Davies, M.C. Garnett, P.M. Williams, D. Armitage, L. Bailey, M. Vamvakaki, S.P. Armes, S. Stolnik, The effect of poly (ethylene glycol) molecular architecture on cellular interaction and uptake of DNA complexes, *Journal of controlled release* 97(1) (2004) 143-156.
- [53] R.E. Horch, Future perspectives in tissue engineering: 'Tissue Engineering' Review Series, *Journal of cellular and molecular medicine* 10(1) (2006) 4-6.
- [54] R.E. Horch, J. Kopp, U. Kneser, J. Beier, A.D. Bach, Tissue engineering of cultured skin substitutes, *Journal of cellular and molecular medicine* 9(3) (2005) 592-608.
- [55] J.-H. Jang, T.L. Houchin, L.D. Shea, Gene delivery from polymer scaffolds for tissue engineering, *Expert review of medical devices* 1(1) (2004) 127-138.
- [56] J. Bonadio, S.A. Goldstein, R.J. Levy, Gene therapy for tissue repair and regeneration, *Advanced drug delivery reviews* 33(1) (1998) 53-69.
- [57] A.K. Pannier, L.D. Shea, Controlled release systems for DNA delivery, *Molecular Therapy* 10(1) (2004) 19-26.
- [58] F.C. van de Watering, J.J. van den Beucken, X.F. Walboomers, J.A. Jansen, Calcium phosphate/poly (d, l-lactic-co-glycolic acid) composite bone substitute materials: evaluation of temporal degradation and bone ingrowth in a rat critical-sized cranial defect, *Clinical oral implants research* 23(2) (2012) 151-159.
- [59] K.M. Huh, Y.W. Cho, K. Park, PLGA-PEG block copolymers for drug formulations, *Drug Deliv Technol* 3(5) (2003) 42-44.
- [60] H.K. Makadia, S.J. Siegel, Poly lactic-co-glycolic acid (PLGA) as biodegradable controlled drug delivery carrier, *Polymers* 3(3) (2011) 1377-1397.
- [61] S. Fredenberg, M. Wahlgren, M. Reslow, A. Axelsson, The mechanisms of drug release in poly (lactic-co-glycolic acid)-based drug delivery systems—a review, *International journal of pharmaceutics* 415(1) (2011) 34-52.
- [62] A. Göpferich, Mechanisms of polymer degradation and erosion, *Biomaterials* 17(2) (1996) 103-114.
- [63] Y. Xu, C.S. Kim, D.M. Saylor, D. Koo, Polymer degradation and drug delivery in PLGA-based drug-polymer applications: A review of experiments and theories, *Journal of Biomedical Materials Research Part B: Applied Biomaterials* (2016).
- [64] R.C. Mundargi, V.R. Babu, V. Rangaswamy, P. Patel, T.M. Aminabhavi, Nano/micro technologies for delivering macromolecular therapeutics using poly (D, L-lactide-co-glycolide) and its derivatives, *Journal of Controlled Release* 125(3) (2008) 193-209.
- [65] C. Raman, C. Berkland, K.K. Kim, D.W. Pack, Modeling small-molecule release from PLG microspheres: effects of polymer degradation and nonuniform drug distribution, *Journal of Controlled Release* 103(1) (2005) 149-158.
- [66] R.A. Jain, The manufacturing techniques of various drug loaded biodegradable poly (lactide-co-glycolide)(PLGA) devices, *Biomaterials* 21(23) (2000) 2475-2490.
- [67] J.A. Wolff, R.W. Malone, P. Williams, W. Chong, G. Acsadi, A. Jani, P.L. Felgner, Direct gene transfer into mouse muscle in vivo, *Science* 247(4949) (1990) 1465-1468.

- [68] C. Oliveira, A.J. Ribeiro, F. Veiga, I. Silveira, Recent Advances in Nucleic Acid-Based Delivery: From Bench to Clinical Trials in Genetic Diseases, *Journal of Biomedical Nanotechnology* 12(5) (2016) 841-862.
- [69] B.K. Muralidhara, R. Baid, S.M. Bishop, M. Huang, W. Wang, S. Nema, Critical considerations for developing nucleic acid macromolecule based drug products, *Drug discovery today* 21(3) (2016) 430-444.
- [70] J. Devoldere, H. Dewitte, S.C. De Smedt, K. Remaut, Evading innate immunity in nonviral mRNA delivery: don't shoot the messenger, *Drug discovery today* 21(1) (2016) 11-25.
- [71] H.R.R. Ramay, M. Zhang, Biphasic calcium phosphate nanocomposite porous scaffolds for load-bearing bone tissue engineering, *Biomaterials* 25(21) (2004) 5171-5180.
- [72] I. Khairoun, M.G. Boltong, F.C.M. Driessens, J.A. Planell, Effect of calcium carbonate on clinical compliance of apatitic calcium phosphate bone cement, *Journal of Biomedical Materials Research* 38(4) (1997) 356-360.
- [73] M. Ginebra, E. Fernández, M. Boltong, O. Bermúdez, J. Planell, F. Driessens, Compliance of an apatitic calcium phosphate cement with the short-term clinical requirements in bone surgery, orthopaedics and dentistry, *Clinical materials* 17(2) (1994) 99-104.
- [74] M. Bohner, G. Baroud, Injectability of calcium phosphate pastes, *Biomaterials* 26(13) (2005) 1553-1563.
- [75] L. Xin, M. Bungartz, S. Maenz, V. Horbert, M. Hennig, B. Illerhaus, J. Günster, J. Bossert, S. Bischoff, J. Borowski, Decreased extrusion of calcium phosphate cement versus high viscosity PMMA cement into spongy bone marrow—an ex vivo and in vivo study in sheep vertebrae, *The Spine Journal* 16(12) (2016) 1468-1477.
- [76] J.W.M. Hoekstra, J. Ma, A.S. Plachokova, E.M. Bronkhorst, M. Bohner, J. Pan, G.J. Meijer, J.A. Jansen, J.J. van den Beucken, The in vivo performance of CaP/PLGA composites with varied PLGA microsphere sizes and inorganic compositions, *Acta biomaterialia* 9(7) (2013) 7518-7526.
- [77] R.P.F. Lanao, S.C. Leeuwenburgh, J.G. Wolke, J.A. Jansen, Bone response to fast-degrading, injectable calcium phosphate cements containing PLGA microparticles, *Biomaterials* 32(34) (2011) 8839-8847.
- [78] O. Borges, A. Cordeiro-da-Silva, J. Tavares, N. Santarém, A. de Sousa, G. Borchard, H.E. Junginger, Immune response by nasal delivery of hepatitis B surface antigen and codelivery of a CpG ODN in alginate coated chitosan nanoparticles, *European Journal of Pharmaceutics and Biopharmaceutics* 69(2) (2008) 405-416.
- [79] F. Danhier, E. Ansorena, J.M. Silva, R. Coco, A. Le Breton, V. Prétat, PLGA-based nanoparticles: an overview of biomedical applications, *Journal of controlled release* 161(2) (2012) 505-522.
- [80] R.M. Mainardes, R.C. Evangelista, PLGA nanoparticles containing praziquantel: effect of formulation variables on size distribution, *International journal of pharmaceutics* 290(1) (2005) 137-144.
- [81] M.I. Worldwide, Dynamic light scattering common terms defined, Inform white paper (2011).
- [82] Z. Potential, An introduction in 30 minutes, Zetasizer Nano Series technical note (MRK654-01), Malvern Instruments, Worcestershire, UK (2006).
- [83] T. Katagiri, A. Yamaguchi, M. Komaki, E. Abe, N. Takahashi, T. Ikeda, V. Rosen, J.M. Wozney, A. Fujisawa-Sehara, T. Suda, Bone morphogenetic protein-2 converts the differentiation pathway of C2C12 myoblasts into the osteoblast lineage, *The Journal of cell biology* 127(6) (1994) 1755-1766.

- [84] M. Bio, Label IT Nucleic Acid Labelink Kits, 2014.
- [85] D.P. Link, J. van den Dolder, J.J. van den Beucken, V.M. Cuijpers, J.G. Wolke, A.G. Mikos, J.A. Jansen, Evaluation of the biocompatibility of calcium phosphate cement/PLGA microparticle composites, *Journal of Biomedical Materials Research Part A* 87(3) (2008) 760-769.
- [86] H. Katou, A.J. Wandrey, B. Gander, Kinetics of solvent extraction/evaporation process for PLGA microparticle fabrication, *International journal of pharmaceutics* 364(1) (2008) 45-53.
- [87] P.Q. Ruhe, E.L. Hedberg, N.T. Padron, P.H. Spauwen, J.A. Jansen, A.G. Mikos, rhBMP-2 release from injectable poly (DL-lactic-co-glycolic acid)/calcium-phosphate cement composites, *J Bone Joint Surg Am* 85(suppl 3) (2003) 75-81.
- [88] S.E. Lupold, T. Johnson, W.H. Chowdhury, R. Rodriguez, A real time Metridia luciferase based non-invasive reporter assay of mammalian cell viability and cytotoxicity via the  $\beta$ -actin promoter and enhancer, *PLOS one* 7(5) (2012).
- [89] M. Doube, M. Kłosowski, I. Arganda-Carreras, F. Cordelières, R. Dougherty, J. Jackson, B. Schmid, J. Hutchinson, S. Shefelbine, BoneJ: free and extensible bone image analysis in ImageJ., *Bone* 47(1076-9) (2010).
- [90] S.K. Sahoo, J. Panyam, S. Prabha, V. Labhasetwar, Residual polyvinyl alcohol associated with poly (D, L-lactide-co-glycolide) nanoparticles affects their physical properties and cellular uptake, *Journal of controlled release* 82(1) (2002) 105-114.
- [91] H. Uchida, K. Itaka, T. Nomoto, T. Ishii, T. Suma, M. Ikegami, K. Miyata, M. Oba, N. Nishiyama, K. Kataoka, Modulated protonation of side chain aminoethylene repeats in N-substituted polyaspartamides promotes mRNA transfection, *Journal of the American Chemical Society* 136(35) (2014) 12396-12405.
- [92] K. Itaka, A. Harada, Y. Yamasaki, K. Nakamura, H. Kawaguchi, K. Kataoka, In situ single cell observation by fluorescence resonance energy transfer reveals fast intracytoplasmic delivery and easy release of plasmid DNA complexed with linear polyethylenimine, *The journal of gene medicine* 6(1) (2004) 76-84.
- [93] K. Itaka, A. Harada, K. Nakamura, H. Kawaguchi, K. Kataoka, Evaluation by fluorescence resonance energy transfer of the stability of nonviral gene delivery vectors under physiological conditions, *Biomacromolecules* 3(4) (2002) 841-845.
- [94] M. Huang, E. Khor, L.-Y. Lim, Uptake and cytotoxicity of chitosan molecules and nanoparticles: effects of molecular weight and degree of deacetylation, *Pharm Res* 21(2) (2004) 344-353.
- [95] W. Jiang, R.K. Gupta, M.C. Deshpande, S.P. Schwendeman, Biodegradable poly (lactic-co-glycolic acid) microparticles for injectable delivery of vaccine antigens, *Advanced Drug Delivery Reviews* 57(3) (2005) 391-410.
- [96] C. Wischke, S.P. Schwendeman, Principles of encapsulating hydrophobic drugs in PLA/PLGA microparticles, *International Journal of Pharmaceutics* 364(2) (2008) 298-327.
- [97] S.D. Allison, Analysis of initial burst in PLGA microparticles, *Expert Opinion on Drug Delivery* 5(6) (2008) 615-628.
- [98] N. Faisant, J. Siepmann, J. Benoit, PLGA-based microparticles: elucidation of mechanisms and a new, simple mathematical model quantifying drug release, *European Journal of Pharmaceutical Sciences* 15(4) (2002) 355-366.
- [99] D. Klose, F. Siepmann, K. Elkharraz, S. Krenzlin, J. Siepmann, How porosity and size affect the drug release mechanisms from PLGA-based microparticles, *International Journal of Pharmaceutics* 314(2) (2006) 198-206.
- [100] E. GmbH, 30 years of Resomer, 2016.

- [101] K. Tahara, T. Sakai, H. Yamamoto, H. Takeuchi, Y. Kawashima, Establishing chitosan coated PLGA nanosphere platform loaded with wide variety of nucleic acid by complexation with cationic compound for gene delivery, *International journal of pharmaceutics* 354(1) (2008) 210-216.
- [102] H. Ragelle, R. Riva, G. Vandermeulen, B. Naeye, V. Pourcelle, C.S. Le Duff, C. D'Haese, B. Nysten, K. Braeckmans, S.C. De Smedt, C. Jérôme, V. Pr at, Chitosan nanoparticles for siRNA delivery: Optimizing formulation to increase stability and efficiency, *Journal of Controlled Release* 176 (2014) 54-63.
- [103] G. Maurstad, B.T. Stokke, K.M. V rum, S.P. Strand, PEGylated chitosan complexes DNA while improving polyplex colloidal stability and gene transfection efficiency, *Carbohydrate Polymers* 94(1) (2013) 436-443.
- [104] N.L. Dhas, P.P. Ige, R.R. Kudarha, Design, optimization and in-vitro study of folic acid conjugated-chitosan functionalized PLGA nanoparticle for delivery of bicalutamide in prostate cancer, *Powder Technology* 283 (2015) 234-245.
- [105] H. Bordelon, A.S. Biris, C.M. Sabliov, W.T. Monroe, Characterization of plasmid DNA location within chitosan/PLGA/pDNA nanoparticle complexes designed for gene delivery, *Journal of Nanomaterials* 2011 (2011).
- [106] N. Nafee, M. Schneider, U.F. Schaefer, C.-M. Lehr, Relevance of the colloidal stability of chitosan/PLGA nanoparticles on their cytotoxicity profile, *International journal of pharmaceutics* 381(2) (2009) 130-139.
- [107] E.H. Care, *Controlled Release*. <<http://healthcare.evonik.com/product/healthcare/en/products/biomaterials/resomer/pages/controlled-release.aspx>>).
- [108] A. Alshamsan, A. Haddadi, V. Incani, J. Samuel, A. Lavasanifar, H. Uludag, Formulation and delivery of siRNA by oleic acid and stearic acid modified polyethylenimine, *Molecular pharmaceutics* 6(1) (2008) 121-133.
- [109] T. Nisisako, S. Okushima, T. Torii, Controlled formulation of monodisperse double emulsions in a multiple-phase microfluidic system, *Soft Matter* 1(1) (2005) 23-27.
- [110] L.-H. Hung, A.P. Lee, Microfluidic devices for the synthesis of nanoparticles and biomaterials, *Journal of Medical and Biological Engineering* 27(1) (2007).
- [111] S. Mishra, P. Webster, M.E. Davis, PEGylation significantly affects cellular uptake and intracellular trafficking of non-viral gene delivery particles, *European journal of cell biology* 83(3) (2004) 97-111.
- [112] L. Chronopoulou, M. Massimi, M.F. Giardi, C. Cametti, L.C. Devirgiliis, M. Dentini, C. Palocci, Chitosan-coated PLGA nanoparticles: a sustained drug release strategy for cell cultures, *Colloids and surfaces B: biointerfaces* 103 (2013) 310-317.

## 5 Appendix

### 5.1 Abbreviations

PLGA	poly(lactic-co-glycolic acid
RNA	ribonucleic acid
DNA	deoxyribonucleic acid
cmRNA	chemically modified messenger RNA
siRNA	small interfering RNA
pDNA	plasmid DNA
FRET	fluorescence resonance energy transfer
MTT	3-(4,5-Dimethylthiazol-2-yl)-2,5-diphenyltetrazoliumbromid
SEM	scanning electron microscopy
$\mu$ -CT	micro-computer tomography
O/W/O	oil in water in oil emulsion
O/W	oil in water emulsion
TLR	toll-like receptor
s2U/U	2-thio-uridine/uridine
<i>i.e.</i>	id est
EPO	erythropoietin
hBMP-2	human bone morphogeneic protein- 2
<i>et al.</i>	et alii
DOPE	(1,2-dioleoyl-sn-glycero-3-phosphoethanolamine
PEG	poly(ethylene glycol)
LA	lactic acid
GA	glycolic acid
Mw	molecular weight
PVA	poly(vinyl alcohol)
DMSO	dimethylsulfoxide
DCM	dichloromethane
WFI	water for injection
PBS	phosphate-based saline

---

CaP	calcium phosphate
DMEM	dulbecco's modified eagle medium
EDTA	ethylenediaminetetraacetic acid
Pen/Strep	penicillin streptomycin
FBS	fetal bovine serum
FCS	fetal calf serum
GFP	green fluorescent protein
HCl	hydrochloric acid
ISO	international organization of standardization
DLS	direct light scattering
rBMSC	rat bone marrow stem cell
NIH3T3	National institute of health, mouse fibroblast line
C2C12	mouse myoblast line
DBCO	dibenzocyclooctyne
DMG-PEG 2k	diacylglycerol poly(ethylene glycol); Mw= 2000 kD
kD	kilo Dalton
N/P	nitrogen to phosphate
UK	United Kingdom
Fig.	Figure
3D	three dimensional
brPEI	branched polyethyleneimine
rpm	rotations per minute
TRIS	tris(hydroxymethyl)aminomethane
Cy	cyanin
% (w/w)	weight to weight ratio in percent

---

## 5.2 Publications

### *Publications as a first author:*

cmRNA/lipoplex encapsulation in PLGA microspheres enables transfection *via* calcium phosphate cement (CPC)/PLGA composites (Utzinger, Jarzebinska, Haag, Schweizer, Winter, Dohmen, Rudolph, Plank. - Journal of Controlled Release – 2016) PMID: 28161466)

Co-formulation of chitosan/cmRNA complexes with PLGA enhances biocompatibility and nucleic acid compaction (Utzinger, Beck, Winter, Dohmen, Rudolph, Plank, International Journal of Nanomedicine – submitted)

### *Publications as second author:*

Chemically modified RNA induces osteogenesis of stem cells and human tissue explants as well as accelerates bone healing in rats (Balmayor, Geiger, Aneja, Berezhansky, Utzinger, Mykhaylyk, Rudolph, Plank – Biomaterials – 2016) PMID: 26923361

Transcript-activated collagen matrix as sustained mRNA delivery system for bone regeneration (Badiyan, Berezhansky, Utzinger, Aneja, Emrich, Erben, Schüler, Altpeter, Ferizi, Hasenpusch, Rudolph, Plank – Journal of Controlled Release – 2016) PMID: 27586186

### *Patents:*

Compositions for introducing nucleic acids into cells of the gastrointestinal tract (Dohmen, Utzinger, Hasenpusch, Rudolph, Plank – Ethris GmbH - 06.02.2014 - WO2015/128030 A1)

---

### 5.3 Supplementary information

Macroinstruction for the automatic analysis of microparticles mean sizes by image post processing *via* ImageJ:

```
run("Clear Results");

dir = getDirectory("Choose a Directory");
list = getFileList(dir);
for (i=0; i<list.length; i++) {
    path = dir+list[i];
    if (endsWith(path, ".jpg")) {
open(path);
name=getTitle;
run("Set Scale...", "distance=2313 known=1000 pixel=1 unit=µm global");
makeRectangle(2115, 1683, 405, 195);
setBackground(255, 255, 255);
run("Clear", "slice");
run("8-bit");

run("Select None");

setAutoThreshold("IsoData");
setThreshold(50, 110);
setOption("BlackBackground", false);
run("Convert to Mask");

run("Watershed");
run("Fill Holes");
run("Dilate");
run("Fill Holes");
run("Watershed");
run("Fill Holes");
```

---

```
run("Watershed");
run("Fill Holes");
run("Set Measurements...", " perimeter feret's limit redirect=None decimal=3");
run("Analyze Particles...", "size=50-8000 circularity=0.5-1.00 show=Nothing
exclude add");
roiManager("Measure");
waitForUser;

run("Close All");
}
}
roiManager("Delete");
saveAs("Results", dir + "Resultsnew.txt");
```

Macroinstruction for the automatic definition of CPC/PLGA specimens investigated for porosity by image post processing *via* ImageJ:

```
makeOval(375, 396, 244, 244);
makeRectangle(256, 132, 350, 341);
```

Macroinstruction for the automatic image post processing of fluorescence microscopy images *via* ImageJ for microparticle investigation:

```
dir = "C:\\\"
list = getFileList(dir);
```

---

```
for (i=0; i<list.length; i++) {

    if (endsWith(list[i], "+++518/")) {

        open(dir + list[i] + "protein.tif");
        run("8-bit");
        setThreshold(3,255);
        run("Create Selection");
        run("Multiply...", "value=30");
        run("Select None");
        resetThreshold();

        open(dir + list[i] + "mRNA.tif");
        run("8-bit");
        setThreshold(3,255);
        run("Create Selection");
        run("Multiply...", "value=5");
        run("Select None");
        resetThreshold();

        open(dir + list[i] + "DNA.tif");
        run("8-bit");
        setThreshold(2,255);
        run("Create Selection");
        run("Multiply...", "value=5");
        //run("Add...", "value=50");
        run("Select None");
        resetThreshold();

        run("Merge Channels...", "c1=mRNA.tif c4=protein.tif c3=DNA.tif create keep");
        rename(list[i] + " composite");
        run("Set... ", "zoom=50 x=696 y=520");
```

```
close("mRNA.tif");
close("protein.tif");
close("DNA.tif");

};

if (endsWith(list[i], "++519/")) {

open(dir + list[i] + "lipid.tif");
run("8-bit");
setThreshold(4,255);
run("Create Selection");
run("Multiply...", "value=3");
run("Select None");
resetThreshold();

open(dir + list[i] + "mRNA.tif");
run("8-bit");
setThreshold(2,255);
run("Create Selection");
run("Multiply...", "value=5");
run("Select None");
resetThreshold();

open(dir + list[i] + "DNA.tif");
run("8-bit");
setThreshold(2,255);
run("Create Selection");
run("Multiply...", "value=5");
//run("Add...", "value=50");
run("Select None");
```

---

```
resetThreshold();

run("Merge Channels...", "c1=mRNA.tif c2=lipid.tif c3=DNA.tif create keep");
rename(list[i] + " composite");
run("Set... ", "zoom=50 x=696 y=520");

close("mRNA.tif");
close("lipid.tif");
close("DNA.tif");

};

if (endsWith(list[i], "520/")) {

open(dir + list[i] + "lipid.tif");
run("8-bit");
setThreshold(5,255);
run("Create Selection");
run("Multiply...", "value=3");
run("Select None");
resetThreshold();

open(dir + list[i] + "protein.tif");
run("8-bit");
setThreshold(4,255);
run("Create Selection");
run("Multiply...", "value=30");
run("Select None");
resetThreshold();

open(dir + list[i] + "DNA.tif");
run("8-bit");
setThreshold(2,255);
```

```
run("Create Selection");
run("Multiply...", "value=5");
//run("Add...", "value=50");
run("Select None");
resetThreshold();

run("Merge Channels...", "c2=lipid.tif c3=DNA.tif c4=protein.tif create keep");
rename(list[i] + " composite");
run("Set... ", "zoom=50 x=696 y=520");

close("protein.tif");
close("lipid.tif");
close("DNA.tif");

}}
```

### 5.3.1 Supplementary Information to 2.3.9 $\mu$ -CT analysis of composites

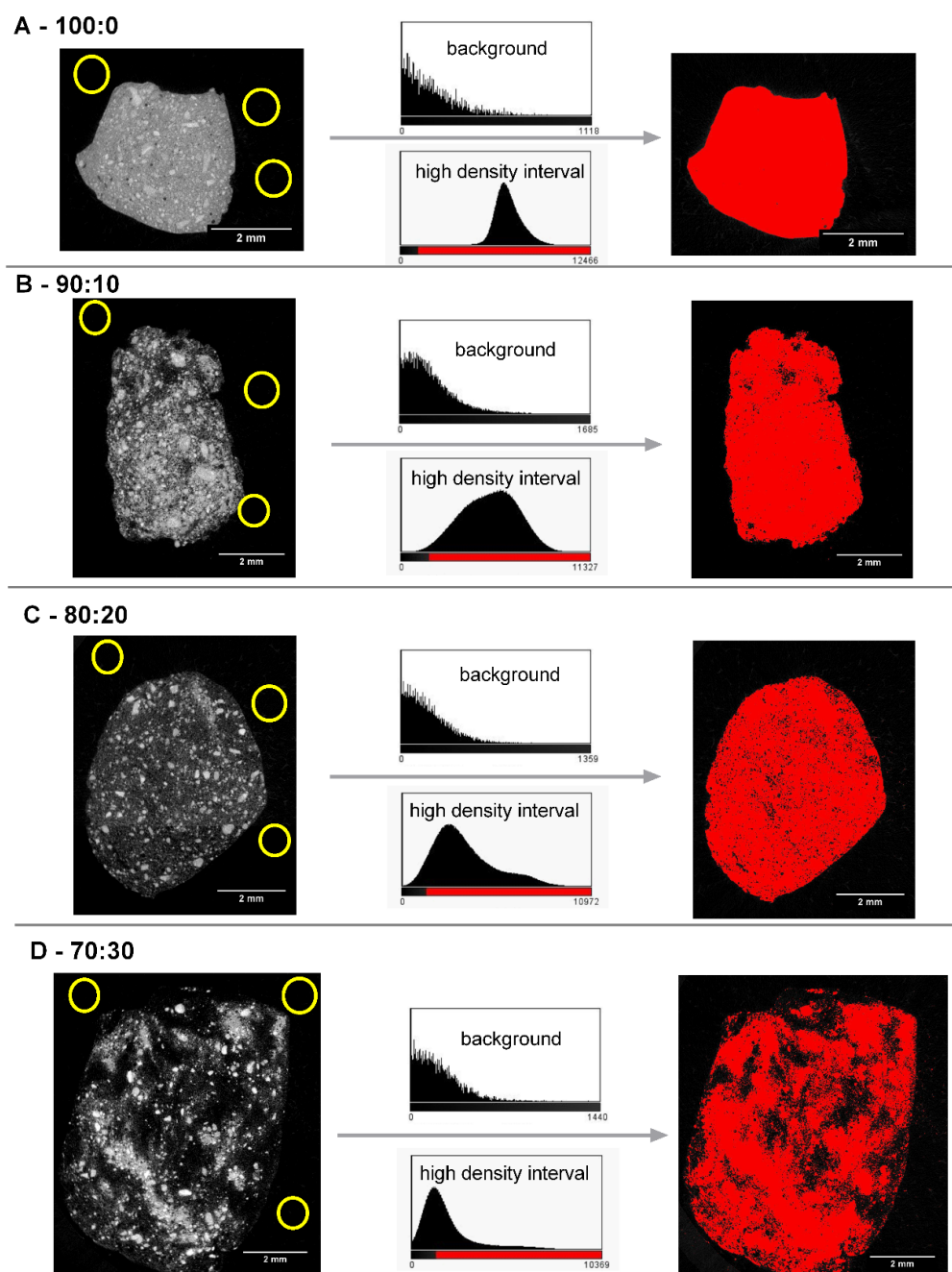


Fig. 47 - Schematic representation of the definition of greyscale thresholds for all specimens including A) pure calcium phosphate cement and CPC/PLGA composites of B) 90:10, C) 80:20 and D) 70:30 % (w/w). Background areas indicated by yellow circles in the exemplary  $\mu$ -CT slice images represent areas where the background greyscale levels were measured. Exemplary greyscale histograms are labelled as "background". The greyscale intervals of those histograms were defined representing the low density fractions of the specimens and were measured in triplicates. Consequently, the greyscale interval above those histograms determined the threshold for higher density/greyscale intervals which was defined as the CPC phase.

## 6 Acknowledgements

This thesis is the product of three and a half years of working at a company which made my exit out of academia and the entry in the corporate world as easy as possible. I had the privilege to enjoy working with very different characters in a huge variety of working areas and I would like to take the advantage to thank each one of these marvelous characters for what they taught me professionally and personally over the last years.

First and foremost, I would like to thank Prof. Gerhard Winter who made this doctorate possible. Thank you for your supervision and support over the years. Next I want to thank Tamara Pasewald for being my oldest friend at Ethris. Also Anita Jarzebinska who was my partner and friend from the beginning and the one who I contacted first when good or bad news came. I am very thankful for having shared all the ups and downs of a doctorate with her.

I would like to thank Linda Kümmerling for being one of the most impressive personalities I have ever met and for being a role model in everyday life decisions. I would like to thank Laura Maccarrone for just being herself and for making every day at work just a little easier, smoother and funnier.

I would also like to thank both Martins who shared my out-of-the-ordinary taste of humor and for each meeting at the “Wilde Hirsch”.

I would like to thank Prof. Christian Plank and PD Carsten Rudolph for giving a mechanical engineer the chance to make his Ph.D. in pharmaceutical technology. Thank you for your support over the years.

Of course, I want to thank my supervisor, mentor and friend Dr. Christian Dohmen for basically getting me through this process of maturing professionally, academically and mentally to finally graduate as a Ph.D.

The most important people however who made this graduation possible in the first place are my family. I want to thank Andreas Hallweger for the inspiration, Angelika Hallweger for being my moral compass, Franz-Xaver Utzinger sen. for giving me perspective, Verena Utzinger for being the sister I never had and my Franz-Xaver Utzinger jun. for being the Yin to my Yang.

In the end I would like to thank most of all, my way better half and companion Susanne Schlosser who contributed most in this story, by simply making my life better on a daily basis.

Thank you